UNITED STATES DEPARTMENT OF THE INTERIOR

GEOLOGICAL SURVEY

Geology of a part of the southern Monte Cristo Range, Esmeralda County, Nevada

By

Steven W. Moore

Open-File Report 81-710

1981

CONTENTS

ILLUSTRATIONS

Page

TABLES

Geology of a part of the southern Monte Cristo Range, Esmeralda County, Nevada

By Steven W. Moore

ABSTRACT

The Blair Junction sequence of the Esmeralda Formation in the southern Monte Cristo Range, Esmeralda County, Nevada, is informally defined as a discrete local stratigraphic assemblage of middle to upper Miocene, dominantly lacustrine sedimentary rocks. The Blair Junction sequence, which is divided into four informal members, is interpreted as being deposited in shallow, fresh, alkaline water of a marginal lacustrine environment with local influences of intermittent paludal and fluvial depositional conditions and contemporaneous volcanic activity. Older stratigraphic units include middle Miocene andesite units and upper Oligocene to lower Miocene ash-flow tuff. The Cenozoic volcanic and sedimentary rocks unconformably overlie the Ordovician Palmetto Formation. Post-Esmeralda Formation units include upper Miocene to Pliocene andesite, rhyolite, and Quaternary alluvial deposits.

Member 1 of the Blair Junction sequence of the Esmeralda Formation is correlative with the coal-bearing unit at the north base of the Silver Peak Range. However, the amount and the grade of coal (lignite or carbonaceous shale) generally decreases northward. In fine-grained lacustrine rocks, authigenic minerals include montmorillonite, opal-CT, authigenic potassium feldspar, and minor zeolites.

The southern flank of the Monte Cristo Range is traversed by three major sets of faults, the trends of which average N. 57 E., N. 77 E., and N. 42 E., respectively. These trends are anomalous with respect to the more northerly trends typical of the Basin and Range Province. These faults, some with large vertical throw, offset upper Oligocene to Pliocene rocks. Slickensided fault planes provide some evidence for left-oblique slip on these northeast-trending faults, which is analogous in part to the relative sense of movement along the fault system in the nearby Candelaria Hills. A zone of locally intense folding, suggestive of compressional stresses acting subparallel to an adjacent fault, also suggests a lateral or oblique component of movement along this fault.

INTRODUCTION

Background, Purpose, and Scope

Coal was discovered north of the Silver Peak Range in Esmeralda County, Nevada in 1893. This discovery spurred great local interest in the early 1900's because of scarcity of fuel in the region and the energy demand of mining operations in the nearby gold-boom towns of Goldfield, Candelaria, and Tonopah. In 1911, lands in four townships in this area, including much of the Monte Cristo Range, were designated by Presidential order as Nevada Coal Withdrawal No. 1 (fig. 1), in accordance with the General Withdrawal Act of 1910 ("Pickett Act"). Under the provisions of this act, Federal lands enclosed were withheld from settlement, sale, location, or entry pending classification of the land for coal resources by the U.S. Geological Survey. The withdrawal has been only partially classified since its designation in 1911.

Recent Federal legislation, in particular the Federal Land Policy Management Act of 1976, requires the Bureau of Land Management (BLM) to review all mineral and other withdrawals to determine the need for extention or revocation in view of the public interest. This project was undertaken as part of the U.S. Geological Survey's effort to provide basic geologic data necessary to support the mandated BLM withdrawal review.

Past studies of this area have been of a more regional nature, providing only general descriptions of the geology of the area, which

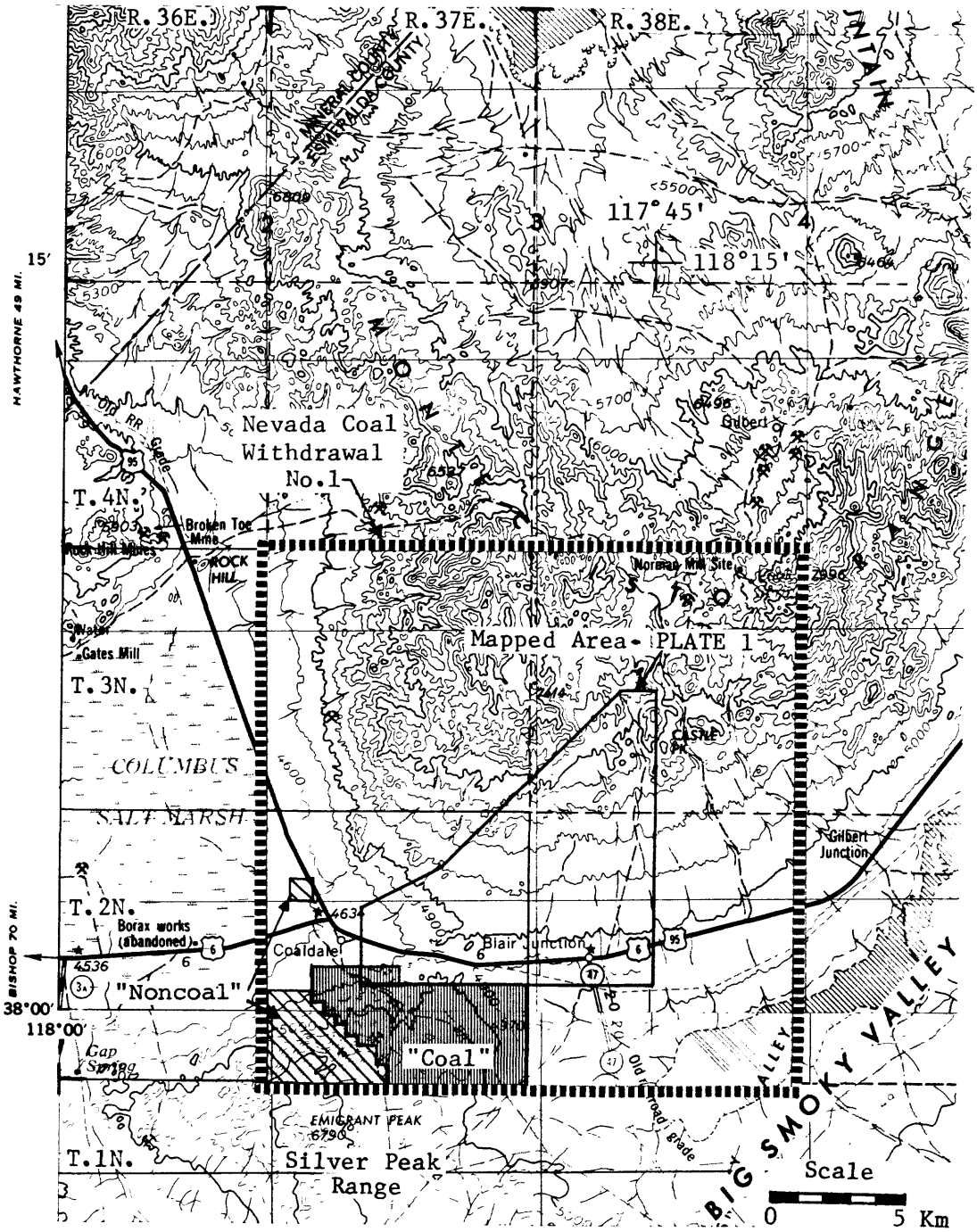

Figure 1.--Location map showing the mapped area within Nevada Coal Withdrawal No. 1. Lands classified as "coal" lands shown by vertical pattern. Diagonal pattern indicates "noncoal" classified lands. The remainder of the lands within the withdrawal are withdrawn pending classification.

were unsuitable for determination of the extent of coal deposits in the area. Therefore, this study was proposed to investigate the sequence of Tertiary sedimentary and volcanic rocks that extends northward from classifed "coal land" into the Monte Cristo Range. The emphasis of this project is on geologic mapping, physical stratigraphy, and depositional sedimentary environments of the area. Of major interest has been the relationship and correlation of the sedimentary sequence of this area to the coal-bearing rocks exposed at the base of the Silver Peak Range, south of the study area.

Location and Geographic Setting

The project area is located in Esmeralda County, which lies in southwestern Nevada adjacent to the California border (fig. 2). The project area, as shown on figures 1 and 2, extends south and southwestward from southern Monte Cristo Range towards the northern base of the Silver Peak Range. The project area lies entirely within the Blair Junction 7.5-minute quadrangle.

The topography of Esmeralda County is conspicuously dominated by several mountain ranges, or combinations of mountain ranges, which together form distinctive, large, concave-north, arcuate structures (Albers and Stewart, 1972, p. 42). This arcuate topographic trend represents a significant departure from the common northerly trending mountain ranges and intervening valleys typical of the Basin and Range Province. The Monte Cristo Range and the Cedar Mountains together define one of these arcuate geomorphic trends. Likewise,

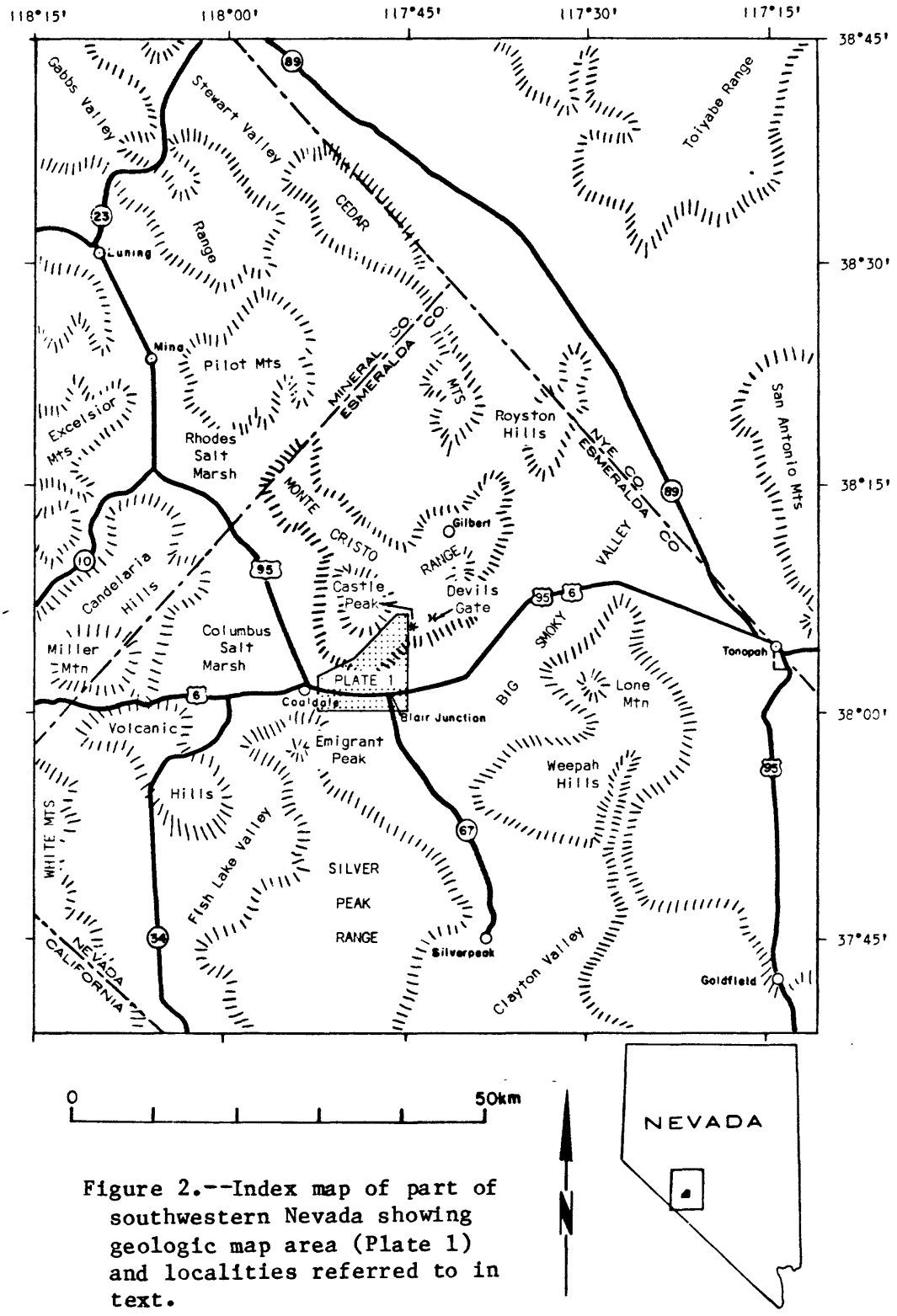

Figure 2.--Index map of part of southwestern Nevada showing geologic map area (Plate 1) and localities referred to in text.

the Silver Peak Range is also part of another large, concave-north arc. The project area lies between these two mountain-range arcs. In addition, the project area constitutes a relative topographic high separating the large intermontane valleys of the Big Smoky Valley, to the east, and Columbus Salt Marsh, to the west.

Elevations within the project area range from about 1,460 m (4,800 ft) to 1,950 m (6,400 ft). The southern part of the project area is characterized by subdued relief with low, dissected hills and gullies that extend across alluvial slopes towards the Monte Cristo Range. The northern extreme of the project area has more rugged terrain with relatively high local relief up to about 180 m (590 ft) developed in the thick pile of volcanic rocks. Landmarks nearby include Castle Peak, elevation 1,873 m (6,145 ft), which lies immediately east of the project area. Devils Gate, a narrow opening between high andesite ridges, lies northeast of the Castle Peak. Three informal geographic names, Jackrabbit Draw, Dragonback Hills, and Gilbert Road, are informally proposed to aid in description of localities described in the text and are shown on plate 1.

Methods Used in the Investigation

A total of 47 days of field work was accomplished during the period from October 1977 to March 1979 for this investigation. Initial field reconnaissance and selection of the project area occurred in October 1977 and March 1978. The bulk of the field work including detailed geologic mapping, measurement of stratigraphic

sections, and collection of lithologic and fossil samples was accomplished during July, September, and October 1978.

Geologic mapping of approximately 85 km^2 was done at a scale of 1:24,000 using the U.S. Geological Survey Blair Junction 7.5-minute topographic quadrangle as a base map. In addition, to increase the precision of location, some geologic data such as sample localities and some fault and lithologic contacts were plotted on 1:20,000-scale, black and white, vertical aerial photographs. Other black and white, vertical aerial photographs at scales of 1:37,000 and 1:60,000 occasionally were used for further location control. Stratigraphic sections were measured using a 30-m tape and Brunton compass, or a Jacob's staff, where applicable. Rock colors were described using the standard rock color chart of Goddard and others (1975). Geologic data from aerial photography was subsequently transferred to the base map using a PG-2 stereographic plotter at the U.S. Geological Survey in Menlo Park, California.

The laboratory part of this investigation included further examination of some of the samples with a binocular microscope. Thin sections of volcanic and sedimentary rocks were examined in detail, in plane and polarized light, to determine mineral composition, texture and other microscopic features. A Zeiss, model 9901, standard petrographic microscope was used. Where applicable, Michel-Levy's method was used to determine the anorthite composition of plagioclase in selected samples of volcanic rocks.

X-ray diffraction patterns were made of 36 bulk samples of fine-grained sedimentary rocks, tuff, and various volcanic rocks. Bulk samples were crushed to a fine powder, mounted on a glass slide, air dried, and then exposed to nickel-filtered Cu K-alpha radiation using a Rigaku Miniflex X-ray diffractometer. Scanning speed used was 0.5° 2θ/minute and the machine was set at 500 counts/second. Minerals were identified by use of using reference patterns and other standard methods.

Some tentative fossil identifications of molluscan fossils were made by the author. J.R. Firby of the University of Nevada, Reno, later substantiated and added to these identifications. G.R. Smith of the University of Michigan identified some fossil fish bones. C.A. Repenning and R.M. Forester, both of the U.S. Geological Survey, provided fossil identifications on a mammal fossil and ostracodes, respectively.

Previous Investigations

Knapp (1897), in an early report, described the coal prospects, first discovered about 1894, at the north end of the Silver Peak Range. Knapp noted a high ash content of 30 percent, in selected coal beds, suggesting clay and sand being washed into the organic matter during deposition. Turner (1900) named the Esmeralda Formation for widespread lacustrine deposits in Esmeralda County and published a map showing the formation's distribution over a widespread area in and north of the Silver Peak Range, along the east

and west sides of Big Smoky Valley, in Clayton Valley, and in the Fish Lake Valley area. Turner interpreted these rocks, some of which contain coal, as representing Miocene to Pliocene deposits of a single, extensive, fresh water "Lake Esmeralda." Knowlton (1900) initially described a fossil flora from the Esmeralda Formation. Berry (1927) and Axelrod (1940) continued work on flora of the Esmeralda Formation and considered it representative of early Pliocene age.

Early investigations by Spurr (1904, 1906) and Hance (1913) summarized the general geology and coal deposits north of the Silver Peak Range, which became known as the Coaldale district. Hance (1913) reported that the coal is confined mostly to four main horizons in sections 27, 28, 33, and 34, T. 2 N., R. 37 N., Mount Diablo Meridian. Hance (1913) described coal as being limited to four main beds: coal from the upper two having dull luster, and the lower two containing coal with a more vitreous, brilliant luster. Hance also noted the rather high amount of folding and faulting in these beds, making measurement of true stratigraphic thickness difficult. On the basis of mammalian fossils, Stirton (1932) correlated Esmeralda Formation lacustrine rocks of Fish Lake Valley with those of Cedar Mountain, north of the Monte Cristo Range.

During World War II, the U.S. Geological Survey and the U.S. Bureau of Mines conducted surface and some subsurface exploration and analyzed coal in the vicinity of Coaldale. These investigations suggest that coal is discontinuous laterally, due to faults, folds, local

igneous intrusions, and sporadic increases in shaly strata. Tests of coal by Toenges and others (1946) show a wide range in coal rank from lignitic shales to rare high volatile-A bituminous coal. These analyses revealed that the coal has a caloric value ranging from about 4,000 to 14,000 BTU, low sulfur content, and an ash content averaging 50 to 59 percent.

Ferguson and others (1953) mapped the geology of the Coaldale quadrangle, which includes the Monte Cristo Range, at a scale of 1:125,000. In that work, the Esmeralda Formation in the Monte Cristo Range was subdivided into a lower rhyolitic breccia unit and an upper sedimentary unit. The stratigraphy of the Esmeralda Formation and other Cenozoic rocks in the Silver Peak region has been described by Robinson (1964), Robinson and others (1968), and Moiola (1969).

Albers and Stewart (1965, 1972) mapped geology of Esmeralda County at scales of 1:200,000 and 1:250,000, respectively. Nearby published geologic quadrangle maps include those of Robinson and others (1976) and Stewart (1979). Recent work in the Candelaria Hills, by Speed and Cogbill (1979a-c), has provided a basis for comparison with some of the volcanic rocks and structures in the project area.

Geologic Time Scale Used

During the past 20 years, the geologic time scale has undergone numerous revisions, mostly on the basis of an ever-growing data base of radiometric ages and their application to the stratigraphic and fossil record. Most notably, the Miocene-Pliocene boundary used

with regard to much of the earlier published literature on the Esmeralda Formation has changed significantly. In this report, the Tertiary epoch boundaries correspond to 1980 U.S. Geological Survey standards (USGS, Geologic Names Committee, written commun., 1980). Informal geologic-time divisions "early", "middle", and "late" for the Oligocene and Miocene epochs are based upon definitions of Ryan and others (1974). Boundaries between North American Land Mammal Ages are based upon current USGS recommendations (C.A. Repenning and J.M. Armentrout, personal commun., 1979), which are in part derived or modified from Evernden and others (1964). In addition, most of the radiometric ages available for southwestern Nevada were done prior to the 1976 adoption of new decay and abundance constants for the calculation of potassium-argon ages (Steiger and Jager, 1977). Therefore, the potassium-argon ages referred to in this report have been recalculated using the conversion tables of Dalrymple (1979), and have been summarized in appendix A. Potassium-argon ages quoted in the text also have been recalculated, but referenced by original sources of the ages. The time scale adhered to in this report follows that illustrated in figure 3.

Period	Epoch	Informal Epoch Subdivision	North American Land Mammal Ages
Tertiary	Pliocene		Blancan
	5		
	Miocene	Late	Hemphillian
			8
			Clarendonian
		11.5	
			12
		Middle	Barstovian
			16
		16.5	
		Early	Hemingfordian
			21
			Arikareean
	24		
	Oligocene	Late	26
			Whitneyan
			29

Figure 3.--Late Cenozoic geologic time scale. Numbers on age boundaries are currently accepted estimates in millions of years before present, based on radiometric age dates. (Ryan and others, 1974; and U.S. Geological Survey, Geologic Names Committee, written commun., 1980).

Acknowledgments

I am grateful to David W. Andersen, Department of Geology, San Jose State University, for providing direction and helpful comment and advice throughout this investigation. I also thank William H. Lee, U.S. Geological Survey, Menlo Park, for his encouragement in the selection of this project and review of the manuscript, and Scott Creely, San Jose State University, for his time and useful suggestions during the preparation of the report.

I also express my gratitude to James R. Firby, Department of Geological Sciences, MacKay School of Mines, University of Nevada, Reno, for identification of molluscs; Charles A. Repenning, U.S. Geological Survey, Menlo Park, for a fossil mammal identification; to Richard M. Forester, U.S. Geological Survey, Denver, for ostracode identification; and to Gerald R. Smith, Museum of Paleontology, University of Michigan, for fossil fish identification. Miles L. Silberman, John H. Stewart, and Joseph R. Davis, all of the U.S. Geological Survey, Menlo Park, contributed useful comments during the project.

STRATIGRAPHY

Ordovician System

Palmetto Formation

The oldest rock unit in the mapped area is the Ordovician Palmetto Formation. Turner (1900, p. 265) originally named this formation on the basis of exposures in the Palmetto Mountains in southern Esmeralda County. The Palmetto Formation is widespread in Esmeralda County and dominantly consists of shale and siltstone with lesser amounts of interbedded chert and limestone. Locally, shale and siltstone are metamorphosed to hornfels. Interlayered quartzite also occurs in the Palmetto Formation, but it probably is limited to the basal 150 m (500 ft), according to Albers and Stewart (1972, p. 23).

Distribution, Contact Relations, and Thickness. Exposures of the Palmetto Formation in the southwestern and central Monte Cristo Range cover about 28 km^2. The Palmetto Formation is limited to exposures in the northern part and along the north-central boundary of the study area (pl. 1). The lower contact of the Palmetto Formation with older rock units is not exposed within the study area or in other parts of the Monte Cristo Range (Albers and Stewart, 1972, pl. 1). The Palmetto Formation is overlain, with angular unconformity, by the upper Oligocene or lower Miocene Castle Peak tuff.

Thickness of the Palmetto Formation is indeterminable from the extent of mapping in the study area. Limited exposures of the

Palmetto Formation within the study area typically are tightly folded and faulted and exhibit no consistent bedding from one outcrop to the next. Ferguson and others (1954) report a thickness of the Palmetto Formation greater than 1,200 m (4,000 ft) in Mineral County.

Lithology. In the southern Monte Cristo Range, the Palmetto Formation principally consists of thin-bedded chert interbedded with lesser amounts of phyllitic to hornfelsic, silicified shale (fig. 4). Outcrops appear rugged and dark. Exposures of the Palmetto Formation are dominated by black to medium-gray (N 5), 2- to 10-cm-thick beds of chert that commonly pinch out laterally over a few meters. Chert beds generally are weathered to yellowish gray (5Y 7/2) or moderate yellow (5Y 7/6). Interbedded phyllitic to hornfelsic shale, commonly a small percentage of each exposure, occurs in 1-to 2-cm-thick, fissile plates, which are medium gray (N 5) to medium dark gray (N 4). Chert beds typically are undulatory or tightly folded into small-scale folds.

Age and Correlation. No fossils were found within the Palmetto Formation in the study area. However, in other parts of Esmeralda County, abundant graptolites and the associated crustacean, Caryocaris sp., are indicative of a Middle Ordovician Age (Ross and Berry, 1963, p. 22-24; Albers and Stewart, 1972, p. 24). Although most fossil collections are representative of a Middle Ordovician age, Early and Late Ordovician age assemblages also are subordinately represented

Figure 4.--Folded, thin-bedded chert of the Ordovician Palmetto Formation at the northern end of the mapped area.

(Albers and Stewart, 1972, p. 24). In the western Silver Peak Range, Buckley (1971, p. 11) reported Early Ordovician graptolites in the lower Palmetto Formation. The exposures within the Monte Cristo Range can be correlated with the type locality in the Palmetto Mountains and other well-exposed areas throughout Esmeralda County.

Depositional Environment. The assemblage of rocks in the Palmetto Formation suggests relatively quiet, deep-water marine deposition. In the Silver Peak Range, the lower carbonate, higher clastic and chert content, and lack of sedimentary structures are suggestive of an off-shore marine facies (Buckley, 1971, p. 26). According to Buckley (1971, p. 26), this facies contrasts with a more shallow-water, transitional, platform section of Ordovician rocks found further westward in the Inyo Mountains, as described by Ross (1966), and in the Sierra Nevada.

Tertiary System

The Tertiary System in the southern Monte Cristo Range is late Oligocene or early Miocene to Pliocene(?). Correlations of units in the project area with units in adjacent and nearby areas of southwestern Nevada reveal that similar stratigraphy is also present on a more regional level (fig. 5).

Oligocene to Miocene Series

Castle Peak Tuff. In this report, rhyolitic tuffs of dominantly an ash-flow origin are included in and informally referred to as the

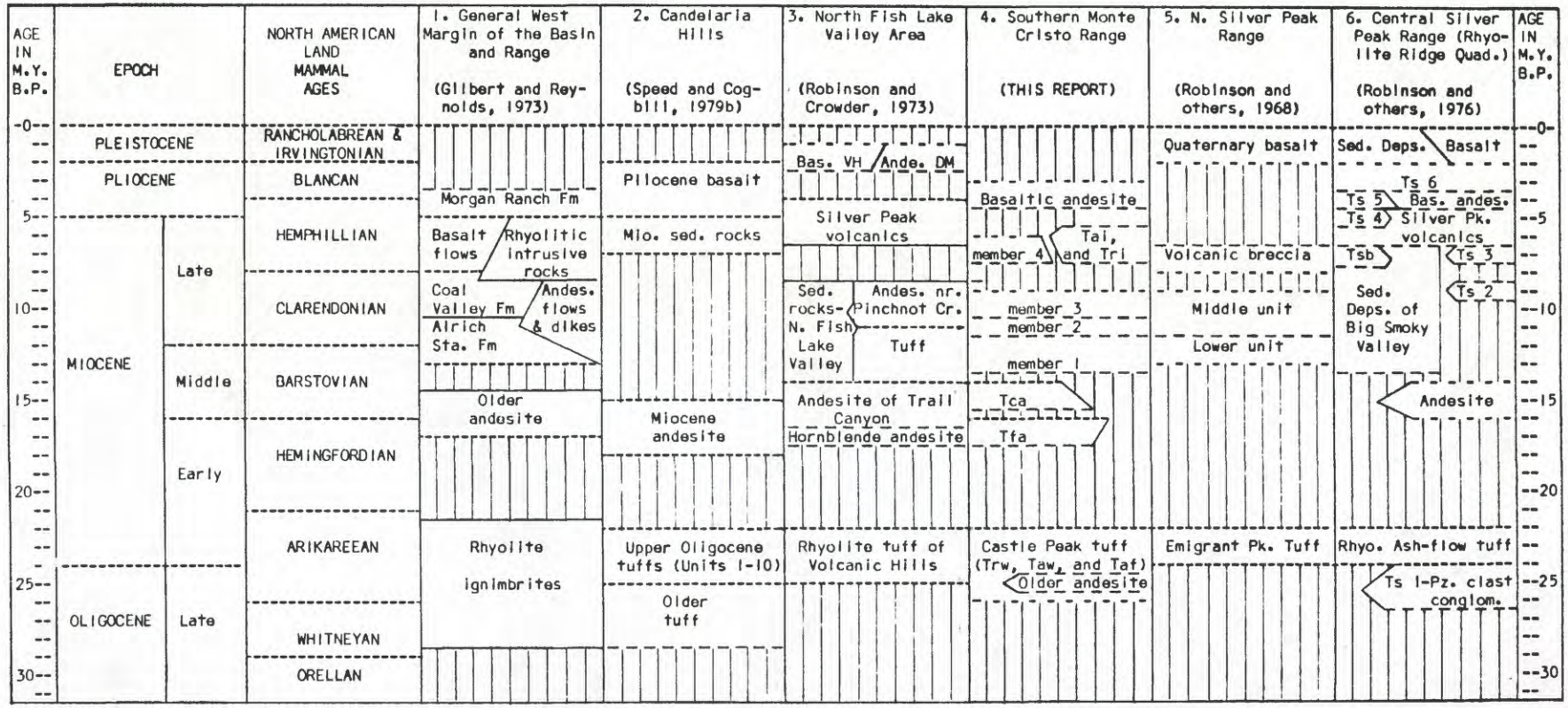

Figure 5.--Regional correlation of Cenozoic rocks (late Oligocene and younger; excluding Quaternary unconsolidated deposits) in selected areas of southwestern Nevada. Vertical lines indicate strata absent. Local unconformities are not shown. At area 3, Bas. VH= Basalt of Volcanic Hills; and Ande. DM= Andesite of Davis Mountain. At area 4 (project area), Tai= intrusive andesite; Tri= intrusive rhyolite; members 1 to 4= members of the Blair Junction sequence of the Esmeralda Formation; Tca= course-grained andesite; Tfa= fine-grained andesite; and Trw, Taw, and Taf= members of the Castle Peak tuff. At area 5, Volcanic breccia, Middle unit, and Lower unit= subunits of the Coaldale sequence. At area 6, Ts 1 to Ts 6= sedimentary units 1 to 6; Tsb= volcanic breccia; and Sedimentary Deposits of Big Smoky Valley include the Alum and Vanderbilt sequences of Moiola (1969), and Robinson and others (1968).

Castle Peak tuff, a name here introduced for exposures at Castle Peak, immediately east of the project area (fig. 6). Three distinct, informal members have been differentiated within the Castle Peak tuff: unwelded tuff member (Taf), white welded tuff member (Taw), and red welded tuff member (Trw). These three members comprise distinct zones within the Castle Peak tuff representative of different degrees of welding in an ash-flow tuff as documented, in the general case, by Smith (1960 a,b). The Castle Peak tuff crops out over much of the central and northern part of the project area (pl. 1).

The thickness of the Castle Peak tuff is apparently variable, dependent, in part, on the amount of local relief on the topographic surface over which it flowed. In the northern extreme of the project area, the exposed thickness of the tuff ranges from about 80 to 120 m. At one locality, the vertical succession consists of about 30 m of unwelded tuff conformably overlain by an erosion-resistant ledge of the white welded tuff that is 50 m thick.

Lithology of the Unwelded Tuff Member. The unwelded tuff member (Taf) is the most extensively exposed subunit of the Castle Peak tuff in the project area. This tuff is generally white (N 9) to very light gray (N 8) or light greenish gray (5G 8/1). Overall, the tuff is poorly sorted, poorly stratified, and thick. The unwelded tuff contains abundant pumice and locally is rich in lithic clasts. Although undifferentiated, the unwelded ash-flow tuff is composed of multiple flow units. Locally, the tuff displays a silicified, case-hardened effect on the surface. This localized surface silicification probably

Figure 6.--North-looking view of Castle Peak, which lies immediately east of the northern end of the mapped area. Erosion-resistant, white welded tuff member (Taw), which forms Castle Peak, overlies the unwelded tuff member (Taf) of the Castle Peak tuff.

is produced by release of silica from ash and redeposition as chalcedony or opal by evaporation at the surface or to fumarolic activity (Ross and Smith, 1961, p. 20). Pinnacles or conical erosional forms, characteristic of the unwelded tuff, evidently result from inequalities in the erosional pattern corresponding to the irregular distribution of the silicification (fig. 7).

In the northern extreme of the mapped area (pl. 1), the basal part of the unwelded tuff is well exposed. The lower 25 m, unconformably overlying the Ordovician Palmetto Formation, is relatively friable and easily eroded. The crystal-rich tuff contains about 20 percent phenocrysts of quartz, potassium feldspar, and minor biotite. This mineralogy is confirmed both by thin section and X-ray diffraction analysis of a representative bulk sample (Taf, table 1). No flattening of pumice fragments is evident. Notable in the basal 20 m of the tuff are angular and unsorted lithic clasts, mostly of black chert, which average 5 to 10 cm in diameter and range up to 20 cm. Lithic clasts constitute about 3 percent of the basal 20 m of the tuff. The succeeding 5 m of the unwelded white tuff is progressively compacted upward and becomes partially welded below the sharp contact with the white welded tuff member (Taw). Near the contact the tuff locally shows strongly flattened vesicles and is appreciably denser than tuff at the base.

Included and undifferentiated within the unwelded tuff are local, thin-bedded and planar-crossbedded lapilli tuffs of probable air-fall origin. These tuffs, although distinctive because of

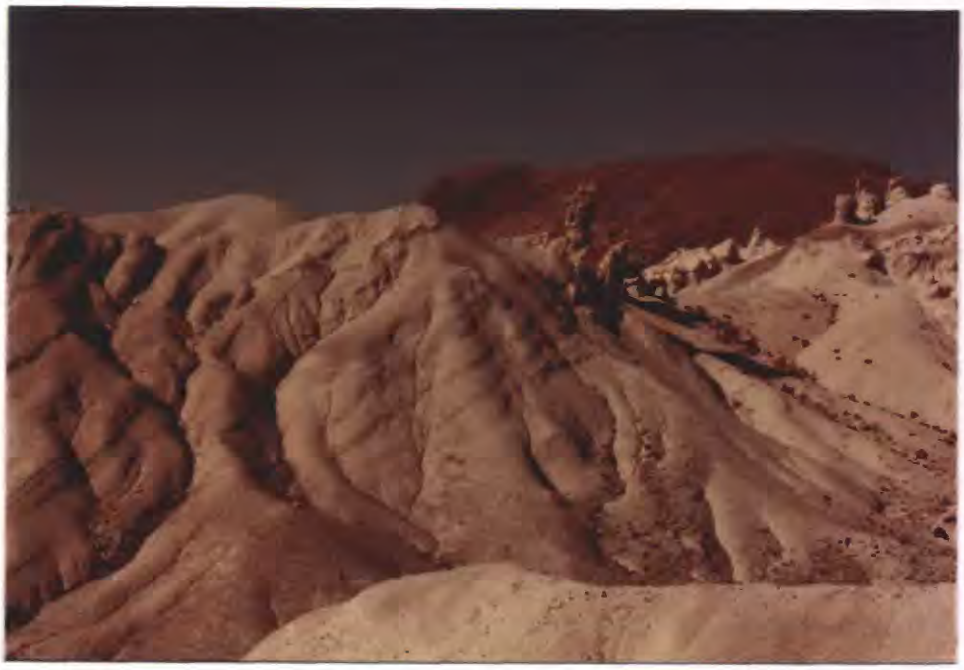

Figure 7.--Unwelded member (Taf) of the Castle Peak tuff, on right, overlain by bedded air-fall tuff, on left. Note prominent erosional pinnacles in the ash-flow tuff. This view is located in the central part of the mapped area, 1.2 km northeast of Dragonback Hills.

MAP UNIT	SAMPLE NUMBER	LITHOLOGY	MAJOR MINERALS IDENTIFIED BY X-RAY DIFFRACTION																
			Albite	Biotite	Calcite	Clinoptilolite	Clinopyroxene	Erionite	Glass	Gypsum	Halite	Hornblende	Hypersthene	Montmorillonite	Opal-CT	Plagioclase	Potassium Feldspar	Quartz
----Blair Junction sequence of the Esmeralda Formation----------																			
Member 3	C-4	limestone			1													2
	C-8le	tuff							1									
	C-113e	tuffaceous, silty sandstone					2										3	1
	C-113e'	efflorescent coating and fracture filling									1							
	C-117	tuff		2		4							6	5			3	1
	C-120c	siliceous siltstone															2	1
	C-171b	tuff														3	2	1
	C-197b	silicified tuff															2	1
	C-297	siliceous sandstone															2	1
	C-339	tuff							1									
Member 2	C-44b	sandstone	3														2	1
	C-50	sandstone														3	2	1
Member 1	C-2c	limestone			1													2
	C-2d	altered tuff		2										1		4	3	
	C-60a	carbonaceous altered tuff												2	1			
	C-64b	efflorescent coating									1							
	C-66b	papery shale							4					3	1			2
	C-70a	papery shale							3						1			2
	C-70d	tuffaceous claystone												1	2			
	C-70e	tuffaceous sandstone														3	2	1
	C-70e'	secondary coating and fracture filling								1								
	C-243a	silicified wood																1
	C-279	carbonaceous shale												1	2		3	
	C-280	carbonaceous claystone						4						1	3		2	
	C-359	tuffaceous siltstone										3		4	1		2	
	C-384	sandy limestone			1													2
-------Volcanic Rocks of other Units--------																			
Tba	C-14a	basaltic andesite		2									3			1		
Tai	C-13a	andesite										2				1		
Tfa	C-14b	andesite										2				1		
Toa	C-14c	andesite										2	3			1		
Toa	C-55b	altered andesite					3					2				1		
Trw	C-198	welded rhyolite tuff		3													2	1
Trw	C-265b	welded rhyolite tuff														3	2	1
Trw	C-352	jasperoid breccia																1
Taw	C-90	welded rhyolite tuff															2	1
Taf	C-29a	unwelded rhyolite tuff		3													2	1

Table 1.--Samples analyzed by X-ray diffraction. Bulk samples of rocks were ground to fine powder, smear slides were prepared, air-dried, and then exposed to nickel-filtered copper radiation. Numbers shown on chart represent a qualitative estimate of major mineral abundance (1= most abundant mineral).

prominent bedding, have not been mapped separately because of the tuffs' local extent and common truncation by faults, commonly with neither top nor bottom of the bedded section exposed. In one locality near measured section SS III (fig. 14), the bedded tuff conformably overlies the unwelded ash-flow tuff (fig. 7). Individual layers of poorly sorted lapilli tuff, 5 to 30 cm thick, typically pinch out or are crossbedded with similar layers over a distance of a few meters. Partially flattened lapilli-sized pumice, 2 to 5 cm long, constitute up to 30 percent of the beds, with the remainder being ash. Where exposed, the tuff above the layered, air-fall lapilli tuff is the more common, unsorted and unbedded ash-flow tuff like that below the air-fall tuff. The air-fall tuff represents a break in ash-flow tuff deposition, and is interpreted to be a break between different major flow units.

The unwelded rhyolite tuff (Taf) member, is the most areally extensive and is stratigraphically thickest of the three members. Where observable, the unwelded rhyolite tuff can be seen to lie with angular unconformity over the Ordovician Palmetto Formation. The erosional surface, upon which the tuffs were deposited, was highly irregular, attested to by the irregular contact of the tuffs with the Palmetto Formation. Also, several scattered knobs of Palmetto Formation are completely surrounded by the tuff.

Lithology of the White Welded Tuff Member. The white welded tuff member (Taw) is informally named for its light color, which is generally white (N 9) to very light gray (N 8) on fresh surfaces,

and pinkish gray (5YR 8/1) or yellowish gray (5Y 8/1) on more weathered surfaces. The white welded tuff member forms a hard, erosion-resistant ledge, 10 to 50 m thick, which typically displays prominent, fairly well-formed columnar joints or other closely spaced vertical joints (fig. 8). Columns are irregular in cross section and range in diameter from about 0.5 to 1.5 m. Where columnar joints are absent, closely spaced near-vertical to vertical joints transect the welded tuff.

In hand specimen, the white welded tuff shows many features distinctive of a strongly welded ash-flow tuff. Although textural detail varies from place to place within the welded tuff, a typical sample of this unit shows common white, flattened, coarse ash- to lapilli-sized pumice fragments, which constitute about 7 to 15 percent of the rock. Flattening of the pumice is parallel to the plane of compaction of the ash flow, as indicated by cross-sectional elongation of individual lapilli-pumice fragments, which are 3 to 6 times larger than they are thick. Another megascopic property of these welded tuffs is the presence of clear, medium-grained quartz and sanidine phenocrysts, 1 to 5 mm in diameter, which comprise about 10 to 15 percent of the rock. A virtual elimination of all pore s]ace within the rock has occurred due to the complete welding and collapse of pumice fragments.

Analysis of several thin sections of this unit confirm that this rock is a strongly welded, rhyolitic crystal tuff. A representative thin section includes 10 percent quartz and 15 percent sanidine

Figure 8.--Columnar joints in white welded tuff member (Taw) of the Castle Peak tuff. Outcrop is located in the northern part of the mapped area, 0.75 km southwest of the northernmost fork in Gilbert Road. Height of the welded tuff outcrop is about 15 m.

phenocrysts with 8 percent coarse-ash- to small-lapilli-sized, collapsed pumice fragments. Phenocrysts and pumice fragments are within a vitroclastic groundmass composed of highly flattened, parallel glass shards and glass dust. Glass shards are easily recognizable by their curved or cuspate outlines, which represent fragmented walls of bubbles within the ash flow (Ross and Smith, 1961, p. 32). Quartz and feldspar phenocrysts typically are anhedral to subhedral and embayed, or resorbed. Some thin sections show well-developed, parallel, axiolitic, microcrystalline intergrowths of feldspar and cristobalite. These axiolites, which are products of devitrification, commonly are molded against phenocrysts or shaped around relict glass shards. Radial aggregates of feldspar and cristobalite occur in some thin sections. These microcrystalline intergrowths are best developed within the outlines of pumice fragments.

The white welded tuff represents a zone of strong welding, which lies conformably above unwelded tuff in the northern project area. The overall appearance of the lower contact between the unwelded and the welded tuff is extremely sharp and well defined (fig. 6).

Lithology of the Red Welded Tuff Member. The red welded tuff member (Trw) is differentiated from the other subunits of the Castle Peak tuff on the basis of a pervasive reddish color, a generally higher degree of welding than that of the other subunits, and a large amount of textural inhomogeneity. The red welded tuff ranges in

color from moderate orange pink (10R 7/4) to pale red (5R 6/2). Exposures typically are well jointed, displaying irregular, nearly vertical jointing patterns.

The red welded tuff displays a large amount of textural inhomogeneity, ranging from a phenocryst-rich, porphyritic texture to a strongly eutaxitic texture. In thin section, the groundmass is strongly vitroclastic, containing well-preserved, although moderately flattened to well-flattened, spindle- and cusp-shaped glass shards. Most glass shards are devitrified to microcrystalline aggregates of minute cristobalite and potassium feldspar crystals. In a representtative thin section, the rock is composed of about 35 percent phenocrysts. The rock contains 20 percent quartz, 12 percent sanidine, and 3 percent biotite phenocrysts. Quartz and sanidine phenocrysts generally are subhedral, with embayed outlines and have diameters of 0.5 to 3.0 mm. Up to 10 percent angular lithic fragments of rhyolitic tuff also are present in most samples. Secondary hematite and goethite constitute 2 to 3 percent of the rock, accounting for the overall reddish color of the rock.

The eutaxitic textural variant of this rock unit is characterized by extremely flattened and bleached, very-light-gray (N 7) pumice fragments, which generally are lapilli-sized and range from 0.5 to 4 cm long (fig. 9). Individual, compacted lapilli-sized pumice fragments typically are disc shaped and flattened uniformly in the subhorizontal plane of compaction. Flattened pumice constitutes 20 to

Figure 9.--Eutaxitic texture in the red welded tuff member (Trw) of the Castle Peak tuff. Locality is 0.75 km south of Castle Peak. Hammer handle is about 0.3 m long.

35 percent of the rock, within a highly devitrified, vitroclastic groundmass displaying strongly flattened and deformed glass shards.

The contact relationships of the red welded tuff are somewhat ambiguous. This unit is exposed in the central part of the map area where it crops out as small, separate erosional remnants of a once more continuous unit. Individually, erosional remnants of the red welded tuff form resistant caps over underlying unwelded tuff. However, immediately east of the mapped area, south of Castle Peak, the red welded tuff is areally more extensive and lies directly above the white welded tuff. Because of these seemingly incongruent contact relationships, the red welded tuff is interpreted to grade laterally into the white welded tuff, in the mapped area. South of Castle Peak, the gradation between these units is vertical. This interpretation is supported both by the similar mineralogy of the two welded tuffs, and by the textural inhomogeneity of the red welded tuff, which seems consistent with a gradational relationship. However, lateral gradation between the two welded tuff units is difficult to demonstrate because of a lack of exposures of either unit over a distance of about 3 km between the north and central parts of the mapped area.

Age and Correlation. The Castle Peak tuff is assigned an age of latest Oligocene or earliest Miocene. These rocks were previously considered as Pliocene, and were included as a basal rhyolite breccia member of the Esmeralda Formation by Ferguson and others (1953).

However, a late Oligocene or early Miocene age is here inferred from the unconformable relationship of the Castle Peak tuff under both the middle Miocene member 1 of the Blair Junction sequence of the Esmeralda Formation and middle Miocene andesite flows.

Although no radiometric ages are yet available for the Castle Peak tuff, a late Oligocene or early Miocene age is inferred from lithologic and stratigraphic correlations with radiometrically dated units in adjacent areas (fig. 5; app. A). Radiometrically dated rhyolitic ash-flow tuffs in adjacent mountain ranges span ages from about 22 to 28 m.y. B.P. (app. A, numbers 33 to 43). In the Candelaria Hills, a thick succession of similar rhyolitic ash-flow tuffs is well exposed. These tuffs were described by Page (1959) and more recently described by Speed and Cogbill (1979b), who describe them as the "upper Oligocene tuffs" of the Candelaria Hills. Potassium-argon ages ranging from 22.0±0.9 to 25.4±0.8 m.y. have been obtained for the "upper Oligocene tuffs" (Marvin and others, 1977; app. A, numbers 33, 37, 39, and 41). On the basis of descriptions of 10 subunits of the "upper Oligocene tuffs" by Speed and Cogbill (1979b) and brief reconnaissance in the Candelaria Hills, the Castle Peak tuff appears to be lithologically similar and is probably in part correlative with these tuffs. Other correlative rhyolite tuffs west of Miller Mountain have potassium-argon ages of 22.6±0.4 and 22.7±0.3 m.y. (Gilbert and others, 1968; app. A, numbers 35 and 36). A rhyolitic welded tuff at the north end of

the Silver Peak Range unconformably underlies the Esmeralda Formation and is named the Emigrant Peak Tuff by Moiola (1969). This tuff has a potassium-argon age of 22.1±1.0 m.y. (Robinson and others, 1968; app. A, no. 34) and is stratigraphically and lithologically equivalent to the Castle Peak tuff. Similar age ash-flow tuffs also occur in the Volcanic Hills, and on the southeast flank of Miller Mountain where a potassium-argon age of 23.4±1.0 m.y. has been obtained (Robinson and others, 1968; app. A, no. 38).

A somewhat older and regionally extensive sequence of ash-flow tuffs has been described by Ekren and others (1980), in the Gabbs Valley and Gillis Ranges, northwest of the Monte Cristo Range. These tuffs include tuffs in the Benton Spring Group and the Tuff of Gabbs Valley, which range in age from about 24 to 28 m.y. (Ekren and others, 1980, p. 12-14). Correlative rocks may exist in northwestern flanks of the Monte Cristo Range, as suggested by the distribution of the "older tuff" of Speed and Cogbill (1979b). Although the lack of radiometric ages in the Castle Peak tuff does not rule out the possible equivalence with the "older tuff" or the tuffs of the Gabbs Valley and Gillis Ranges, lithologic and stratigraphic correlation with the younger, "upper Oligocene tuffs" seems most likely.

Mode of Deposition. With the exception of local, undifferentiated, bedded lapilli tuff in the unwelded tuff member (Taf), the Castle Peak tuff is interpreted as an ash-flow tuff. An ash-flow tuff results from a nuee ardente, or glowing avalanche of turbulent

gas and pyroclastic materials, which was explosively ejected from a crater or fissure, at high temperatures, and traveled swiftly down the slopes of a volcano along the ground surface (Ross and Smith, 1961, p. 3). An ash-flow origin for the Castle Peak tuff is supported by the following characteristics: massive, unsorted, and unbedded nature; the presence of distinct zones of welding and compaction; columnar joints and pinnacle-like conical erosional forms; pumice fragments and glass shards showing distortion, stretching, and eutaxitic textures due to welding and compaction; and presence of features suggesting devitrification.

The Castle Peak tuff is interpreted as essentially a simple cooling unit as defined by Smith (1960b). The three members of the tuff represent zones of varying degrees of welding. The welded tuffs are interpreted as stratigraphic equivalents, one grading into the other laterally over distance, in the mapped area. This lateral gradation, as well as the relatively sharp transition upward from the white welded tuff to the red welded tuff, south of Castle Peak, can be explained by large local variations in welding temperature or in duration of welding. These variations could have been caused by large local differences in thickness of the ash flow due to flowage over a locally irregular surface, as is indicated by the basal unconformity of the Castle Peak tuff. Local, bedded, pumice-rich tuff found stratigraphically high in the unwelded tuff member is interpreted as air-fall tuff, which constitutes a break between different flow units, and possibly represents the top of the the cooling unit.

Older Andesite. The older andesite is mapped at Dragonback Hills (fig. 10). This unit was previously included in the Gilbert Andesite by Ferguson and others (1953). Exposures at Dragonback Hills reveal that the older andesite locally overlies the Castle Peak tuff with apparent conformity. Elsewhere, the younger flow units of unwelded Castle Peak tuff contain clasts that are lithologically similar to the older andesite flows. These geologic relationships suggest that the older andesite is in part contemporaneous with the Castle Peak tuff. Older andesite flows at Dragonback Hills reach a maximum thickness of about 50 m, with individual flows averaging about 5 to 10 m thick. Bases of flows typically are marked by poorly sorted, volcanic breccia and agglomerate.

Lithology. The older andesite flows differ from other andesites in the project area in color, texture, and in having a higher degree of weathering. The older andesite varies from greenish gray (5G 6/1) to a more bleached, grayish orange pink (5YR 7/2). The older andesite is porphyritic with an aphanitic groundmass. In thin section, the groundmass is hyalopilitic and is composed mostly of brown glass and microcrystalline material. In most samples, phenocrysts constitute 30 to 35 percent of the rock. A representative thin section contains 25 percent euhedral phenocrysts of zoned plagioclase 0.4 to 1.6 mm long. Other phenocrysts include 4 percent short, prismatic augite phenocrysts and 3 percent small, oxidized hornblende phenocrysts. The groundmass consists of 20 percent plagioclase microlites within

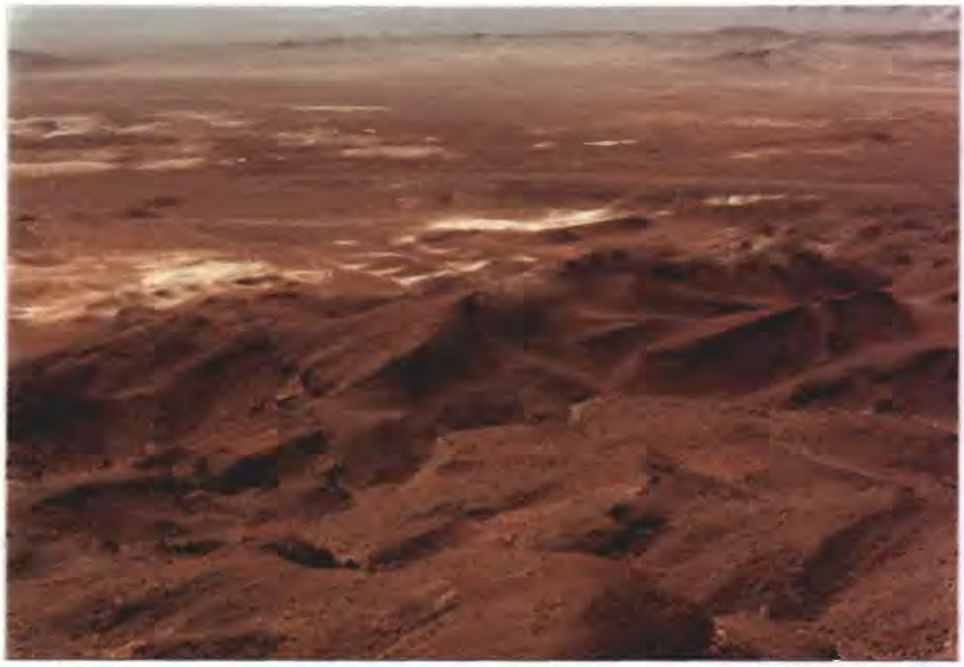

Figure 10.--Dark flows of older andesite unit (Toa) at Dragonback Hills. View is southwest. The white unit in the middle distance is member 3 of the Blair Junction sequence of the Esmeralda Formation.

altered, interstital glass. Secondary minerals include 3 percent magnetite and hematite, with 1 percent sericite.

Age and Correlation. The older andesite is assigned a late Oligocene or possibly early Miocene age on the basis, in part, of the conformable relationship of older andesite flows over the the Castle Peak tuff. However, the occurrence of pebbles of apparent older andesite within the uppermost unwelded portions of the Castle Peak tuff suggests that the older andesite is older than, or in part contemporaneous with some of the upper, unwelded flow units of the Castle Peak tuff. Clasts of similar andesite which appear in unit 6 of the "upper Oligocene tuffs" of the Candelaria Hills (Speed and Cogbill, 1979b) may be correlative. In addition, a potassium-argon date of 24.7±0.7 m.y. (Morton and others, 1977; app. A, no. 40) has been obtained from a stratigraphically correlative andesite on the east side of the Pilot Mountains. The older andesite unit may also be correlative with andesite underlying rhyolitic ash-flow tuffs southwest of Gilbert, and andesite described as "pre-Esmeralda lavas" by Ferguson (1927, p. 131-133).

Miocene Series

Miocene Andesite Flows. Two mineralogically similar, but texturally distinct, andesites of Miocene age and older than the Esmeralda Formation are distinguished in the project area. Both andesites occur as flows in the northern half of the project area (pl. 1). These flows are not restricted to the project area, but appear to be

quite extensive throughout the rest of the Monte Cristo Range, on the basis of reconnaissance and aerial photograph interpretation. Voluminous andesite flows in the Monte Cristo Range all were previously mapped as the Gilbert Andesite, as named by Ferguson and others (1953). As described by Ferguson and others (1953), the Gilbert Andesite consists of andesitic flows, agglomerates, and minor basalt that cover the crest of the Monte Cristo Range with a composite thickness of 150 to 300 m (500 to 1000 ft). In the project area, two andesites that compose the bulk of the Gilbert Andesite, as previously mapped, are differentiated. These two andesites are distinguished mainly on grain size and color and are informally referred to in this report as the "fine-grained andesite" and the "coarse-grained andesite."

Lithology of the Fine-grained Andesite. The fine-grained andesite (Tfa) is the stratigraphically lower of the two andesites. The fine-grained andesite lies unconformably above the Castle Peak tuff (fig. 11). The cumulative thickness of fine-grained andesite flows in the project area varies from about 40 to as much as 190 m. Individual flows may be as thin as 5 m.

Although porphyritic, the fine-grained andesite is named for its groundmass that consists of crystals less than 1 mm in diameter. The overall color of the fine-grained andesite is light gray (N 7) where fresh, or pale red (10YR 6/2) where more weathered. The fine-grained groundmass is interrupted by conspicuous phenocrysts of weathered and oxidized hornblende needles that constitute 5 to 10 percent of the rock. In thin section, phenocrysts of hornblende are strongly

Figure 11.--Fine-grained andesite (Tfa) overlying the unwelded tuff member (Taf) of the Castle Peak tuff. Locality is adjacent Gilbert Road in the northern part of the mapped area.

alined parallel to the direction of flow and are 0.5 to 4 mm in length. A typical thin section of fine-grained andesite is composed of 7 percent euhedral to subhedral hornblende phenocrysts with a pliotaxitic groundmass of euhedral, subparallel plagioclase laths 0.2 mm or less in length, hornblende microlites, and interstitial cryptofelsite and glass. Plagioclase in the groundmass ranges in composition from An_{40} to An_{55}. Secondary minerals, hematite and magnetite, occur as rims around hornblende crystals or as total replacements of smaller crystals, and account for 4 to 6 percent of the rock composition.

Lithology of the Coarse-grained Andesite. The coarse-grained andesite (Tca) is mineralogically similar to the fine-grained andesite. Where the base of the unit is exposed, a basal agglomerate or volcanic breccia, 3 to 5 m thick, unconformably overlies either the fine-grained andesite or lies directly on Castle Peak tuff (fig. 12). The basal volcanic breccia is typically monolithologic, composed of 70 to 80 percent, angular, lapilli- to block-sized clasts of coarse-grained andesite in a matrix of comminuted andesite and tuffaceous material.

The coarse-grained andesite ranges from medium light gray (N 6) to a more weathered pale red (5R 6/2). The most distinctive characteristic of this andesite is the abundance of large, lath-shaped light-colored plagioclase phenocrysts that sharply contrast with the darker groundmass. Plagioclase phenocrysts are generally 2 to 6 mm long and and are euhedral to subhedral. In thin section the coarse-grained andesite has a porphyritic texture dominated by large, twinned

Figure 12.--Basal breccia of the coarse-grained andesite (Tca). Staff is 1.5 m long. Photograph taken at a locality along the west side of Gilbert Road, about 6 km north of intersection with U.S. Highway 6/95.

plagioclase phenocrysts, with less abundant, euhedral hornblende phenocrysts. An average mineral composition determined from thin sections includes 20 percent plagioclase phenocrysts and 15 percent hornblende phenocrysts. The plagioclase is andesine, which ranges from An_{37} to An_{47}. The groundmass is pilotaxitic and is composed of 38 percent plagioclase microlites, 6 percent hornblende and augite, with the remainder composed of brown glass and interstitial cryptofelsite. Magnetite occurs as a secondary mineral in the groundmass and constitutes about 5 percent of the rock.

Age and Correlation. The age of andesites in the Monte Cristo Range is not well known. Ferguson and others (1953) considered the Gilbert Andesite to be younger than the Esmeralda Formation and Pliocene in age. This age assignment mostly was based on the topographically high position of the andesites at the crest of the Monte Cristo Range, the absence of overlying units with the exception of Quaternary or Tertiary basalt, and the stratigraphic position over what Ferguson and others (1953) considered the "lower pyroclastic unit" of the Esmeralda Formation.

The results of this study and recent radiometric dating of andesitic rocks in the Monte Cristo Range, however, indicate that most of the Gilbert Andesite is older than the Esmeralda Formation and is of middle Miocene age. Mapping in the project area suggests that andesite of at least four general ages is present, the oldest being the previously discussed older andesite unit. The fine-grained

andesite and the coarse-grained andesite, although separated by an erosional unconformity, are interpreted to be relatively close in age because of the mineralogic similarity and close stratigraphic association. Potassium-argon ages obtained from Gilbert Andesite in the Monte Cristo Range have been reported as 15.5±0.5 m.y. (Silberman and others, 1975; app. A, no. 29) and 15.5±0.6 m.y. (Albers and Stewart, 1972; app. A, no. 30). A thin section of the sample (GL-2), which was radiometrically dated by Silberman and others (1975), was examined and found to be similar to the coarse-grained andesite of the project area. Also similar is the stratigraphic position of this dated sample, and the fine-grained and coarse-grained andesite units above the upper Oligocene-lower Miocene Castle Peak tuff. In addition, weathered, rounded clasts of these andesites are found in conglomerates of member 1 of the Blair Junction sequence of the Esmeralda Formation. On the basis of preceding evidence, the fine-grained and coarse-grained andesites are assigned a middle Miocene, or early Barstovian age.

Andesites of middle Miocene age are particularly common in adjacent areas of western Nevada (fig. 5). Andesite in and adjacent to the Candelaria Hills has yielded potassium-argon ages of 16.1±0.5 and 17.9±0.6 m.y. (Marvin and others, 1977; app. A, numbers 31 and 32). These andesites overlie the upper Oligocene tuffs of Speed and Cogbill (1979b). The "older andesite" of Gilbert and Reynolds (1973), north of Coal Valley, has a potassium-argon age of 15.3±0.5 m.y. (app. A, no. 26). The andesites of Mt. Ferguson and Stewart Valley,

north of the Monte Cristo Range, both have a potassium-argon age of 15.4±0.5 m.y. (Morton and others, 1977; app. A, numbers 27 and 28). Also, other undated andesitic rocks of the Fish Lake Valley area and in the central Silver Peak Range underlie the Esmeralda Formation (Robinson and Crowder, 1973; Stewart and others, 1974; fig. 5). Descriptions and stratigraphic position of andesitic rocks in the Red Mountain Mining District of the Silver Peak Range (Keith, 1977) are also similar to that of the andesitic rocks in the mapped area.

Esmeralda Formation--Blair Junction Sequence. In this report, four informal, local lithostratigraphic members have been described and mapped separately in Tertiary sedimentary rocks of the Esmeralda Formation. Herein, these four members are collectively and informally designated the "Blair Junction sequence" of the Esmeralda Formation. Ferguson and others (1953) mapped these sedimentary rocks as the "upper sedimentary unit" of the Esmeralda Formation. The Esmeralda Formation as defined by Turner (1900, p. 198) includes lacustrine shale, marlstone, and sandstone, with local breccia and conglomerate. Turner's type section of the Esmeralda Formation is located at the coal mines at the north end of the Silver Peak Range and continues eastward, interrupted by the Big Smoky Valley, to the Alum area in the Weepah Hills. Turner further included other lithologically similar exposures of rock throughout much of the Silver Peak region (Turner, 1900, Pl. XXIV).

Owing to general lithologic and interpreted paleoenvironmental similarities, the term "Esmeralda Formation" has been used regionally over much of southwestern Nevada by many authors (for example, Berry, 1927; Van Houten, 1956). Widespread use of the term Esmeralda Formation and inclusion of interbedded volcanic units, such as by Ferguson (1924, p. 133) and Ferguson and others (1953), has led to confusion and overgeneralization of the term far beyond Turner°s original definition. More recent detailed studies and the application of radiometric dating to Cenozoic rocks in western Nevada (Evernden and others, 1964; Evernden and James, 1964; Robinson and others, 1968; Gilbert and Reynolds, 1973) have demonstrated a need for local distinction or a discontinuation of use of the term Esmeralda Formation. Therefore, in this report, the use of the term Esmeralda Formation conforms approximately with the usage of Robinson and others (1968, p. 581-582), Moiola (1969, p. 23), and Albers and Stewart (1972, p. 34).

The term Esmeralda Formation is used to designate predominately tuffaceous sedimentary rocks at or near the type locality of Turner (1900, p. 199-202) at the southern end of Big Smoky Valley. In this report, the "Blair Junction sequence" of the Esmeralda Formation is defined as a discrete local assemblage of informal lithostratigraphic members of the Esmeralda Formation. Areally, the Blair Junction sequence, as herein described, lies in and is limited to the southern half of the Blair Junction 7.5-minute quadrangle (fig. 2; pl. 1).

This use of the term "sequence" corresponds to the use of Robinson and others (1968). Different sequences of the Esmeralda Formation contain similar lithologies, but each is distinct from the others in specific stratigraphic succession and detail.

The Blair Junction sequence of the Esmeralda Formation consists of 3 sedimentary members and 1 volcanic breccia and sandstone member. Members are numbered 1 through 4, in ascending stratigraphic order. Numbers are given to each member for ease of reference since each member is composed of a combination of lithologies. Dominant characteristic lithologies of these members are: member 1--claystone, carbonaceous to lignitic shale, and tuff, with minor limestone, conglomerate, and sandstone; member 2--volcaniclastic sandstone and siltstone; member 3--siliceous siltstone, coarse-grained arkosic sandstone, and tuff, with minor shale, granule conglomerate, and limestone; member 4--volcanic breccia with interbedded sandstone.

Distribution and Thickness. The Esmeralda Formation in the study area crops out discontinuously from the north base of the Silver Peak Range, northeastward towards the southern Monte Cristo Range, and eastward towards the southern end of Big Smoky Valley. Informal members 1 to 4 of the Blair Junction sequence of the Esmeralda Formation crop out in the southern 60 percent of the mapped area (pl. 1).

The thickness of the Blair Junction sequence of the Esmeralda Formation was determined by a composite of measured sections SS I through SS IV (fig. 13; app. B). Owing to extensive faulting and

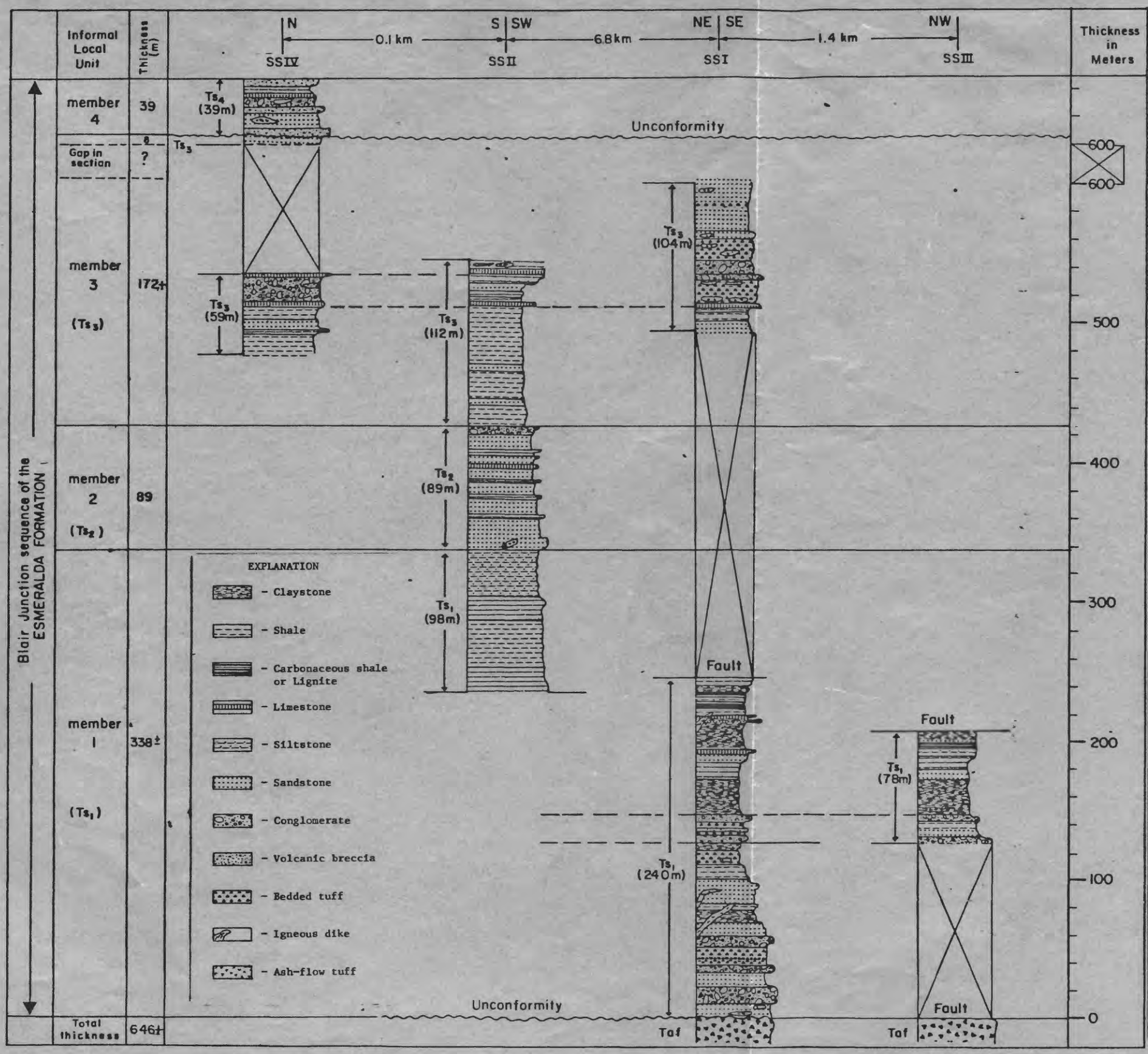

Figure 13.—Correlation of measured stratigraphic sections SS I through SS IV.

incomplete exposure, continuous, uninterrupted stratigraphic section was not measurable. However, by the use of distinctive, fossil-rich limestone beds, lignitic shale horizons, tuff beds containing silicified wood, and similar conglomerate intervals, the four overlapping measured sections can be lithologically correlated (fig. 13, 14). A composite of the measured sections SS I through IV reveals a minimum thickness of 646 m for the Blair Junction sequence of the Esmeralda Formation. The vertical stratigraphic succession determined for the Blair Junction sequence and that of the adjacent Coaldale sequence of Robinson and others (1968, p. 589) and Moiola (1969, p. 72-75) are closely comparable in lithology and probably are equivalent as shown in figure 15. However, the Blair Junction sequence as measured is apparently thinner.

Because of structural complexities, the thickness of the Esmeralda Formation at its type locality has been disputed. Turner (1900) reported a minimum thickness of 690 m (2250 ft) at the type locality of the Esmeralda Formation at the north end of the Silver Peak Range. However, Turner did not measure the entire exposed thickness. Instead, he correlated beds east across Big Smoky with those at Weepah Hills (Alum area) and continued measurement stratigraphically upward, resulting in a superposed stratigraphic sequence with a combined thickness of about 4500 m (14,800 ft). Robinson and others (1968), and Moiola (1969), extended the measurement of section at the northern Silver Peak Range locality and report a thickness of about 930 m (3050 ft) for the Coaldale sequence. The net difference in thickness

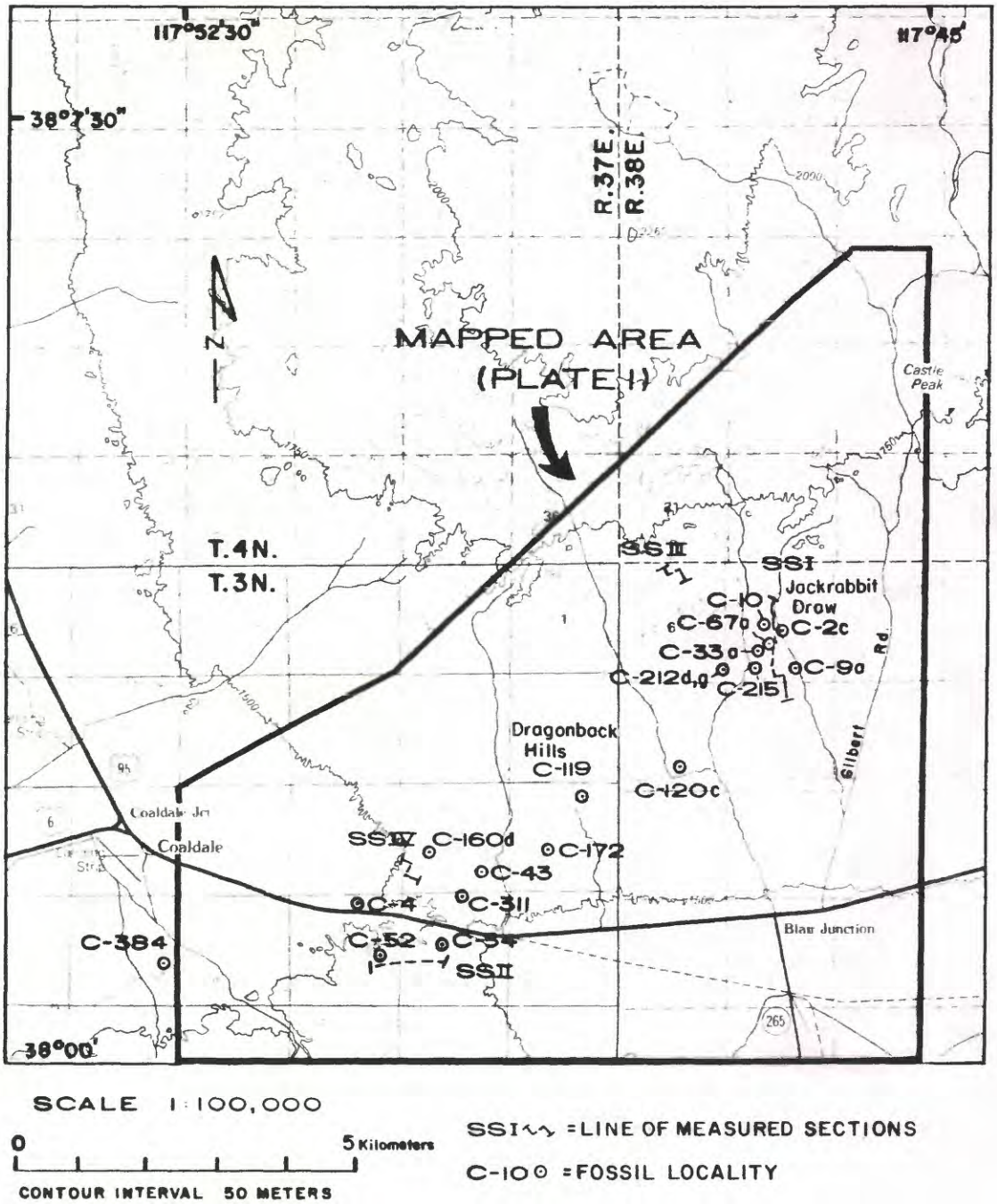

Figure 14.--Map showing locations of measured sections and fossil localities discussed in text.

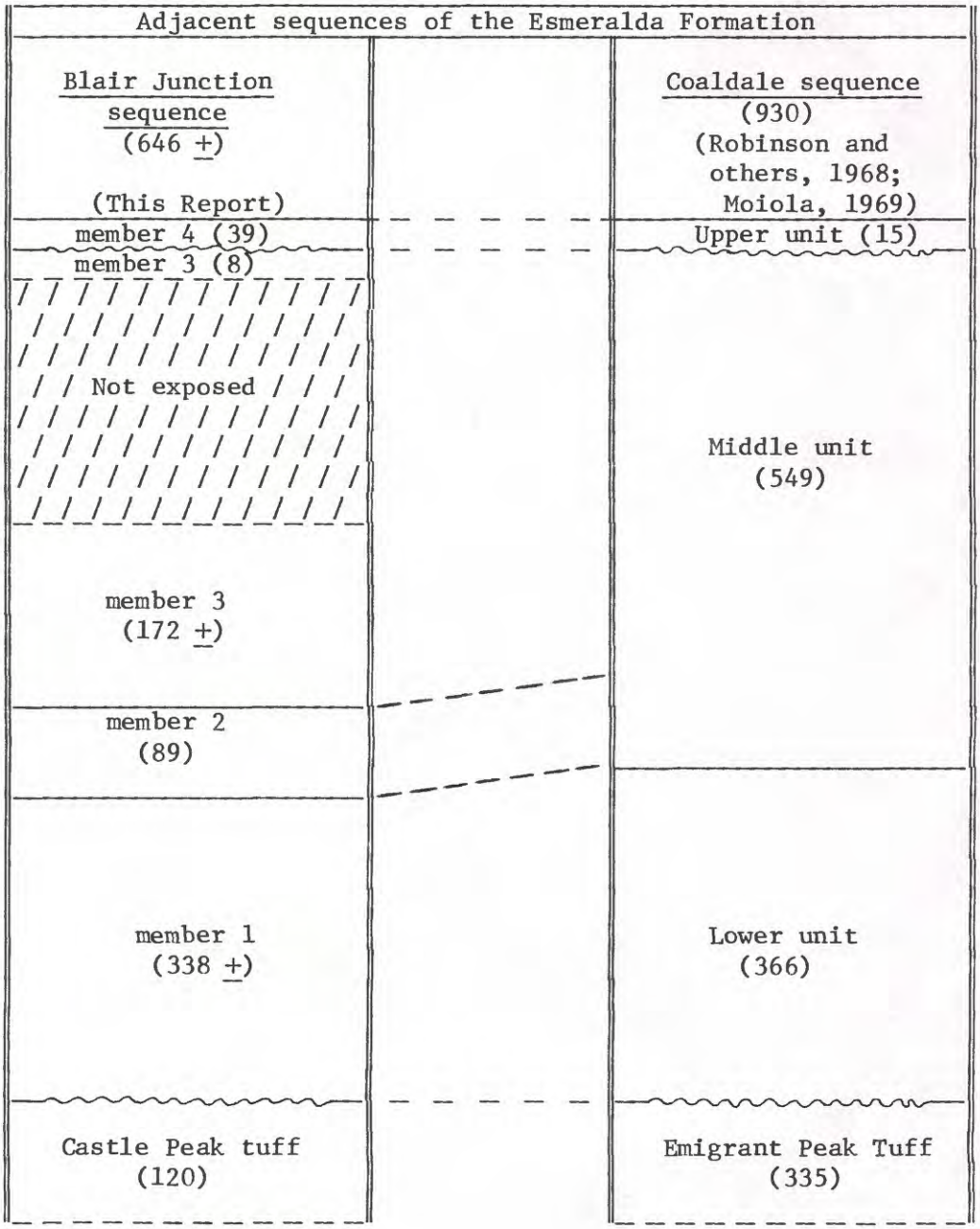

Figure 15.--Correlation of the Blair Junction and Coaldale sequences of the Esmeralda Formation. Relative thicknesses are shown in meters.

between the correlative Coaldale sequence and Blair Junction sequence is then about 280 m (fig. 15). This discrepancy in measured thickness is interpreted to be the result of faulting and incomplete exposure of member 3, due to alluvial cover in the project area (fig. 13).

Lithology of Member 1. Member 1 consists of claystone, siltstone, carbonaceous shale with notable lignite, tuff, limestone, and minor sandstone and conglomerate. The overall character of member 1 is predominantly of fine-grained rocks, including claystone, clay and silt shale, siltstone, and tuff. Pebble conglomerate and sandstone also occur sporadically throughout the lower part of the member, with a particular concentration near the base of member 1.

The base of member 1 in measured section SS I is a thick, moderate-reddish-brown (10 R 4/6), pebbly sandstone which overlies, in erosional unconformity, the unwelded member of the Castle Peak tuff (fig. 16). Pebbles and rare cobbles within this bed are almost exclusively weathered, olive-gray (5Y 6/1) andesite of the older andesite unit (Toa), with lesser amounts of clasts of the coarse-grained andesite unit (Tca). Other sandstone and conglomerate beds of the same composition, which are lensoidal and intercalated with fine-grained rocks throughout the lower 150 m of member 1, all display a moderately high degree of weathering and a reddish color suggestive of oxidation from subaerial exposure shortly after deposition. Alternating with the sandstone and conglomerate are thick-bedded, very light-gray (N 8) to very pale-orange (10YR 8/2) tuffs, and

Figure 16.--Basal conglomerate of member 1 of the Blair Junction sequence of the Esmeralda Formation unconformably overlying Castle Peak tuff at the base of measured section SS I. Arrows indicate contact (surficial material covering precise contact between arrows).

Figure 16.--Basal conglomerate of member 1 of the Blair Junction sequence of the Esmeralda Formation unconformably overlying Castle Peak tuff at the base of measured section SS I. Arrows indicate contact (surficial material covering precise contact between arrows).

pale-yellowish-brown (10YR 6/2) to pale-yellowish-orange (10YR 6/6) claystone or clay shale. The tuffs and claystone typically are soft, friable, and erodible, and are poorly exposed and mantled with a 0.2- to 0.5-m-thick, crumbly surface with "popcornlike" texture suggestive of expansive clays (fig. 17).

X-ray diffraction results (table 1) indicate that the claystone units are largely composed of montmorillonite with subordinate amounts of potassium feldspar and opal-CT. Montmorillonite was identified in X-ray diffractograms of air-dried bulk samples by strong peaks between 12.5 and 15.0 A. The peaks near 15.0 A probably are from more hydrated, Na or Ca montmorillonites (Walton, 1975, p. 617). Authigenic potassium feldspar in samples produce a X-ray diffraction pattern very similar to that of Sheppard and Gude (1969, p. 3). Samples that contain montmorillonite also display X-ray diffractogram peaks characteristic of opal-CT, as it is defined by Jones and Segnit (1971, p. 57-59). Opal-CT differs from more highly amorphous forms of opal in having a higher degree of crystallinity. Opal-CT was identified by broad, but well defined X-ray diffractogram peaks of cristobalite and tridymite, at 4.04 to 4.08 A, and 4.3 A, respectively.

Fragments of very pale-orange (10 YR 8/2), and pale-yellowish-orange (10 YR 8/6) to dusky-yellowish-brown (10 YR 2/2) silicified wood are locally abundant in three thick tuffaceous units in the lower part of member 1. Commonly, silicified wood fragments are 10 to 15 cm across, but range up to trunk segments or branches 0.6 to 1.2 m in diameter. Most silicified wood is clearly banded with

Figure 17.--Tuffs and claystones of the lower part of member 1 of the Blair Junction sequence exposed at the locality of measured section SS III. The hill in the foreground is about 20 m high.

concentric 1- to 2-mm growth rings. Some pockets of silicified wood are associated with local lenses of pebble and cobble conglomerate. Also notable in the lower part of member 1, beginning about 45 m above the base of the unit, are thin- to thick-bedded, clay-rich tuffs that contain carbonized plant remains. These plant remains appear within clay-rich tuffs as discrete, carbonized, woody chips or twig-like fragments from several millimeters up to 4 cm in length.

Above a sequence of pebble conglomerates about 150 m above the base of member 1, in measured section SS I (app. B), the rocks are dominantly fine grained. This part of member 1 consists, to a large degree, of rhythmically interbedded thin siltstone and shale, interrupted by two main, laterally persistent, thin limestone horizons. Siltstone and shale commonly are very pale orange (10YR 8/6). Siltstones are thin bedded, with discrete beds 1 to 4 cm thick that exhibit either a porcellaneous or siliceous nature and break into hard, roughly equant angular chips. The siltstone is evenly interbedded with similarly thin-bedded, softer shale or claystone. Some of the shale, which characteristically breaks into paper-thin flexible flakes, is carbonaceous to lignitic. Minor partings and fractures in the shale commonly are filled with secondary gypsum.

The lignitic shale is particularly abundant in the interval between 228 and 232 m above the base of member 1 (between units 55 and 67, app. B, SS I; fig. 18). In this portion of the sequence, four or more thin lignite beds exist, the thickest of which is 0.7 m thick.

Figure 18.--Thin-bedded, porcellaneous, siliceous, and lignitic shale in member 1 of the Blair Junction sequence, at the locality of measured section SS I, along Jackrabbit Draw. Cliff is 3.5 m high.

Poorly preserved plant matter is readily visible in most of the lignite and interbedded carbonaceous shales. These lignite beds are extremely "ashy", containing about 25 to 50 percent inorganic material, and numerous thin 5- to 30-mm-thick, shale or bony coal partings. Even the most carbonaceous of these lignitic coals is very high in inorganic constituents (vitric material, clay, and silt) and may be classified as "bone coal" for the harder lignite, or carbonaceous shale for the softer, "ashy" lignite. Carbonaceous shale and thin lignitic coal zones in this unit generally are poorly exposed and are discontinuously traceable laterally for a distance of a few meters up to about 0.5 km.

Interbedded within the shale are three thin (0.3- to 0.5-m-thick) pale-yellow-orange (10YR 8/6) to dark-yellowish-brown (10YR 4/2), sandy to clayey limestone beds. These limestone beds are interbedded with other fine-grained sedimentary rocks in the stratigraphic interval from 188 to 210 m above the base of member 1. Most limestone beds are discontinuously traceable laterally for a few hundred meters. The most distinctive feature about these limestones is their general abundance of fresh-water molluscan fossils, ostracodes, and scattered, fragmented fish bones. X-ray and petrographic examination of these limestones reveals that calcite is the only carbonate mineral present (table 1).

Member 1 has a minimum thickness of about 338 m as determined from a composite of parts of measured sections SS I and II (fig. 13).

The lower contact is at the base of the basal conglomerate, which unconformably overlies the Castle Peak tuff (fig. 16).

Lithology of Member 2. Member 2 is predominantly composed of alternating sandstone and siltstone with very minor limestone and conglomerate. Member 2 is best exposed south of U.S. Highway 6/95 at location of measured section SS II, which is given as a representative stratigraphic section (fig. 14; app. B). A massive, mound-shaped outcrop of a sandstone unit with a thickness of 9 m occurs at the base of member 2, in measured section SS II, which conformably overlies member 1 (fig. 19). This sandstone unit and other similar sandstone units in this member typically are light olive brown (5Y 5/6) or dusky yellow (5Y 4/4) on weathered, exposed surfaces. The base of the sandstone bed is flat or slightly undulatory. Texturally, most sandstone beds are moderately well sorted with angular grains. Individual beds, ranging in thickness from several centimeters up to a meter, are generally graded, fining upward from medium- to fine-grain size. Thicker beds are commonly laminated with 3- to 5-mm-thick laminae. Some partings between laminations have impressions of lath-like reedy and woody plant material, up to several centimeters in length. Sandstone in this member locally has small-scale, trough crossbedding.

Examination of thin sections of sandstone in member 2 reveals that subangular, 0.05- to 0.3-mm diameter grains are supported in a mostly clay matrix. Large grains, in a representative thin section of the basal sandstone of member 2, consist of 25 percent lithic

Figure 19.--Thick-bedded sandstone at the base of member 2 of the Blair Junction sequence, along measured section SS II, south of U.S. Highway 6/95. Outcrop is 5 m high.

fragments, mostly of fine-grained porphyritic andesite with lesser rhyolite, 20 percent plagioclase, 15 percent quartz, and 1 percent hornblende. The remainder of the sandstone is matrix, composed of 36 percent clay and biotite with 3 percent minor hematite, which acts as interstitial cement. The feldspar commonly has prominent albite twinning. This is a fairly immature sandstone which can be classified as a volcanic wacke.

Siltstone or silt shale that alternates with sandstone is dark yellowish orange (10YR 6/6) or grayish orange (10YR 7/4) and is thin-bedded and laminated. Siltstone, which is very well indurated, siliceous, and flaggy or platy, forms highly erosion-resistant ledges (fig. 20). Impressions of reedy plant material are also present in these siltstone units. The siltstone is moderately to well sorted and predominantly contains silt-sized particles, although particles range in size from clay to fine sand. In thin section, identifiable grains are plagioclase, potassium feldspar, lithic fragments (chert and volcanic rocks), and quartz, supported by a matrix of clay minerals and vitric material. Some siltstone has minor iron-oxide staining.

Of other lithologies, only two very thin limestone beds were recognized in measured section SS II. These minor limestones are each about 0.5 m thick and are dark yellowish brown (10YR 6/2), fissile, platy, and are similar in appearance to other limestone units in members 1 and 3. The limestone locally contains molds and casts of gastropods. A minor conglomerate composed of pale-brown (5YR 4/4), weathered andesite cobbles and pebbles defines the top of member 2 in

Figure 20.--Platy siltstone overlying thick-bedded sandstone in member 2 of the Blair Junction sequence south of U.S. Highway 6/95 along measured section SS II. Outcrop is about 3 m high.

measured section SS II. The clasts in this conglomerate are poorly sorted and supported in a sandy matrix.

Member 2 is 89 m thick in measured section SS II (app. B). The lower contact of member 2 is defined as the base of the lowest thick-bedded volcanic-wacke sandstone that conformably overlies a thick succession of tuffaceous and porcellaneous shale of member 1.

Lithology of Member 3. Member 3 primarily consists of interbedded siliceous siltstone, coarse-grained to pebbly, arkosic sandstone, tuff, and some minor shale and limestone. Member 3 is generally recognizable for the predominance of extremely platy to flaggy siliceous siltstone, which commonly forms erosion-resistant, tilted ledges, conspicuous in otherwise gently rolling topography. The siltstone commonly splits into flagstones less than 5 cm thick to 10-cm-thick slabs. The siltstone ranges from yellowish gray (5Y 7/2) to dark yellowish orange (10YR 6/6) and is thinly laminated. This siltstone is lithologically similar to that of member 2; however, the siltstone in member 3 is associated with channel-form lenses of calcareous, coarse-grained sandstone.

Lensoidal sandstone in this member is generally yellowish gray (5Y 7/2) or grayish yellow (5Y 8/4). The sandstone typically is moderately to poorly sorted and mostly composed of subangular to subrounded grains of quartz, with lesser amounts of feldspar and biotite in a tuffaceous to calcareous matrix. Locally, granule to small-pebble conglomerate is associated with sandstone. Pebble and granule conglomerate is channel-form and exhibits medium-scale trough cross-

stratification. Crossbeds are graded, fining upward from small-pebble or granule conglomerate to coarse sandstone (fig. 21).

Bedded vitric tuff units are interbedded with siltstone, sandstone, and granule conglomerate. Tuff units range from less than 0.5 m to more than 10 m thick. Tuff is typically very light gray (N 8) and is composed of vitric material with accessory biotite and quartz phenocrysts. Sandstone lenses less than 1 cm thick are locally abundant within the tuff units. Papery, very-light-gray (N 8) tuffaceous shale, similar to that in member 1, is interbedded with tuff units, although is not as abundant as shale in member 1. Vitric material in some samples of tuff and tuffaceous shale, siltstone, and sandstone is diagenetically altered to potassium feldspar, montmorillonite, and minor clinoptilolite (table 1).

Minor, but distinctive, fossil-bearing limestone also occurs in member 3. These limestone beds generally are less than 1 m thick and are laterally persistent. The limestone commonly is sandy and moderate yellowish brown (10YR 5/4) to dark yellowish brown (10YR 4/2) and is locally ferruginous. Numerous ostracodes, molluscs, and fragmented fish bones are concentrated in these limestones. Calcite is the carbonate mineral present in these limestone beds, as shown by X-ray diffraction analysis (table 1). Calcite is also present in spheroidal concretions, 5 to 20 cm in diameter, which are locally abundant in sandy limestone.

Member 3 has a minimum thickness of 172 m as determined from a composite of measured sections (SS I, II, and IV), which are given

Figure 21.--Crossbedded, coarse-grained, pebbly sandstone overlain by vitric tuffs in member 3 of the Blair Junction sequence, at measured section SS I, along Jackrabbit Draw. Staff shown is 1.5 m long.

as representative of this member (fig. 13; app. B). The lower contact of member 3 is defined as the base of the lowest fine-grained rocks (siltstone, shale, and tuff) above the upper conglomerate and volcanic-wacke sandstone units of member 2 (app. B, SS II).

Lithology of Member 4. Member 4 is characterized by the dominance of volcanic breccias of laharic origin with interbedded sandstones. Interbedded conglomerate, siltstone, tuff, and limestone occur as a minor counterpart of the member 4. The volcanic breccias, or lahars, are the most distinctive feature of member 4, forming irregularly bedded, erosion-resistant ledges that crop out along U.S. Highway 6/95 in the project area (fig. 22). Member 4 is described, and thickness given in measured section SS IV (app. B; fig. 13).

Four individual lahars were encountered within interbedded fluvial sedimentary rocks in measured section SS IV. The overall color of the lahars is yellowish gray (5Y 7/2) to pale olive (10Y 5/2). Locally, the surface of lahars is greenish black (5GY 2/1) with desert varnish. The lahars measured in member 4 are individually about 1.5 to 5.0 m thick. Each lahar is strongly indurated and characteristically displays a strongly brecciated texture (fig. 23). Each lahar is very poorly sorted, unbedded, and contains angular to subangular heterolithologic clasts ranging in diameter from a few millimeters to about 1.5 m. The dominant lithologies of blocks are rhyolite or andesite, with lesser, but commonly present, black chert and other Paleozoic rock fragments. The matrix ranges from sandy to tuffaceous and typically is dark, ranging from light olive

Figure 22.--Prominent exposure of the upper lahar in member 4 of the Blair Junction sequence showing lenses of sandstone. Outcrop is located north of U.S. Highway 6/95, in SW 1/4 of section 14, T. 2 N., R. 37 E. Staff shown is 1.5 m long.

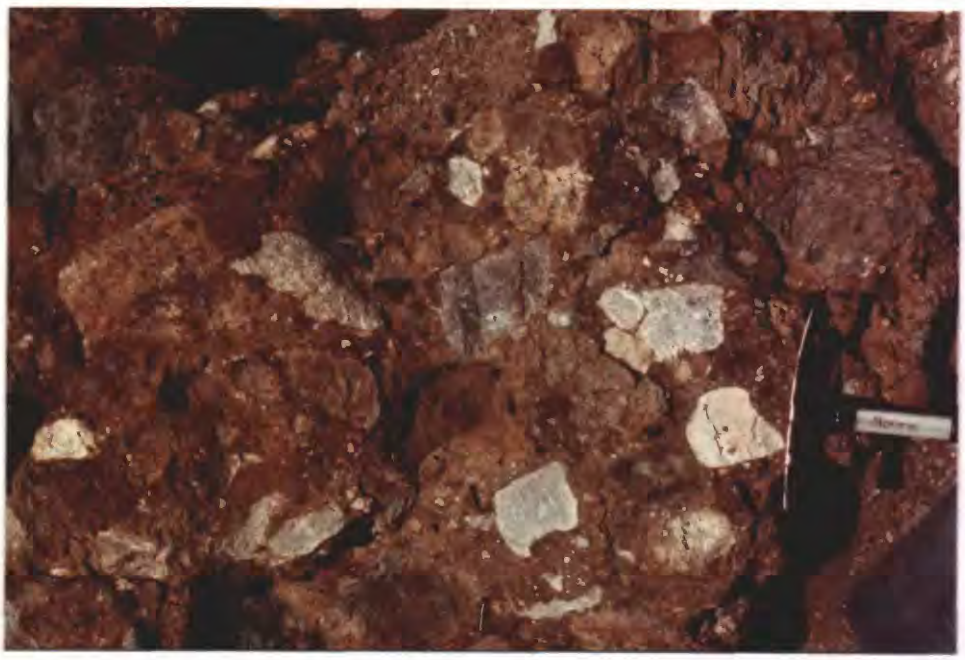

Figure 23.--Angularity of clasts and poorly sorted nature of a lahar in member 4 of the Blair Junction sequence. Hammerhead shown is 20 cm long.

gray (5Y 5/2) to dark yellowish brown (10YR 4/2). The matrix is composed, to a large degree, of smaller fragments of comminuted volcanic rocks of the same multiple lithologies as the larger clasts.

Locally, exposures of the lahars display features similar to those described by (Schmincke, 1967). The lahar shown in figure 24 consists of a 0.5-m-thick basal layer of moderately sorted, medium- to coarse-grained sandstone, which abruptly grades upward into the massive, poorly sorted volcanic breccia. The volcanic breccia is reversely graded, with larger clasts that increase from about 2 cm to 15 cm upward. Above the brecciated portion of this lahar is bedded sandstone that has small-scale trough crossbedding.

Sandstone interbeds in member 4 are light-olive-gray (5Y 6/1) to yellowish-gray (5Y 8/1) volcanic wackes or tuffaceous lithic wackes. These sandstone beds alternate with tuffaceous siltstone and brittle fracturing, grayish-orange (10YR 7/4) siliceous tuff and conglomerate. The sandstone in member 4 generally is poorly sorted to moderately sorted and consists of medium-grained sand to granule-size, angular to subangular lithic clasts, quartz, and feldspar in a tuffaceous, silty matrix. A representative thin section is composed of 35 percent lithic fragments, 15 percent quartz, 20 percent feldspar, and 2 percent biotite, in a silty ash matrix. Lithic fragments are mostly welded rhyolite tuff, basalt and andesite. Minor iron-oxide staining locally coats grain surfaces. Sandstones commonly are lensoidal and range in maximum thickness from a few centimeters to over a meter thick. Minor, small-scale trough crossbeds are evident within

Figure 24.--Lahar of member 4 of the Blair Junction sequence which shows a relatively fine-grained basal sandstone layer which grades rapidly upward into a volcanic breccia. The volcanic breccia shows distinct reverse grading. Staff is 1.5 m long.

thicker sandstone beds. Crossbeds are, in general, graded, fining up from coarse- or very coarse- to medium-grained sandstone.

Conglomerate with subrounded pebble- to cobble-size volcanic clasts is interlensed with sandstone. The conglomerate beds of member 4 can be distinguished from the laharic breccias by their much higher degree of sorting and rounding of the cobbles.

The overall thickness of member 4 in measured section SS IV is 39 m. However, individual lahars, although sheetlike, appear to vary greatly in overall thickness, as does the proportion of interbedded sandy lenses from place to place. The exposures of member 4 in the project area suggest a range in thickness from about 5 to 40 m. The lower contact of member 4 is defined by a disconformity between the lowest observed lahar and the sandstone and siltstone of member 3.

Fossils. Fossils generally are common and highly concentrated in selected horizons of the Blair Junction sequence of the Esmeralda Formation. The best preserved and most abundant fossils found in the the project area occur in member 1 and include molluscs, ostracodes, fish, a mammal, pollen, carbonized plant material, worm burrows, and silicified wood (table 2). Most fossils are found within or associated with thin limestone beds. These limestones are dominated by large concentrations of complete or fragmented, flattened mollusc shells, which typically are replaced by silica. The molluscan assemblage in member 1 includes the gastropods Viviparus turneri,

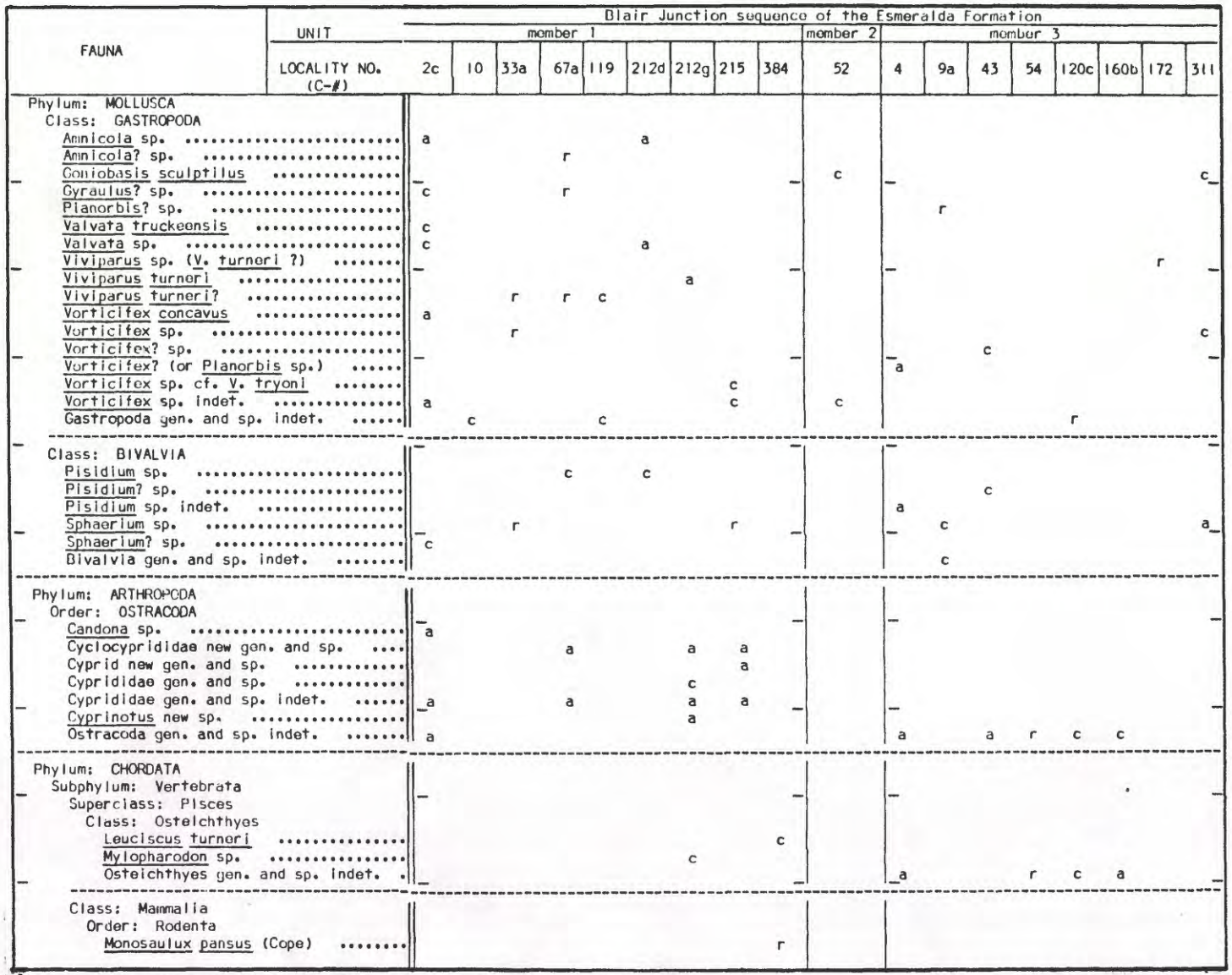

Table 2.--Checklist of fossils from the Blair Junction sequence of the Esmeralda Formation. Relative abundance is indicated by letters: a= abundant; c= common; r= rare.

Valvata truckeensis, Vorticifex concavus, Amnicola sp., and Gyraulus sp. (J.R. Firby, written commun., 1980). Large individuals of Viviparus turneri, up to 35 mm in diameter, erode out of limestone matrix and are found scattered over the ground surface. Associated bivalves identified by Firby are Pisidium sp. and Sphaerium sp. In a minor limestone of member 2, the gastropods Vorticifex sp. indet., and Goniobasis sculptilus were identified (J.R. Firby, written commun., 1980).

Some of the same molluscs that occur in thin limestone beds of member 1 also occur in member 3. The gastropod assemblage in member 3 includes Vorticifex sp. indet., Planorbis sp. indet., Viviparus turneri, and Goniobasis sculptilis. Bivalves Pisidium sp. and Sphaerium sp. also are identified in member 3.

Ostracodes are easily visible and are abundant in sandy limestone beds of member 1. However, identifications are only partially diagnostic due to poor preservation. Ostracodes identified in samples from member 1 include Candona sp., Cyprinotus new sp., Cyprididae, gen. and sp. indet., Cyclocyprididae, new gen. and sp., and Cyprididae, new gen. and sp. (R.M. Forester, written commun., 1979). According to Forester, the large number of ostracodes in these sandy limestone beds is probably due to mechanical concentration. This is further substantiated by large concentrations of fragmented molluscs and other fossils. The mechanical concentration and abrasion of ostracodes during transport has destroyed many of the the delicate features necessary for more specific identification. In addition, the diversity

of species represented has probably increased or altered during transport.

Fossil fish also are common in thin limestones of members 1 and 3 and in closely associated or interbedded fish-bone-hash calcareous claystone. Fish fossils found are thoroughly disarticulated and concentrated in thin layers rich with light-brown (5YR 6/4) to moderate-brown (5YR 4/4), thin, needle-like bones, vertebrae and well preserved simple, conical, teeth. Among the samples examined by G.R. Smith (written commun., 1979), one sample (C-212g) yielded a well preserved pharyngeal arch with teeth that belongs to an undescribed, primitive species of Mylopharodon (Cypriniformes-Cyprinidae; fig. 25). In another sample (C-384), Smith has identified small teeth as being from the Cyprinid fish Leuciscus turneri (Lucas). Also found at locality C-384, in a coarse, sandy limestone of member 1, was a partial jaw and the teeth of the small, primitive beaver Monosaulux pansus (Cope), identified by C.A. Repenning (written commun., 1979).

Fossil plant material in member 1 occurs in carbonaceous shale, lignitic beds, pollen, and silicified wood. Pollen was identified by J.P. Bradbury in coal from the area at the base of the Silver Peak Range in rocks correlative with member 1. Pollen was poorly preserved, but the following types were tentatively identified: Pinus (pine), Picea (spruce), Quercus (oak), Alnus (alder), and Myrica type (J.P. Bradbury, written commun., 1979).

Abundant fragments of Dryopteris obscura (Knowlton) fern pinnae have been reported associated with coal beds and interbedded shale

Figure 25.--Sample C-212g, pharyngeal arch of a primitive fish (a minnow), Mylopharodon sp., from member 1 of the Blair Junction sequence.

near Coaldale (Axelrod, 1940, p. 170). Axelrod (1940, p. 165) also stated that the flora of this general area is dominated by oaks and junipers. Large and abundant pieces of silicified wood, up to 0.5 m across, within tuffs of lower member 1 indicate the past existence of large trees comparable to the size of modern oaks (fig. 26).

Age and Correlation. On the basis of fossil evidence and radiometric ages of closely correlative rocks, the Blair Junction sequence of the Esmeralda Formation is inferred to range in age from late Barstovian (middle Miocene) to Hemphillian (late Miocene). These ages correspond to about 13 to 6 m.y. ago. Member 1 is assigned an age of late Barstovian (middle Miocene) or very early Clarendonian (late Miocene) on the basis, in part, of the fossil beaver Monosaulux pansus collected near the base of the unit. In addition, the molluscan and fish assemblages are consistent with a late Barstovian to very early Clarendonian age. A potassium-argon age of 13.0 m.y. from a tuff interbedded with coals of stratigraphically and lithologically correlative beds of the Coaldale sequence provides further evidence of a late Barstovian to early Clarendonian age (Evernden and James, 1964; app. A, no. 24). Although not acutely time restricted, the ostracode assemblage in member 1 is probably no younger than middle Miocene, according to R.M. Forester (written commun., 1979).

Members 2 and 3 are assigned an age of Clarendonian (late Miocene) on the basis of the conformable relationship of member 2 over member 1 and a molluscan assemblage including Goniobasis sculptilus,

Figure 26.--Silicified wood in a tuff of member 1 of the Blair Junction sequence along Jackrabbit Draw.

Planorbis sp., Vorticifex sp., and Viviparus turneri. Member 4, the volcanic breccia-sandstone member, is probably of Hemphillian (late Miocene) age on the basis of the disconformable relationship to Clarendonian age member 3 and a potassium-argon date of 7.1±0.3 m.y. on an air-fall tuff in a lithologically similar and probably correlative unit, which also unconformably overlies Clarendonian strata, in the Weepah Hills (Robinson and others, 1968; app. A, no. 10).

On the basis of these age relationships and the general lithology of the stratigraphic sequence, the Blair Junction sequence is temporally and closely lithologically equivalent to the Coaldale sequence of Robinson and others (1968) and Moiola (1969). The Coaldale sequence is divided into 3 subunits: a "lower unit" of predominately fine-grained rocks; a "middle unit" of alternating coarse- and fine-grained rocks; and an "upper unit" composed of a laharic breccia. The Coaldale and Blair Junction sequences are correlative as shown in figures 5 and 15.

Many lithologic similarities are evident between the coal-bearing lower unit of the Coaldale sequence and member 1 of the Blair Junction sequence, which contains similar carbonaceous and lignitic shales. Both units also contain tuffs with abundant silicified wood and interbedded, thin, molluscan limestones are associated with the carbonaceous sequence. The coaly portion of member 1 is very similar to that represented in the lithologic logs of Bureau of Mines coreholes 3-28, 1-28, and 2-33 at the base of the Silver Peak Range (Toenges and others, 1946, p. 20). The three coreholes, spaced about 0.9 km

(0.5 mi) apart and drilled to depths between 160 and 210 m (520 and 680 ft), each encountered coaly zones. However, even over this relatively close spacing, coal beds were not precisely correlative bed-for-bed, but were discontinuous and irregularly mixed with varying amounts of tuff, shale, and sandstone. Similarly, the coaly zone of member 1 can be roughly correlated to the coaly zones in corehole logs. The correlation is again imprecise, attesting to the inherent variability in the thickness and lateral discontinuity of coaly deposits in the Esmeralda Formation. From comparison of these logs and other available stratigraphic data at the north end of at the Silver Peak Range (including Hance, 1913) with measured section SS I, even less coal or carbonaceous shale is present in the Blair Junction sequence than at the north end of the Silver Peak Range.

In contrast to the general lithologic continuity between the Blair Junction and Coaldale sequences, the other sequences, as described by Moiola (1969) and Robinson and others (1968), exhibit appreciably more lithologic variability. On the basis of fossil and radiometric age evidence, those authors suggest that the stratigraphic sequences around Big Smoky Valley (Alum, Coaldale, and Vanderbilt sequences) represent contemporaneous, local facies on opposite sides of the same depositional basin. These correlations are shown on figure 5. The correlation of the Coaldale and Alum sequences across Big Smoky Valley indicate that Turner (1900, p. 199-202) was probably incorrect in interpreting rocks from these two areas as representing a continuous superposed stratigraphic succession (Moiola, 1969, p. 23; Robinson and others 1968, p. 582).

Sedimentary rocks and tuffs that crop out in the Fish Lake Valley are also temporally correlative to the Blair Junction sequence. In the northern Fish Lake Valley, teeth from the early Clarendonian horse Nannippus tehonensis are associated with tuffs which have potassium-argon ages of 11.4 and 11.7 m.y. (Evernden and others, 1964; app. A, numbers 17 and 19). The basal part of the sedimentary sequence at the southern end of Fish Lake Valley has a potassium-argon age of 13.4 m.y., the oldest reliable date for tuffaceous sedimentary rocks of the Esmeralda Formation (Robinson and others, 1968; app. A, no. 25). Stirton (1932) used mammalian assemblages to correlate the Fish Lake Valley beds with those at Cedar Mountain. Since then, this correlation has been substantiated by corroborating potassium-argon ages between 11.8 and 10.9 m.y. (Evernden and others, 1964; app. A, numbers 20 and 16). The potassium-argon ages are associated with tuffs above an assemblage of mammals of early Clarendonian age. The beaver Monosaulax pansus also is associated with the Stewart Spring Fauna of Barstovian age at Cedar Mountain (Teilhard de Chardin and Stirton, 1934). These beds correlate well with the time range represented by members 1 through 3.

The sedimentary rocks in Coal Valley were originally included in the Esmeralda Formation by Berry (1927). Axelrod (1956) later described the geology and distinguished three formations on the basis of lithology and floral assemblages that implied local depositional conditions. On the basis of fossil mammal evidence and potassium-argon ages ranging from about 11 to 9 m.y. (Gilbert and Reynolds 1973; app. A,

numbers 21, 15, and 14), two of these formations in Coal Valley correspond well with ages of members 1 to 3 of the Blair Junction sequence. Together these formations compose the Wassuk Group, which comprises, from oldest to youngest, the Alrich Station Formation, the Coal Valley Formation, and the Morgan Ranch Formation. The Alrich Station and Coal Valley Formations are temporally correlative to members of the Blair Junction sequence of the Esmeralda Formation as shown in figure 5. In addition, the stratigraphic position of this sedimentary sequence above older andesites, dated at 15.3±0.5 m.y. (Gilbert and Reynolds, 1973; app. A, no. 26), is strikingly similar to the southern Monte Cristo Range stratigraphy (fig. 5). However, the different floral assemblages, as described by Axelrod (1956), together with contrasting specific stratigraphic detail, lack of evidence for a physical depositional connection, and distance from the Blair Junction sequence, indicate separate depositional basins.

Depositional Environment. The Esmeralda Formation has long been considered by geologists as consisting of rocks of mainly lacustrine origin (Turner, 1900; Toenges and others, 1946; Ferguson and others, 1953; Van Houten, 1956; Robinson, 1964; Firby, 1966; and Moiola, 1969). The Blair Junction sequence of the Esmeralda Formation is interpreted as a local succession of lithologic units that were deposited in a shallow-water, marginal-lacustrine environment with local influences of paludal and fluvial conditions and associated volcanic activity. The dominance of a lacustrine environment generally is indicated by fossils, thin limestone beds, relatively good lateral

continuity of rhythmically bedded fine-grained rocks (probably formed by tractive currents), and by the general paucity of sedimentary structures.

The vertical succession in member 1 is interpreted to represent a transition from a dominantly alluvial to a marginal-lacustrine or paludal environment. In the lower 150 m of member 1, poorly to moderately sorted and lensoidal, andesitic conglomerate and sandstone units are interpreted as rapidly deposited braided-stream deposits that accumulated at the distal end of an alluvial fan system. Reddish coloration of conglomerates and sandstones is probably due to subaerial exposure and oxidation shortly after deposition. Interbedded with coarser channel-form beds are thick claystone and bentonitic tuff units, which represent overbank deposits. Fragmented, carbonaceous plant material dispersed throughout some of the tuff units suggests a nearby source of abundant vegetation. Also, large silicified logs and wood fragments that are localized in pockets within conglomerates, sandstones, and adjacent claystone or tuff units, suggest concentration by fluvial processes.

The upper part of member 1, which typically is more fine grained, thin bedded, and contains carbonaceous shale and low-grade lignite beds, suggests a shallow lacustrine to paludal environment. Similar lithologic assemblages produced from this type of environment occur in the Luman tongue of the Green River Formation, which represents the early facies of Eocene Lake Gosiute in Wyoming (Surdam and Wolfbauer, 1975, p. 336). The general lateral discontinuity of organic coaly

deposits between member 1 and correlative, but more concentrated, thicker coal beds at the north end of the Silver Peak Range (lower unit of the Coaldale sequence) also suggests local pond environments, with variable supplies and mixtures of organic and inorganic matter. Thin, brown, mud- to grain-supported limestone with abundant whole and fragmented molluscs, ostracodes, and fish-bone fragments resemble lake-margin, carbonate-flat units such as those described by Surdam and Wolfbauer (1975, p. 339), Ryder and others (1976, p. 504-505), and Surdam and Stanley (1979, p. 102-103). The ostracodes identified, including the families Cyprididae and Cyclocyprididae, generally are suggestive of a marginal-lacustrine, pond, or other small aquatic environment with abundant aquatic vegetation, and shallow water (less than 3 m deep), according to R.M. Forester (written commun., 1979). The ostracodes and identified molluscs, including Viviparus turneri, Valvata sp., Sphaerium sp., and Pisidium sp., suggest a permanent, fresh-water lake, containing alkaline water with a pH of 7.0 to 8.4, and low total dissolved solids. In addition, the lake probably exhibited seasonal flucuations (Firby, oral commun., 1979). The fossilized jaw of the beaver Monosaulux pansus (Cope) from a sandy limestone of member 1 also is consistent with a pond or marshy environment adjacent to a fresh-water lake. In addition, the Cyprinid fish identified in member 1 is associated with low salinity, high alkalinity, and moderately high temperatures of perhaps 25°C (G.R. Smith, written commun., 1979).

The depositional environment of member 2, which is dominantly composed of alternating volcanic-wacke sandstone and platy silicified siltstones, is interpreted as a marginal-lacustrine-deltaic environment. Although alternating sandstone-siltstone units are relatively thick bedded, the horizontal laminae, very-fine-sand grain size, the flat to slightly undulatory bed bases, and fining-upward, grain-size sequences are similar to the lacustrine-deltaic environment described within the Cretaceous through Eocene age Lake Uinta in Utah (Ryder and others, 1976, p. 505-507). Minor, thin-bedded limestone within member 2, containing the lacustrine molluscs Goniobasis sculptilus and Vorticifex sp., suggests minor flucuations with an adjacent carbonate-flat environment. The poorly sorted conglomerate marking the top of member 2 in measured section SS II may represent lag deposits of a deltaic channel.

The depositional environment of member 3 is similar to that of the upper part of member 2 and is interpreted as marginal lacustrine. Platy, silicified siltstone, water-laid tuffs, and tuffaceous sedimentary rocks attest to concurrent volcanic activity in the region. The influence of a carbonate-flat environment is evidenced by laterally pervasive, thin, fossil-rich limestone beds with locally abundant, large spheroidal calcite concretions. Calcite concretions and calcareous cement are considered characteristic of the marginal-lacustrine facies of Eocene Lake Gosiute of the Green River Formation (Surdam and Wolfbauer, 1975, p. 339). The mollusc and ostracode

assemblages suggest a sedimentary environment with fresh, alkaline water and low total dissolved solids, similar to that of member 1. In member 3, channel-form, coarse-grained sandstone and granule- to pebble-conglomerate, with medium-scale, trough crossbeds are interpreted as bar deposits of small deltaic, braided, distributary streams.

Member 4, mostly composed of distinctive volcanic breccias with coarse, interbedded conglomerate and sandstone, is interpreted as a dominantly fluvial unit containing volcanic mudflows or lahars. A laharic origin is also suggested for volcanic breccias of the correlative upper unit of the Coaldale sequence (Moiola, 1969, p. 77). The interpretation of these volcanic breccias as lahars is based on: massive, resistant, cement-like outcrops; angularity of fragments; very poor sorting; a matrix of mixed tuffaceous material, sand, and comminuted volcanic clasts; reverse grading of larger clasts; and irregular thickness and sheet-like geometry. These features are consistent with those of other lahars described by Mullineaux and Crandell (1962), Schmincke (1967), and MacDonald (1972, p. 170-181). The lahars in member 4 also resemble similar deposits, which are interbedded with fluvial deposits in the Mehrten Formation of the Sierra Nevada in California, described by Curtis (1954). Two most striking features of lahars, the angularity of fragments and the almost complete absence of bedding and sorting, are explained by unified mass movement and high specific gravity. The viscous mixture of water-rich mud and

fine-grained pyroclastic materials in a mobile lahar tends to buffer or cushion the larger clasts, thus greatly reducing abrasion and allowing the whole mass to move fluidly (Mullineaux and Crandell, 1962, p. 858).

In addition, reverse grading of larger clasts within finer matrix and the presence of a relatively fine-grained sand layer at the base of the lahars is common. This may be explained by pebbles and blocks that have moved up during transport, leaving a fine-grained layer at the base, as explained by Schmincke (1967, p. 446) in analogous deposits of the Ellensburg Formation in south-central Washington. Judging from the extreme angularity of the andesite and rhyolite fragments, these lahars probably were derived from the flanks of a nearby volcano, and were possibly associated with the earliest eruptions of the Silver Peak volcanic center in late Miocene.

The sandstone with minor conglomerate within member 4, which is commonly channel-form, moderately sorted, graded (fining up), and which contains small-scale trough crossbeds, is interpreted to represent deposits of overloaded aggrading, meandering streams. Fine-grained interbeds probably represent overbank deposits.

During most of the deposition of the Blair Junction sequence in middle to late Miocene time, the climate was temperate, as suggested by the fossil record. The coal deposits and locally abundant fossil plant material of the Esmeralda Flora, in beds correlative to member 1, suggest a savana-woodland community dominated by oaks and junipers

(Axelrod, 1940, p. 165). Nearby grasslands are suggested by the temporally equivalent grazing mammal assemblage in the Vanderbilt sequence, to the south of the project area (Robinson and others, 1968, p. 592; Moiola, 1969, p. 81). Ferns probably grew around shallow pond environments, with nearby pine, spruce, and alder also in existence. According to Axelrod (1940, p. 167), precipitation in this area was much greater than at present, probably ranging from 30 to 38 cm (12 to 15 in.) per year, in comparison to the present 10 cm (4 in.) per year. The Esmeralda Flora is similar to the present floral assemblage on the western slopes of the southern Sierra Nevada and in southern Arizona, suggesting comparable temperature ranges, and an average annual temperature of about 15°C (59°F), according to Axelrod (1940, p. 167). The relatively warm climate, reflected in the Esmeralda Flora, may have been associated with a world-wide middle Miocene warm interval, which is referred to by Wolfe (1978, p. 700).

Diagenesis. Minerals resultant from diagenetic processes identified by X-ray diffraction in the Blair Junction sequence (table 1) include montmorillonite, opal-CT, authigenic potassium feldspar, and minor amounts of clinoptilolite, and erionite. Authigenic silicate minerals, including the minerals above, are common in Cenozoic continental tuffs and tuffaceous sedimentary rocks in the western U.S., as has been shown by many authors (Deffeyes, 1959; Hay 1963, 1966; Sheppard and Gude, 1969, 1973; Walton, 1975; Boles and Surdam, 1979; and Glanzman and Rytuba, 1979). In addition, previous work has

demonstrated a significant presence of zeolites and associated montmorillonite in parts of the Esmeralda Formation (Moiola, 1963, 1964, 1969, and 1970). Montmorillonite also is extensively developed in correlative Esmeralda Formation beds at the Blanco clay mine, on the northeast side of the Silver Peak Range, about 13 km south-southeast of Coaldale (Papke, 1970, p. 20).

In the Blair Junction sequence, montmorillonite is by far the most abundant authigenic silicate mineral. Particularly evident in the claystones and altered tuffs of the lower part of member 1 is the occurrence of montmorillonite as a partial to almost total replacement of vitric material (table 1).

Although zeolites are common in other locations of the Esmeralda Formation, they were identified in only 3 of about 20 samples of tuffs or tuffaceous sedimentary rocks. Clinoptilolite and erionite are present in only minor amounts and are associated with potassium feldspar, quartz, and montmorillonite. In one sample, a tuffaceous sandstone, clinoptilolite forms a finely crystalline cement similar to that described by Sheppard and Gude (1973, p. 14), and Moiola (1970, p. 1686).

According to the experimental work by Hemley (1959, 1962), and zeolite studies by Hay (1963, 1966), Moiola (1963, 1964), Moiola and Hay (1964), and Mariner and Surdam (1970), the formation of zeolites and associated minerals is activated by high alkali-ion (Na^+, K^+) to hydrogen-ion (H^+) ratios and high silica activity. Moiola (1970, p. 1689) suggests that this type of chemical environment can be

attained in one of three possible situations: a depositional environment of an alkaline, saline lake; hydrothermal alteration; or a post-depositional diagenetic environment resulting from dissolution and hydrolysis reactions between volcanic glass and subsurface water. The first alternative does not seem plausible, since fossil evidence (molluscs and fish) and absence of saline minerals, other than surface efflorescence, are indicative of a fairly fresh, although alkaline lake. Several hornblende andesite and rhyolite dikes and plugs intrude member 1; however, alteration of vitric material is not confined to the local area or fractures around these intrusive bodies, but rather seems laterally continuous and confined by bedding. In addition, common hydrothermal alteration minerals such as kaolinite and alunite are notably absent; thus an origin from hydrothermal alteration is unlikely. Therefore, the third alternative, that authigenic minerals were formed after deposition by reaction of subsurface groundwater with vitric material seems most plausible.

Given a particular set of conditions, according to Moiola (1970, p. 1688) and Walton (1975, p. 617), montmorillonite is among the first diagenetic minerals to form from hydrolysis of volcanic glass by subsurface water. The initial formation of montmorillonite, over direct formation of zeolites, probably is the result of less alkaline, lower pH, conditions and a relatively low alkali-ion to hydrogen-ion ratio (Hemley, 1962). The hydrolysis reaction releases silica, alumininum species, and alkali ions into solution and precipitates montmorillonite. At this stage, montmorillonite forms clay coatings or rinds

on glass shard and grain surfaces. Excess silica in solution not consumed in this formation of clay would concurrently form opal. According to Hay (1963), the formation of initial montmorillonite by this reaction would in effect raise the $Na^+ + K^+$ activity and raise the pH of interstitial water. This in turn, results in the formation of zeolites, most commonly clinoptilolite, in favor of continued formation of montmorillonite. Various forms of silica, as opal, are thought to continue during the formation of zeolites, and thereafter, as long as excess silica is available (Walton, 1975, p. 621). Formation of potassium feldspar may coincide with the formation of zeolites such as clinoptilolite, or analcime, as is suggested by the coexistence of the two minerals in this study, and in the studies of Deffeyes (1959), Hay (1963), and Moiola (1970).

In view of these concepts, and given the assemblage of authigenic minerals in the Blair Junction sequence, a specific set of local post-depositional chemical conditions is required. In order for montmorillonite to form, initial reactions between fresh volcanic glass and groundwater require a relatively low $Na^+ + K^+$ to H^+ ratio and a relatively alkaline pH. Concurrent with, and subsequent to montmorillonite formation, opal-CT was deposited as a result of groundwater supersaturated in silica. The sparse representation of zeolites in the sampling suggests two alternatives: (1) zeolites were once more extensive and have been subsequently altered; or (2) zeolites were never formed to any large extent. In the first case, zeolites may have been recently removed by surficial weathering. Or in the second case, the

subsurface chemical conditions were such as to halt the formation of zeolites after montmorillonite formed, and favored the direct formation of potassium feldspar. This could be activated by some change in the hydrologic regime, or by the interaction of a specific set of variables which may include: porosity; pH; depth of burial, or temperature and pressure conditions; or influence of the original composition of the unaltered glass. These variables, in combination, could alter the critical equilibrium between the $Na^+ + K^+$ to H^+ ratio and silica concentration, thus determining the stability and presence of authigenic minerals. Conceivably, local concentration of more alkaline, higher pH, pore fluids possibly could have accounted for only very local formation of zeolites; whereas, montmorillonite was more favored in less alkaline, lower pH pore conditions persistent over a larger subsurface area. However, owing to the only minor presence of zeolites, their paragenesis is not clearly evidenced.

In member 1 of the Blair Junction sequence, the abundance of montmorillonite is attributed to a combination of diagenetic and surficial weathering processes. A diagenetic origin for much of the montmorillonite is supported by its association with authigenic potassium feldspar, opal-CT, and minor zeolites, and by the relative abundance of montmorillonite in member 1, as compared to members 2 and 3 (table 1), suggesting depth of burial as a factor. However, similar alteration of volcanic glass is also likely under surficial weathering conditions, apparent from the abundant montmorillonite in the surface weathering rind on claystones and shale units in member 1.

Miocene or Pliocene(?) Series

Post-Esmeralda Formation Volcanic Rocks. Dikes and other small intrusive masses of both rhyolite and hornblende andesite locally intrude the Blair Junction sequence of the Esmeralda Formation and older rock units in the project area. This intrusive relationship is best seen in the Dragonback Hills where north-northwest-trending hornblende andesite dikes transect the older andesite unit. The dikes are commonly 1 to 3 m wide and form resistant, linear features easily differentiated from older rocks (fig. 27). Where narrow dikes intrude member 1 of the Blair Junction sequence, shale and siltstone beds are locally folded and deformed. Dikes are locally brecciated and contain mixtures of angular rhyolite and andesite clasts, with andesite predominant and comprising most of the groundmass material. This common mixture of andesite and rhyolite attests to the bimodal nature of volcanism in the area in post-Esmeralda Formation time. In the area immediately east of Dragonback Hills, an exposure shows a narrow hornblende andesite dike that thickens upward into a small local flow (fig. 28). The area immediately east of Dragonback Hills is dominated by a complex of numerous dikes, small intrusive hornblende andesite masses, and small local flows. Parallelism of many small dikes with northeast-trending faults suggests emplacement along, but not limited to, fault planes. Because dikes are also slickensided and offset by faults, faulting also occurred subsequent to dike emplacement. Other dikes, particulary notable in the Dragonback Hills, trend north or north-northwest, transverse to the trend of faulting.

Figure 27.--View toward the southwest of erosion-resistant dikes of intrusive andesite (Tai) which intrude flows of coarse-grained andesite (Tca). Dikes in the foreground are 0.5 to 1.5 m high. The area of light colored rocks in the middle distance is the Jackrabbit Draw area. The mountain range in the distance, on the left, is the Silver Peak Range; on the right, is the Volcanic Hills.

Figure 28.--Hornblende andesite dike that intrudes the Castle Peak tuff in the central part of the mapped area.

Lithology. Rock types included as post-Esmeralda Formation volcanic rocks are mainly hornblende andesite and minor rhyolite. The more pervasive hornblende andesite (Tai) is distinguished from other andesite by a strong greenish-gray (5GY 6/1) color with abundant large 3- to 8-mm, euhedral phenocrysts of black hornblende. This texture is particularly evident in dikes where hornblende phenocrysts are alined subvertically. The drab greenish color is attributed to propylitic alteration. The hornblende andesite is porphyritic with a hyalopilitic texture. The hornblende phenocrysts commonly constitute 10 to 15 percent of the rock and commonly are partially replaced by chlorite and hematite. The groundmass is composed of nonoriented microlites of plagioclase with interstitial glass and microfelsite.

Small dikes and other intrusive masses of rhyolite very locally intrude the Blair Junction sequence (fig. 29). These rhyolites, of very local areal extent, differ from older rhyolites in the project area by their compact, crystalline igneous texture, as opposed to the pyroclastic nature of the Castle Peak tuff. These intrusive masses consist of commonly flow-banded to brecciated very light-gray (N 8) to pinkish-gray (5YR 8/1) porphyritic rhyolite with quartz, sanidine, and biotite phenocrysts that comprise up to 20 percent of the rock. The groundmass is micro- to cryptofelsitic. Common angular xenoliths of hornblende andesite and other lithic clasts occur within the rhyolite.

Age and Correlation. The intrusive hornblende andesite and rhyolite are assigned an age of latest Miocene to Pliocene. This age is

Figure 29.--Small plug of rhyolite (Tri) that intrudes member 1 of the Blair Junction sequence of the Esmeralda Formation. The plug is about 6 m high. The White Mountains are visible in the far distance.

based on the intrusive relationship with the middle to late Miocene Blair Junction sequence of the Esmeralda Formation, and radiometric ages on nearby, similar, mostly post-Esmeralda Formation volcanic rocks. A glassy rhyolite flow in the eastern Monte Cristo Range has a potassium-argon age of 7.2±0.2 m.y. (Silberman and others, 1975; app. A, no. 11). In addition, possibly correlative trachyandesite and rhyolite associated with the Silver Peak volcanic center have potassium-argon ages of 6.3±0.3, and 6.2±0.5 m.y., respectively (Robinson and others, 1968; app. A, numbers 9 and 8).

Pliocene(?) Series

Basaltic Andesite. The basaltic andesite unit of the project area is another unit that has been differentiated from rocks previously included in the Gilbert Andesite by Ferguson and others (1953). The distribution of the basaltic andesite is limited to areally small remnants that lie in the northernmost part of the project area. However, this andesite also appears to be more extensive in the higher reaches of the Monte Cristo Range, as determined by examination of aerial photographs and reconnaissance outside of the project area. In the project area, the basaltic andesite unconformably lies over the older, fine-grained andesite and has variable thickness that ranges from a less than 2-m-thick layer of blocky rubble to flows over 30 m thick. The locally variable thickness, scattered outcrop pattern, and unconformable relationship with underlying andesite units suggests that the basaltic andesite flowed over irregular, dissected topography.

Lithology. The basaltic andesite is easily distinguished from older andesites by a distinctly darker and less weathered appearance, a subhorizontal upper flow surface, and the stratigraphic position over older, tilted andesite flows. On unweathered surfaces, the basaltic andesite is dark gray (N 3) to grayish black (N 2) or pale olive (10Y 6/2) with reddish iron-oxide staining. Flows erode easily into large blocks of separated columnar joints that form coarse talus slopes downhill from flows (fig. 30). Columnar joints form posts of basaltic andesite that are fairly regular with 5 or 6 sides, commonly being 20 to 30 cm in diameter and up to several meters long. Columns of basaltic andesite are either fairly straight or curved (fig. 31).

The basaltic andesite is coarsely porphyritic with distinctive large pyroxene and plagioclase phenocrysts which constitute 15 to 25 percent of the rock. Pyroxenes present are euhedral augite and hypersthene, which range from 0.6 to 3.5 mm in length. Phenocrysts occur in a microcrystalline, hyalopilitic groundmass composed of plagioclase microlites and interstitial glass. An average mineralogic composition as determined from thin section analysis includes 3 percent augite, 3 percent hypersthene, 3 percent biotite, 12 percent plagioclase phenocrysts. The plagioclase is calcic andesine or labbradorite with a composition of An_{39} to An_{58}. The groundmass consists of 79 percent plagioclase microlites and glass, with 2 percent secondary magnetite and other opaque minerals. The designation of basaltic andesite rather than andesite for this unit is preferred

Figure 30.--Dark basaltic andesite flow (Tba) with coarse talus slope below, in the northern part of the mapped area. The direction of the view is eastward, with Gilbert Road at the base of the flow. Light-colored hill in the foreground is the Castle Peak tuff.

Figure 31.--Columnar-jointed basaltic andesite (Tba) exposed in the northern part of the mapped area, along Gilbert Road. The outcrop is about 15 m high.

because of a fairly high color index, the presence of substantial plagioclase with An content higher than 50, and the relative abundance of pyroxenes. This rock is a borderline andesite or basalt, for which chemical analysis would be needed to be more specific.

Age and Correlation. The age of the basaltic andesite is not precisely known; however, it is probably Pliocene or younger, on the basis of the unconformable position stratigraphically above older Miocene andesites, relatively flat, undeformed flows, mostly unweathered appearance, good preservation of flow features, such as columnar joints, and correlation with nearby, lithologically similar rocks of known Pliocene age. Radiometrically dated basalts occur in the nearby Candelaria Hills that have potassium-argon ages of 3.0±0.1 and 4.0±0.4 m.y. (Marvin and others, 1977; and Silberman and others, 1975, respectively; app. A, numbers 1 and 2). An olivine basalt in the Silver Peak Range has a potassium-argon date of 4.9±0.6 m.y. (Robinson and others 1968; app. A, no. 3). In addition, a Pliocene basaltic andesite is reported in the central Silver Peak Range by Robinson and others (1976; fig. 5).

Quaternary System

Older Alluvium

Older alluvium (Qoa) consists of poorly sorted, unconsolidated deposits of pebbly or cobbly gravel and sand, which lie adjacent to the flanks of the southern Monte Cristo Range. These deposits

represent older, dissected alluvial fans and have surfaces above the present surface of alluvial deposition. These deposits are somewhat better consolidated than the younger alluvium and are noted for overall darker color due to "desert varnish", a thin film of iron and manganese oxides deposited on lithic clasts after a long period of aerial exposure in this arid region. Caliche deposits locally are abundant in the older alluvium. Dissected alluvial fans generally are cone shaped and sheet like with thicknesses as much as 2 or 3 m.

Younger Alluvium

Younger alluvium (Qal) includes unconsolidated poorly sorted gravel, sand, and silt, which is presently being deposited by intermittent streams on the alluvial plain adjacent to the southern Monte Cristo Range. This unit includes colluvium deposited at the base of steep slopes in intercanyon areas in the northern part of the project area. Younger alluvial deposits grade into finer valley fill basinward from the Monte Cristo Range.

STRUCTURAL GEOLOGY

Regional Tectonic Setting

The project area lies along the western margin of the Basin and Range Province, a physiographic and structural province noted for northerly trending, elongate mountain ranges and intervening linear valleys. The structure of this region is largely attributed to regional extensional tectonics that have been dominant in this region from early or middle Miocene time, about 17 m.y. ago, until present (Stewart, 1978, p. 21-22). However, along the western edge of this province lies a northwest-trending zone of topographic and structural disruption and transition between the Sierra Nevada block on the west and the more typical north-northeast trending ranges on the east (Albers and Stewart, 1972, p. 42). This zone of structural disruption is about 600 km long and as much as 100 km wide and is known as Walker Lane (Locke and others, 1940; fig. 32). Walker Lane is interpreted to represent a zone of large-scale, right-lateral shear parallel to, and analogous to the San Andreas fault (Locke and others, 1940; Shawe, 1965; Albers, 1967; Stewart, 1967; Ekren and others, 1980). Along Walker Lane, which merges southward into the Las Vegas Shear Zone, as much as 130 to 190 km of right-lateral displacement has occurred, accounted for by a combination of fault slip and pervasive large-scale drag (Stewart, 1978).

Southwest of the project area lies the northern terminus of the

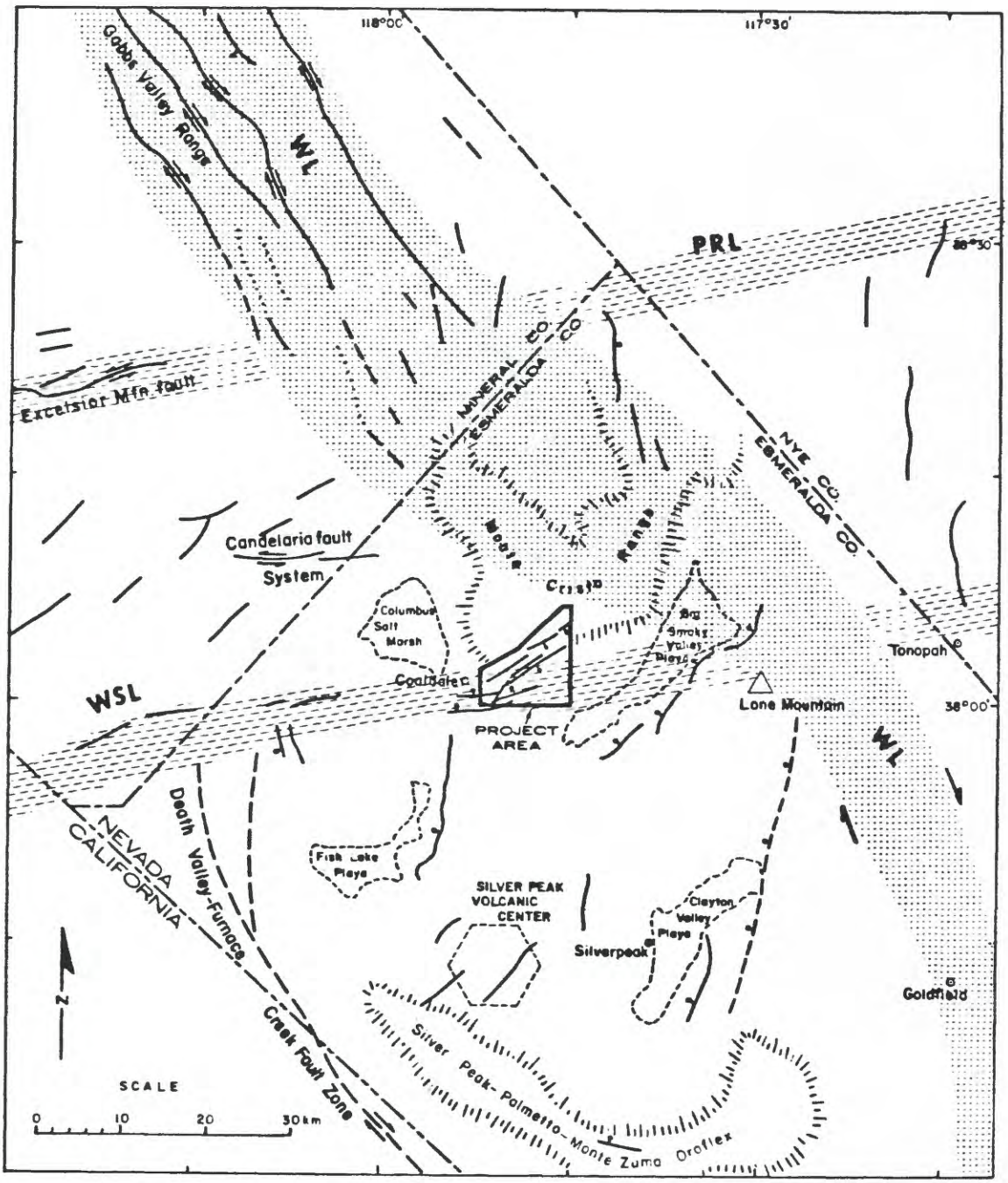

Figure 32.--Generalized map of major fault traces and major regional structural features or lineaments in part of southwestern Nevada. "PRL"= Pancake Range Lineament; "WL"= Walker Lane; "WSL"= Warm Springs Lineament. (Modified after: Shawe, 1965; Albers, 1967; Albers and Stewart, 1972; Ekren and others, 1976; Davis and Vine, 1979; and Speed and Cogbill, 1979a).

Death Valley-Furnace Creek fault zone, which is also a right-lateral strike-slip fault system. Albers (1967) and Stewart (1967) suggest that displacement at the end of this right-lateral fault system is taken up by large-scale tectonic bending. This bending has involved rocks mostly of pre-Cretaceous age and has resulted in large concave-north, arcuate physiographic features conspicuous in this part of western Nevada. These large arcuate features are known as oroflexes (Albers, 1967, p. 145). The pre-Cretaceous cores of the Silver Peak Range, Palmetto Mountains, and the Montezuma Range together constitute an oroflex (fig. 32). A large concave-north, arcuate form is also typical of the combination of the Monte Cristo Range and Cedar Mountains. However, the evidence for the Monte Cristo Range-Cedar Mountains arcuate form as an oroflex is less convincing, since these ranges are composed mostly of Tertiary rocks with discontinuous outcrops of Mesozoic and Paleozoic rocks (Albers and Stewart, 1972, p. 51).

Recent studies in western Nevada also suggest large-scale, east-trending features. The "Warm Springs lineament" of Ekren and others (1976) trends east-northeast through the project area. The Warm Springs lineament trends eastward apparently through Walker Lane, which is diffusely defined at this latitude. Ekren and others (1976) suggest that this lineament, which has topographic and geomagnetic expression, probably does not offset Walker Lane. While the meaning of this lineament is conjectural, similar east-trending faults in the region with left-lateral displacements may represent shears that are conjugate to the right-lateral shears associated with Walker Lane similar to the Garlock fault-San Andreas fault relationship (Shawe, 1965, p. 1372-1373).

Pre-Cenozoic Structure

Pre-Cenozoic structural features in the project area consist of folds and small-scale faults within the Ordovician Palmetto Formation, which crops out along the northwest boundary of the project area (pl. 1). Bedding attitudes are highly variable from one exposure to the next because thin beds of chert and interbedded phyllitic shale typically are undulatory or tightly folded (fig. 4). Folds commonly have wavelengths of 0.5 to 3.0 m. In addition, associated small-scale faults, which offset individual chert beds several centimeters, are abundant.

On a larger scale, the structure of pre-Cenozoic rocks is also found to be complex. Northwest of the project area, the "Monte Cristo thrust" (Ferguson and others, 1953) displaces Ordovician rocks over Triassic, and Permian rocks over Ordovician (Ferguson and Muller, 1949, p. 48-49; Ferguson and others, 1953).

The strong deformation of beds in the Palmetto Formation is probably related to regional tectonic deformation of pre-late Jurassic age, which may be related to the Late Devonian-Early Mississippian Antler Orogeny. In addition, judging from the tectonic activity of the region, these rocks probably have been subjected to repeated deformation. Oroflexural bending, as suggested by Albers (1967), may have contributed to this deformation, although the evidence is weak in the Monte Cristo Range because of limited exposure (Albers and Stewart, 1972).

A major angular unconformity exists between the folded Palmetto Formation and the overlying Castle Peak tuff and can be seen in the northernmost extreme of the mapped area (pl. 1). This unconformity represents major uplift and erosion from Late Ordovician to about late Oligocene time. The unconformity is marked by a highly irregular erosional surface, which underlies the Castle Peak tuff, and isolated Palmetto Formation outcrops surrounded by the tuff.

Cenozoic Structure

Unconformities

Several unconformities also are present within the Cenozoic stratigraphic succession in the mapped area (pl. 1). However, very few of these unconformities are clearly visible in the field, but rather are inferred from the distribution and attitudes of mapped units. These unconformities represent intervals of uplift and erosion. An unconformity between the upper Oligocene or lower Miocene Castle Peak tuff and the middle Miocene, member 1 of the Blair Junction sequence is defined by a basal conglomerate which contains well-rounded cobbles of andesite of an intervening age. The lower contact of member 4 of the Blair Junction sequence is disconformable over member 3, as is indicated by a roughly parallel, but irregular, wavy contact. Another more clearly defined unconformity is evidenced by the irregular distribution of the near horizontal basaltic andesite unit over older tilted andesite flows.

Faults

Faults that transect upper Oligocene to Pliocene rocks are abundant in the project area (pl. 1). Most of this faulting previously was not recognized in the more regional geologic mapping of Ferguson and others (1953) and Albers and Stewart (1965, 1972). Most faults are recognizable both on aerial photographs and on the ground. Locally, bedding is upturned and distorted adjacent to faults (fig. 33). Other features associated with faulting include linear concentrations of calcite or silica cement, local accumulations of silicified or jasperoid breccia, and narrow clayey gouge zones.

The most conspicious feature of faults in the project area is the strong northeasterly trend of fault traces (pl. 1). To better quantify fault trends, the orientations of 88 faults and fault segments were plotted on a polar-coordinate frequency diagram. Trends of longer fault traces were plotted in 0.8 km segments and all fault trends were grouped into 5°-trend intervals (fig. 34). Figure 34 shows that the three most common fault-trend groups all trend northeast. In order of frequency, the trends are N. 55-60 E., N. 75-80 E., and N. 40-45 E. At the base of the Silver Peak Range, south of the project area, Cenozoic faults are strongly east trending (Moiola, 1969, pl. 2; Albers and Stewart, 1972, pl. 1). Where observable, fault planes, or minor planes associated with a fault trace, dip steeply, generally greater than 65°.

Geologic mapping and cross sections (pl. 1) reveal that vertical displacements ranging from a few meters up to about 400 m have occurred

Figure 33.--Upturned siltstone and sandstone beds of member 3 of the Blair Junction sequence along a northeast trending fault that projects across U.S. Highway 95/6.

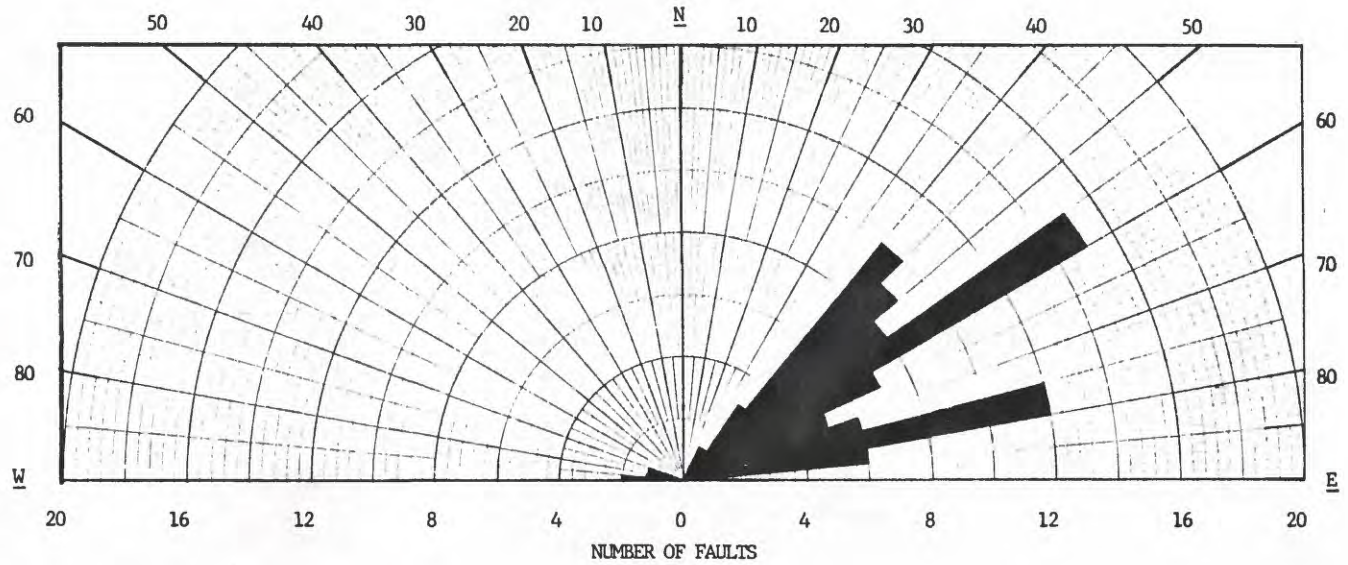

Figure 34.--Frequency diagram of fault trends in the southern Monte Cristo Range.

on faults in the project area. Juxapositon of members 1 and 4 of the Blair Junction sequence along a major fault trending N. 40 E. in the south half of sec. 14, T. 2 N., R. 37 E., indicates a vertical displacement, down to the west, of about 400 m. The fault that trends N. 60 E. through sections 13 and 14, T. 2 N., R. 37 E. and continues northeastward to the Jackrabbit Draw area juxaposes members 1 and 3 of the Blair Junction sequence, which results in an apparent throw of 100 to 150 m. Other faults with a similar sense of movement, but with displacements of only a few meters, are common in the project area.

Slickensides are common on fault planes and are best preserved in andesites. Some striated surfaces are extremely well polished and have a glazed appearance (fig. 35). Because of the steep dips of fault planes, the rake of slickensides generally was measured in the the field and later converted to amount and direction of plunge by rotation on a stereographic net. Figure 36 is an equal-area, lower hemisphere plot of plunges of 23 prominent slickensides measured along faults in the project area. The trends of slickensides generally show the same dominant northeast orientation that was reflected in the trends of fault traces. Points that plot in the northeast quadrant are from slickenslides on both southeast- , and secondarily, northwest-dipping fault planes. In addition, the amounts of plunge vary from near horizontal to as much as 70°, with most between 30° and 70°.

These results suggest that movement on these faults was not pure

Figure 35.--Prominent slickensides along fault at Dragonback Hills in older andesite flows (Toa).

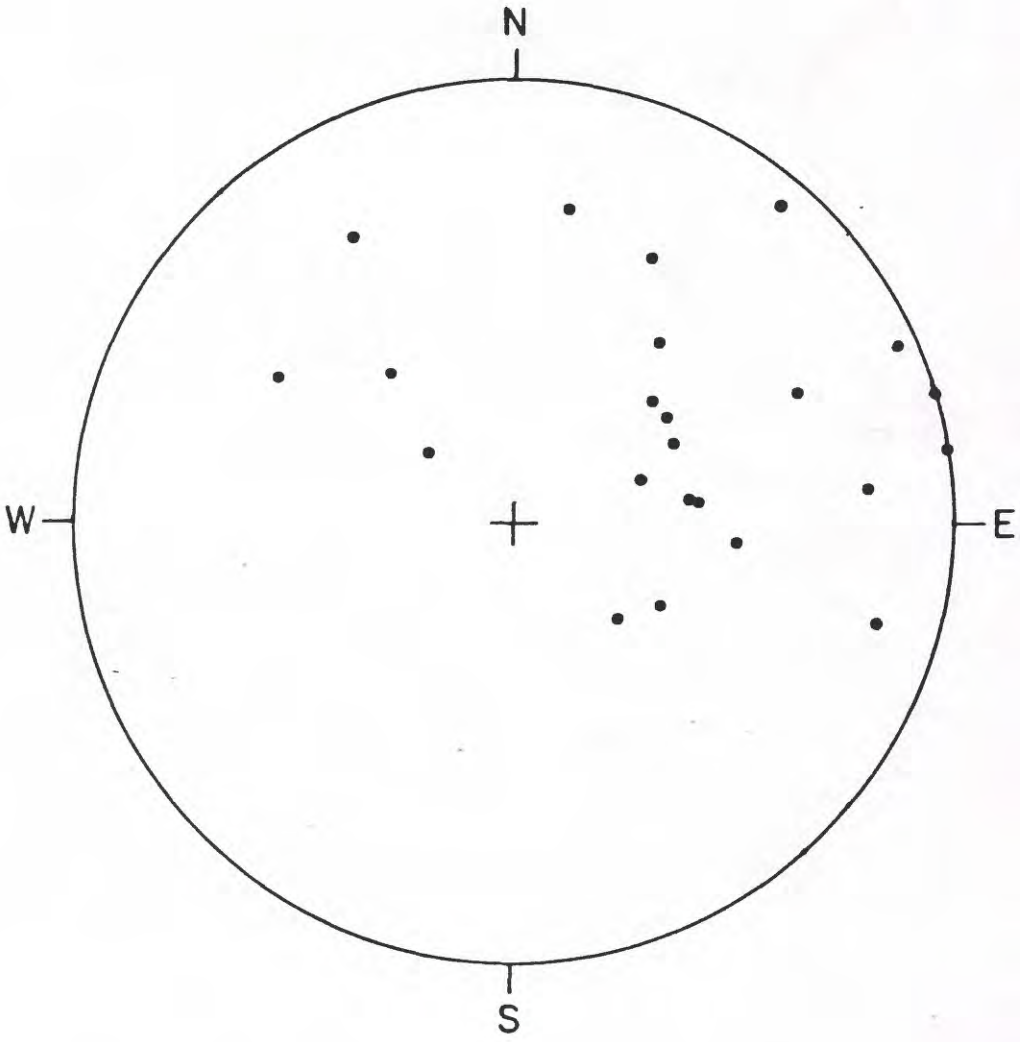

Figure 36.--Equal-area (lower hemisphere) stereographic plot of poles of slickensides associated with faults in the mapped area.

dip slip, but rather normal slip with a horizontal component, or oblique slip. On many southeast-dipping fault planes, slickensides on the upthrown block plunge at relatively low angles northeast, suggesting an overall relative movement of left-oblique slip.

On most faults in the project area, subhorizontal or oblique displacements across faults are difficult to demonstrate, particularly where the strike of bedding is subparallel to the fault trend. However, a fault trending N. 75 E., which crosses the highway in the north half of section 23, T. 2 N., R. 37 E., has an apparent right-strike separation of about 1 km between the offset contact of members 2 and 3. This displacement could have been accomplished by: dip slip along the fault in tilted beds, with subsequent erosion of the northern, upthrown block and/or displacement with a right-lateral horizontal, or oblique movement. A combination of dip slip and right-oblique slip is favored for this fault on the basis of nearby oblique-angled slickensides and vertical displacements in the nearby project area.

Folds

Folds in Cenozoic rocks mostly are confined to a zone approximately 215 m wide and 0.6 km long, adjacent Jackrabbit Draw, along a major fault that trends N. 50 E. (pl. 1). Member 1, which dips southeast of an angle of 14°, just north of the zone of intense folding, is abruptly transformed to a zone of tightly folded and overturned bedding (fig. 37). The thin-bedded lignitic, porcellaneous, and siliceous shale of member 1 of the Blair Junction sequence is folded into a series of tightly compressed, symmetric and asymmetric, similar- and

Figure 37.--Zone of intense folding in shale of member 1 of the Blair Junction sequence adjacent to a fault along Jackrabbit Draw. Height of the folded shale outcrop is about 5.5 m.

chevron-style folds. The folds have wavelengths ranging from less than 20 cm to over 10 m. Fold axes generally plunge southeast at angles ranging from 5° to 30° and averaging about 15°. Axial traces of folds are fairly consistent and average between N. 50 and 55 W. Relatively coherent beds of siliceous shale generally maintain equal thickness throughout the fold, whereas softer, less competent, lignitic shales commonly bunch up and thicken in the hinge zone of folds (fig. 38). A similar intensity of folding has occurred also at the base of the Silver Peak Range, in the vicinity of the old coal mines.

Other folds representing a lesser degree of deformation occur adjacent to mapped faults (fig. 33). Another comparatively broad fold, a syncline that trends N. 20 E., is located in the southwest quarter of section 13, T. 2 N., R. 37 E. (pl. 1).

The overall structure of the basin between the southern Monte Cristo Range and the Silver Peak Range is essentially a broad, faulted syncline. This interpretation contrasts with that of Moiola (1969, p. 72) who considered the strata of the Esmeralda Formation north of the Silver Peak Range to be a north-dipping homocline. At the north base of the Silver Peak Range, bedding in the Coaldale sequence of the Esmeralda Formation generally dips north or northeast. Mapping in the project area reveals that strata of correlative beds in the Blair Junction sequence generally dip southeast in the vicinity of Jackrabbit Draw (pl. 1). This broadly synclinal form probably is the result of the uplift of the Monte Cristo and Silver Peak Ranges subsequent to the deposition of the Esmeralda Formation.

Figure 38.--Thickening of lignitic shale in the hinge of a fold in member 1 of the Blair Junction sequence. Staff is 1.5 m.

Folds in the project area are apparently related to faults. This relationship is suggested by the concentration of the zone of intense folding localized along the major fault crossing Jackrabbit Draw, and the adjacent relationship of small flexures in bedding with mapped faults (fig. 33). These smaller flexures suggest drag along faults, and provide evidence for the sense of relative fault block movement.

Discussion

The fault trends of N. 40-80 E., mapped in the project area, although anomalous to the more northerly trends typical of the Basin and and Range province as a whole, are similar to fault trends indicated by recent work in adjacent areas. Areas with similar structural trends include the Candelaria Hills (Speed and Cogbill, 1979a), the area north of the Volcanic Hills, in the Columbus and Miller Mountain quadrangles (Stewart, 1979), and the northern Silver Peak Range (Robinson and others, 1976). In addition, older Quaternary fault scarps across Big Smoky Valley, at the base of Lone Mountain have similar trends of N. 65 E. and N. 20 E. (Davis and Vine, 1979, p. 422). According to those authors, the fault scarp trends coincide with ages of about 20,000 and 10,000 years, respectively. This similarity suggests that regional tectonic stresses that produced faults in the Blair Junction sequence during the late Miocene or Pliocene were also active, at least intermittently, through Quaternary time.

Most of the fault displacement in the project area appears to be due to vertical movement. Slickensides suggesting oblique slip are

intriguing and invite comparison with left-oblique slip faults in the Candelaria region described by Speed and Cogbill (1979a,c). Those authors suggest that a system of en echelon faults has undergone significant left slip in a N. 82 W. extension direction, along nearly east-trending faults, intermittently from late Oligocene through Pliocene time. In addition, a magnitude 6.3 earthquake produced en echelon fractures with left-oblique slip (Callaghan and Gianella, 1935) in 1934 along the Excelsior Mountain fault. This recent seismic activity suggests possible continuance of east-trending extension to present time. The faults in the project area, particularly those with some oblique slip, could be in part related to the same regional stresses responsible for the left slip in these adjacent areas.

The zone of intensely folded rocks may be analogous to similarly trending folds and associated compressional features in the Candelaria Hills (Speed and Cogbill, 1979a). Those authors describe local concentrations of folds with northwest-trending axial traces, that lie along the north wall of the east-trending Candelaria fault system. These folds intersect the fault system at 45° and suggest that the generation of folds is related to lateral shortening or compression along a northeast-trending axis, concurrent with left-oblique slip along the Candelaria fault system. The orientation of folds in the project area is essentially the same, although the associated fault trends are more northeasterly than the Candelaria Fault system. The similarity of folding between these two areas suggests a similar form of compressive stress along the north wall of the northeast-trending

fault adjacent to the folded zone. The compressive stresses needed to facilitate this folding, therefore, may be also related to at least limited left-oblique slip along this fault, as is also supported by the orientations of measured slickensides along this fault.

In summary, although the areal extent of the project area is very limited, the trends and types of structural features fit well with those described by other workers in the adjacent areas. Fault trends in the project area are anomalous to those of the Basin and Range Province as a whole. Walker Lane and east-trending structural lineaments such as the Warm Springs lineament, may have some control on structural trends in the project area.

GEOLOGIC HISTORY

In the vicinity of the present Monte Cristo Range, chert and phyllitic shale of the Palmetto Formation, in addition to associated graptolite shale in nearby areas, suggest deep, off-shelf, marine deposition in Ordovician time. Marine conditions are in evidence as early as Cambrian from widespread exposures of Cambrian rocks in the nearby Silver Peak Range, Miller Mountain, and Lone Mountain areas (Albers and Stewart, 1972, pl. 1).

The interval between Ordovician and late Oligocene is represented by a pronounced angular unconformity between the Palmetto Formation and the Castle Peak tuff. During that time, regional deformations and intrusions of plutonic rocks occurred leading to a transition from marine to nonmarine, continental conditions. The first major folding and deformation of the Palmetto Formation may have coincided with part of the Antler orogeny during Late Devonian-Early Mississipian time.

The absence of Paleocene through middle Oligocene rocks in the project area and surrounding region suggests that this area was a highland with external drainage during at least part of this time (Moiola, 1969, p. 88). In late Oligocene to early Miocene, voluminous rhyolitic ash-flow tuffs, including the Castle Peak tuff, were deposited on an irregular pre-Tertiary erosional surface that had relatively high local relief. Northwest of the project area, in the vicinity of the Candelaria Hills, an east-trending trough of probable

block-fault origin existed, as suggested by Speed and Cogbill (1979c), and was filled by the correlative "upper Oligocene tuffs."

Subsequent to the eruption of the Castle Peak tuff and the older andesite, probably by about 16 or 15 m.y. ago (middle Miocene, late Hemingfordian-early Barstovian), andesitic volcanism was predominant, represented by the fine-grained and coarse-grained andesite flows. Shortly after, block faulting and associated extensional tectonism produced the basin in which the Blair Junction sequence of the Esmeralda Formation was to be deposited. Moiola (1969, p. 88-90) suggests that the Esmeralda Formation was deposited in two northwest-trending basins formed at this time. A short period of erosion was followed by the beginning of the dominantly lacustrine deposition of the Blair Junction sequence of the Esmeralda Formation, in middle to late Miocene time (late Barstovian to Hemphillian). The basal part of member 1 was deposited by braided streams and as overbank deposits along the distal end of an alluvial fan system. The fine-grained shale and lignitic beds in the upper part of member 1 were subsequently deposited in a marginal-lacustrine to paludal environment. Marginal lacustrine conditions continued throughout the deposition of members 2 and 3, with a deltaic influence that caused flucuating lake shorelines, as represented in member 2. Carbonate mudflat conditions prevailed intermittently adjacent to the lake. The abundance of tuffaceous material in the sedimentary rocks attests to the presence of concurrent volcanic activity in the region.

A period of uplift and erosion followed the deposition of member 3, which was followed by predominantly fluvial deposition accompanied by active volcanism and emplacement of volcanic mudflows from adjacent volcanic vents. Soon thereafter, minor andesite and rhyolite dikes and other small igneous bodies intruded into the Blair Junction sequence and older rocks. Many dikes were intruded along preexisting faults. The period of volcanism occurred in the latest Miocene to early Pliocene (Hemphillian) and was approximately coincident with the activity at the Silver Peak volcanic center.

A period of tilting and associated faulting occurred prior to the eruption of the basaltic andesite in the Pliocene. Active extensional tectonics and uplift continued during Pliocene time, during which oblique slip and dip slip occurred on faults in the project area. Continuing tectonic activity in the region is indicated by historic earthquakes of large magnitude and by Quaternary fault scarps at the base of Lone Mountain.

CONCLUSIONS

The stratigraphic record of the project area provides an example of deposition resulting from a complex interaction of specific tectonic and climatic conditions imposed on this region during late Cenozoic time. The Blair Junction sequence of the Esmeralda Formation, in the southern Monte Cristo Range, represents a succession of lithologic units of fairly local extent, which range in age from middle Miocene (late Barstovian to early Clarendonian) to late Miocene (Hemphillian), or about 13 to 7 m.y. before present. While the other contemporaneous sequences of the Esmeralda Formation, as described in the literature, are similar in general aspect, lithologic detail varies greatly owing to variable local depositional conditions. The Blair Junction sequence correlates with the lithologically similar Coaldale sequence at the northern base of the Silver Peak Range.

Lignitic intervals in member 1 of the Blair Junction sequence generally correlate with coal-bearing horizons at the north base of the Silver Peak Range. However, coaly material in member 1 is even thinner and of lower grade than coal in the coal mine area at the north base of the Silver Peak Range. The general decrease in coal content northward is attributed to the discontinuous nature of the accumulation of vegetative matter and irregular increases of inorganic shale laterally. Because of the low grade and low concentration of coal in the Blair Junction sequence, in addition to the complex structure of the area, determined by surface mapping, the coal deposits of

the southern Monte Cristo Range are considered subeconomic. Therefore, these lands are considered to be below the standards for "coal land" for the purpose of U.S. Geological Survey mineral land classification.

The stratigraphy in the southern Monte Cristo Range reveals a long period of uplift, nondeposition, and erosion from Early or Middle Ordovician to late Oligocene. During that time, regional deformations and intrusions of plutonic rocks occurred in the region and a transition was made from marine to continental conditions. After deposition of upper Oligocene to lower Miocene volcanic rocks, lacustrine conditions prevailed intermittently until Pliocene. The members of the Blair Junction sequence of the Esmeralda Formation were deposited in a mostly marginal-lacustrine to paludal environment. Evidence indicates that the water in the shallow lake was fresh, but alkaline. This lacustrine deposition evidently occurred during a somewhat warmer and considerably less arid climate than that of the present. Fluvial and volcanic influences were predominant during deposition of member 4. Tuffaceous material in the Blair Junction sequence has largely been diagenetically altered to montmorillonite, opal-CT, authigenic potassium feldspar, and minor zeolites.

The Castle Peak tuff is dominantly of an ash-flow origin and is probably correlative with tuffs in the Candelaria Hills and other adjacent areas. The Gilbert Andesite, as mapped by Ferguson and others (1953), is not exclusively of post-Esmeralda Formation or Pliocene age. Rather, different andesites grouped into the Gilbert

Andesite appear to range in age from as old as 25 m.y., to as young as 7 m.y. From regional compilation of radiometric dates, the bulk of the andesite erupted in this region occurred about 17 to 15 m.y. before present.

The structure of the southern Monte Cristo Range and the adjacent region is complex. Although vertical displacements along northeast-trending faults were predominant, there also is some evidence for oblique slip along these faults. This suggests that regional tectonic stresses responsible for deformation in this area were not purely extensional. The relationship between large-scale regional "structural" features such as Walker Lane and the Warm Springs lineament has not yet been substantiated. More regional analysis is necessary. However, the proximity to Walker Lane probably contributes to the rather anomalous fault trends encountered in the southern Monte Cristo Range.

REFERENCES

Albers, J.P., 1967, Belt of sigmoidal bending and right-lateral faulting in the western Great Basin: Geological Society of America Bulletin, v. 78, p. 143-156.

Albers, J.P., and Stewart, J.H., 1965, Preliminary geologic map of Esmeralda County, Nevada: U.S. Geological Survey Mineral Investigations Field Studies Map MF-298, scale 1:200,000.

_____, 1972, Geology and Mineral deposits of Esmeralda County, Nevada: Nevada Bureau of Mines and Geology Bulletin 78, 75 p.

Axelrod, D.I., 1940, The Pliocene Esmeralda Flora of west-central Nevada: Washington Academy of Science Journal, v. 30, p. 163-174.

_____, 1956, Mio-Pliocene floras from west-central Nevada: California University Publications in Geological Sciences, v. 33, 321 p.

Berry, E.W., 1927, Flora of Esmeralda Formation in western Nevada: U.S. Natural Museum Proceedings, v. 72, article 23, 15 p.

Boles, J.R., and Surdam, R.C., 1979, Diagenesis of volcanogenic sediments in a Tertiary saline lake; Wagon Bed Formation, Wyoming: American Journal of Science, v. 279, p. 832-853.

Buckley, C.P., 1971, The structural position and stratigraphy of the Palmetto Complex in the northern Silver Peak Mountains, Nevada [Ph.D. dissert.]: California University, Berkeley, 66 p.

Callaghan, Eugene, and Gianella, V.P., 1935, The earthquake of January 30, 1934, at Excelsior Mountains, Nevada: Seismological Society of America Bulletin, v. 25, p. 161-168.

Curtis, G.H., 1954, Mode of origin of pyroclastic debris in the Mehrten Formation of the Sierra Nevada: California University Publications in Geological Sciences, v. 29, p. 453-502.

Dalrymple, G.B., 1979, Critical tables for conversion of K-Ar ages from old to new constants: Geology, v. 7, p. 558-560.

Davis, J.R., and Vine, J.D., 1979, Stratigraphic and tectonic setting of the lithium brine field, Clayton Valley, Nevada, in Newman, G.W., and Goode, H.D., eds., Basin and Range Symposium and Great Basin Field Conference: Rocky Mountain Association of Geologists and Utah Geological Association, p. 421-430.

Deffeyes, K.S., 1959, Zeolites in sedimentary rocks: Journal of Sedimentary Petrology, v. 29, p. 602-609.

Ekren, E.B., Bucknam, R.C., Carr, W.J., Dixon, G.L., and Quinlivan, W.D., 1976, East-trending structural lineaments in Central Nevada: U.S. Geological Survey Professional Paper 986, 16 p.

Ekren, E.B., Byers, F.M., Hardyman, R.F., Marvin, R.F., Silberman, M.L., 1980, Stratigraphy, preliminary petrology, and some structural features of Tertiary volcanic rocks in the Gabbs Valley and Gillis Ranges, Mineral County, Nevada: U.S. Geological Survey Bulletin 1464, 54 p.

Evernden, J.F., and James, G.T., 1964, Potassium-argon dates and the Tertiary floras of North America: American Journal of Science, v. 262, p. 945-974.

Evernden, J.F., Savage, D.E., Curtis, G.H., and James, G.T., 1964, Potassium-argon dates and the Cenozoic mammalian chronology of North America: American Journal of Science, v. 262, p. 145-198.

Ferguson, H.G., 1924, Geology and ore deposits of the Manhattan district, Nevada: U.S. Geological Survey Bulletin 723, 163 p.

_____, 1927, The Gilbert district Nevada: U.S. Geological Survey Bulletin 795-F, p. 125-145.

Ferguson, H.G., and Muller, S.W., 1949, Structural geology of the Hawthorne and Tonopah quadrangles, Nevada: U.S. Geological Survey Professional Paper 216, 55 p.

Ferguson, H.G., Muller, S.W., Cathcart, S.H., 1953, Geology of the Coaldale Quadrangle, Nevada: U.S. Geological Survey Geologic Quadrangle Map GQ-23, scale 1:125,000.

_____, 1954, Geology of the Mina Quadrangle, Nevada: U.S. Geological Survey Geologic Quadrangle Map GQ-45, scale 1:125,000.

Firby, J.R., 1966, New non-marine mollusca from the Esmeralda Formation, Nevada: Proceedings of the California Academy of Sciences, Fourth Series, v. 33, p. 453-479.

Gilbert, C.M., Christensen, M.N., Al-Rawi, Yehya, and LaJoie, K.R., 1968, Structural and volcanic history of Mono Basin, California-Nevada, in Coats, R.R., Hay, R.L., and Anderson, C.A., eds., Studies in Volcanology: Geological Society of America Memoir 116, p. 275-329.

Gilbert, C.M., and Reynolds, M.W., 1973, Character and chronology of of basin development, western margin of the Basin and Range province: Geological Society of American Bulletin, v. 84, p. 2489-2509.

Glanzman, R.K., Rytuba, J.J., 1979, Zeolite-clay zonation of volcaniclastic sediments within the McDermitt caldera complex of Nevada and Oregon: U.S. Geological Survey Open-File Report 79-1668, 25 p.

Goddard, E.N., Trask, P.D., DeFord, R.K., Rove, O.N., Singewald, J.T., Jr., and Overbeck, R.M., 1975, Rock-color chart: Boulder, Geological Society of America, 11 p.

Hance, J.H., 1913, The Coaldale coal field, Esmeralda County, Nevada: U.S. Geological Survey Bulletin 531-K, p. 313-322.

Hay, R.L., 1963, Stratigraphy and zeolitic diagenesis of the John Day Formation of Oregon: California University Publications in Geological Sciences, v. 42, p. 199-262.

_____, 1966, Zeolites and zeolitic reactions in sedimentary rocks: Geological Society of America Special Paper 85, 130 p.

Hemley, J.J., 1959, Some mineralogical equilibria in the system K_2O-Al_2O_3-SiO_2-H_2O: American Journal of Science, v. 252, p. 241-270.

_____, 1962, Alteration studies in the system Na_2O-Al_2O_3-SiO_2-H_2O and K_2O-Al_2O_3-SiO_2-H_2O [abs.]: Geological Society of America Special Paper 68, p. 196.

Jones, J.B., and Segnit, E.R., 1971, The nature of opal, I. Nomenclature and constituent phases: Journal of the Geological Society of Australia, v. 18, p. 57-68.

Keith, W.J., 1977, Geology of the Red Mountain mining district, Esmeralda County, Nevada: U.S. Geological Survey Bulletin 1423, 45 p.

Knapp, M.A., 1897, The coal fields of Esmeralda County, Nevada: Mining and Science Press, v. 74, p. 133.

Knowlton, F.H., 1900, Fossil plants of the Esmeralda Formation: U.S. Geological Survey 21st Annual Report, pt. 2, p. 209-227.

Locke, Augutus, Billingsley, P.R., and Mayo, E.B., 1940, Sierra Nevada tectonic patterns: Geological Society of America Bulletin, v. 51, p. 513-540.

MacDonald, G.A., 1972, Volcanoes: New Jersey, Prentice-Hall Inc., 510 p.

Mariner, R.H., and Surdam, R.C., 1970, Alkalinity and formation of zeolites in saline alkaline lakes: Science, v. 170, p. 977-980.

Marvin, R.F., Mehnert, H.H., Speed, R.C., and Cogbill, A.H., 1977, K-Ar ages of Tertiary igneous and sedimentary rocks of the Mina-Candelaria region: Isochron/ West, no. 18, p. 9-12.

Moiola, R.J., 1963, Origin of authigenic silicate minerals in the Esmeralda Formation of western Nevada [abs.]: Geological Society of America Special Paper 76, p. 116-117.

_____, 1964, Authigenic mordenite in the Esmeralda Formation, Nevada: American Mineralogist, v. 48, p. 1472-1474.

_____, 1969, Late Cenozoic geology of the northern Silver Peak region, Esmeralda County, Nevada [Ph.D. dissert.]: Berkeley, California University, 139 p.

_____, 1970, Authigenic zeolites and K-feldspar in the Esmeralda Formation, Nevada: American Mineralogist, v. 55, p. 1681-1691.

Moiola, R.J., and Hay, R.L., 1964, Zeolite zones in Pleistocene Recent sediments of China Lake, California [abs.]: Geological Society of America Special Paper 76, p. 215.

Morton, J.L., Silberman, M.L., Bonham, H.F., Garside, L.J., and Noble, D.C., 1977, K-Ar ages of volcanic rocks, plutonic rocks, and ore deposits in Nevada and eastern California--Determination run under the USGS-NBMG Cooperative Program: Isochron/West, no. 20, p. 19-29.

Mullineaux, D.R., and Crandell, D.R., 1962, Recent lahars from Mount St. Helens, Washington: Geological Society of America Bulletin, v. 73, p. 855-870.

Page, B.M., 1959, Geology of the Candelaria mining district, Mineral County, Nevada: Nevada Bureau of Mines and Geology Bulletin 56, 67 p.

Papke, K.G., 1970, Montmorillonite, bentonite, and fuller's earth deposits in Nevada: Nevada Bureau of Mines and Geology Bulletin 76, 47 p.

Robinson, P.T., 1964, Geology of the Silver Peak Range [Ph.D. dissert.]: Berkeley, California University, 107 p.

Robinson, P.T., and Crowder, D.F., 1973, Geologic map of the Davis Mountain Quadrangle, Esmeralda and Mineral Counties, Nevada, and Mono County, California: U.S. Geological Survey Geologic Quadangle Map GQ-1078, scale 1:62,500.

Robinson, P.T., McKee, E.H., and Moiola, R.J., 1968, Cenozoic volcanism and sedimentation, Silver Peak region, western Nevada and adjacent California, in Coats, R.R., Hay, R.L., and Anderson, C.A., eds., Studies in Volcanology: Geological Society of America Memoir 116, p. 577-611.

Robinson, P.T., Stewart, J.H., Moiola, R.J., and Albers, J.P., 1976, Geologic map of the Rhyolite Ridge quadrangle, Esmeralda County, Nevada: U.S. Geological Survey Geologic Quadrangle Map GQ-1325, scale 1:62,500.

Ross, C.S., and Smith, R.L., 1961, Ash-flow tuffs: Their origin, geologic relations, and identification: U.S. Geological Survey Professional Paper 366, 81 p.

Ross, D.C., 1966, Stratigraphy of some Paleozoic formations in the Independence quadrangle, Inyo County, California: U.S. Geological Survey Professional Paper 396, 64 p.

Ross, R.J., Jr., and Berry, W.B.N., 1963, Ordovician graptolites of the Basin Ranges in California, Nevada, Utah, and Idaho: U.S. Geological Survey Bulletin 1134, 177 p.

Ryan, W.B.F., Cita, M.B., Rawson, M.D., Burckle, L.H., and Saito, P., 1974, A paleomagnetic assignment of Neogene stage boundaries and the development of isochronous datum planes between the Mediterranean the Pacific and the Indian Oceans in order to investigate the response of the world ocean to the Mediterranean "salinity crisis": Bivista Italiana di Paleontologia e Stratigrafia, v. 80, p. 631-688.

Ryder, R.T., Fouch, T.D., Elison, J.H., 1976, Early Tertiary sedimentation in the western Unita Basin, Utah: Geological Society of America Bulletin, v. 87, p. 496-512.

Schmincke, Hans-Ulrich, 1967, Graded lahars in the type sections of the Ellensburg Formation, southcentral Washington: Journal of Sedimentary Petrology, v. 37, p. 438-448.

Shawe, D.R., 1965, Strike-slip control of Basin-Range structure indicated by historical faults in western Nevada: Geological Society of America Bulletin, v. 76, p. 1361-1378.

Sheppard, R.A., and Gude, A.J., 1969, Diagenesis of tuffs in the Bartow Formation, Mud Hills, San Bernardino County, California: U.S. Geological Survey Professional Paper 634, 35 p.

_____, 1973, Zeolites and associated authigenic silicate minerals in tuffaceous rocks of the Big Sandy Formation, Mojave County, Arizona: U.S. Geological Survey Professional Paper 830, 36 p.

Silberman, M.L., Bonham, H.F., Jr., and Osborne, D.H., 1975, New K-Ar ages of volcanic and plutonic rocks and ore deposits in western Nevada: Isochron/West, no. 13, p. 13-21.

Smith, R.L., 1960a, Ash-flows: Geological Society of America Bulletin, v. 71, p. 795-841.

_____, 1960b, Zones and zonal variations in welded ash-flows: U.S. Geological Survey Professional Paper 354-F, p. 149-159.

Speed, R.C., and Cogbill, A.H., 1979a, Candelaria and other left-oblique slip faults of the Candelaria region, Nevada: Geological Society of America, Part I, v. 90, p. 149-163.

_____, 1979b, Cenozoic volcanism of the Candelaria region, Nevada: Geological Society of America Bulletin, Part II, v. 90, p. 456-493.

_____, 1979c, Deep fault trough of Oligocene age, Candelaria Hills, Nevada: Geological Society of America, Part II, v. 90, p. 494-527.

Spurr, J.E., 1904, Coal deposits between Silver Peak and Candelaria, Nevada: U.S. Geological Survey Bulletin 225-G, p. 289-292.

_____, 1906, Ore deposits of the Silver Peak quadrangle, Nevada: U.S. Geological Survey Professional Paper 55, 174 p.

Steiger, R.H., and Jager, E. 1977, Subcommission on geochronology. Convention on the use of decay constants in geo- and cosmochronology: Earth and Planetary Science Letters, v. 36, p. 359-362.

Stewart, J.H., 1967, Possible large right-lateral displacement along fault and shear zones in the Death Valley-Las Vegas area, California and Nevada: Geological Society of America Bulletin 78, p. 131-142.

_____,1978, Basin-range structures in western North America: A review in Smith, R.B., and Eaton, G.P., eds., Cenozoic tectonics and regional geophysics of the western Cordillera: Geological Society of America Memoir 152, p. 1-31.

_____, 1979, Geologic map of Miller Mountain and Columbus quadrangles, Mineral and Esmeralda counties, Nevada: U.S. Geological Survey Open-File Report 79-1145, scale 1:24,000.

Stewart, J.H., Robinson, P.T., Albers, J.P., and Crowder, D.F., 1974, Geologic map of the Piper Peak quadrangle, Nevada-California: U.S. Geological Survey Geologic Quadrangle Map GQ-1186, scale 1:62,500.

Stirton, R.A., 1932, Correlation of Fish Lake Valley and Cedar Mountain Beds in the Esmeralda Formation of Nevada: Science, v. 76, p. 60-61.

Surdam, R.C., and Stanley, K.O., 1979, Lacustrine sedimentation during the culminating phase of Eocene Lake Gosiute, Wyoming (Green River Formation): Geological Society of America Bulletin, Part I, v. 90, p. 93-110.

Surdam, R.C., and Wolfbauer, C.A., 1975, Green River Formation: A playa-lake complex: Geological Society of America Bulletin, v. 86, p. 335-345.

Teilhard de Chardin, P., and Stirton, R.A., 1934, A correlation of some Miocene and Pliocene mammalian assemblages in North America and Asia with a discussion of the Mio-Pliocene boundary: California University Bulletin, Department of Geological Science, v. 23, p. 277-290.

Toenges, A.L., Turnbull, L.A., and Schopf, J.M., 1946, Exploration of a coal occurring near Coaldale, Esmeralda County, Nevada: U.S. Bureau of Mines Technical Paper 687, 79 p.

Turner, H.W., 1900, The Esmeralda Formation, a fresh-water lake deposit: U.S. Geological Survey 21st Annual Report, part 2, p. 191-208.

Van Houten, F.B., 1956, Reconnaissance of Cenozoic sedimentary rocks of Nevada: American Association of Petroleum Geologists Bulletin v. 40, p. 2801-2825.

Walton, A.W., 1975, Zeolitic diagenesis in Oligocene volcanic sediments, Trans-Pecos, Texas: Geological Society of America Bulletin, v. 86, p. 615-624.

Wolfe, J.A., 1978, A paleobotanical interpretation of Tertiary climates of the Northern Hemisphere: American Scientist, v. 66, p. 694-703.

APPENDIX A: TABLE OF SELECTED RADIOMETRIC AGES FOR CENOZOIC ROCKS IN SOUTHWESTERN NEVADA

Ages are listed in order from youngest to oldest (Old Age= published age, pre-1976 constants; New Age= recalculated age based on revised decay and abundance constants of Steiger and Jager, 1977; * = number given is an average of several closely spaced ages; Two numbers given indicates a bracketing age range; a dash in the old column= published age was originally calculated using new constants).

Rock Unit (General Locality)	Reference, Sample No., and Material Dated	Age in M.Y. Old	Age in M.Y. New
1. Basalt, olivine (Candelaria Hills)	Marvin and others (1977), USGS-D2392R, whole rock	2.9±0.1	3.0±0.1
2. Basalt, olivine (Candelaria Hills)	Silberman and others (1975), CAN-2, whole rock	3.9±0.4	4.0±0.4
3. Basalt, olivine (Silver Peak Range)	Robinson and others (1968), no. 7, whole rock	4.8±0.6	4.9±0.6
4. Unnamed sedimentary rocks (Smith Valley)	Gilbert and Reynolds (1973), KA 2513, biotite	4.7±0.35	5.1±0.4
5. .....do.....	Gilbert and Reynolds (1973), KA 2491, hornblende	5.02±0.26	5.2±0.3
6. Volcanogenic Sedimentary rocks (southwest of Mina)	Marvin and others (1977), USGS-D2466B, biotite	5.7±0.2	5.9±0.2

Rock Unit (General Locality)	Reference, Sample No., and Material Dated	Age in M.Y. Old	Age in M.Y. New
7. Trachyandesite (Silver Peak Range)	Robinson and others (1968), no. 8, biotite	5.9±0.2	6.1±0.2
8. Rhyolite tuff (Silver Peak Range)	Robinson and others (1968), no. 6, biotite	6.0±0.5	6.2±0.5
9. Trachyandesite welded tuff (Silver Peak Range)	Robinson and others (1968), no. 5, biotite	6.1±0.3	6.3±0.3
10. Esmeralda Fm., air-fall tuff (east side of Big Smoky Valley near Monocline and Alum area)	Robinson and others (1968), no. 13, biotite	6.9±0.3	7.1±0.3
11. Obsidian (northeast Monte Cristo Range)	Silberman and others(1975), Black Balls, obsidian	7.0±0.2	7.2±0.2
12. Sedimentary rocks (north flank of Pilot Mtns.)	Marvin and others (1977), USGS-D2466B?,biotite	7.3±0.2	7.5±0.2
13. Quartz-adularia vein (central Monte Cristo Range, near Gilbert)	Silberman and others(1975) GLA-1, adularia and sanidine	7.9±0.2	8.1±0.2
14. Coal Valley Fm., tuff (Coal Valley)	Gilbert and Reynolds(1973) KA 2439, hornblende	9.14±0.44	9.4±0.5

Rock Unit (General Locality)	Reference, Sample No., and Material Dated	Age in M.Y. Old	Age in M.Y. New
15. Coal Valley Fm.,tuff (Coal Valley)	Gilbert and Reynolds (1973), KA 2432, hornblende	10.42±0.49	10.7±0.5
16. Esmeralda Formation (Cedar Mtn. area)	Evernden and others (1964), KA 452, biotite	10.7	10.9
17. Esmeralda Fm., tuff (Fish Lake Valley)	Evernden and others (1964), KA 480, biotite	11.1	11.4
18. Alrich Station Fm., tuff (near Alrich Station, Coal Valley)	Evernden and others (1964), KA 414, biotite	11.2	11.5
19. Sedimentary rocks, tuff (North Fish Lake Valley)	Evernden and others (1964), KA 499, biotite	11.4	11.7
20. Sedimentary rocks, tuff (Cedar Mtns.)	Evernden and others (1964), KA 577, sanidine	11.5	11.8
21. Alrich Station Fm., tuffs (near Alrich Station, Coal Valley)	Gilbert and Reynolds (1973), KA 2379R, KA 2375, KA 2440, KA 2503, and KA 2501, biotite or hornblende	11.5*	11.8*
22. Andesite, hornblende-biotite, unaltered (southeast of Pine Grove Hills, near East Walker River)	Gilbert and Reynolds (1973), KA 2368, biotite	12.33±0.31	12.7±0.3

Rock Unit (General Locality)	Reference, Sample No., and Material Dated	Age in M.Y. Old	Age in M.Y. New
23. Andesite, hornblende-biotite dike (Southeast of Pine Grove Hills, near East Walker River)	Gilbert and Reynolds (1973), KA 2372, biotite	12.42±0.17	12.8±0.2
24. Esmeralda Fm., tuff, interbedded with coal, type locality (North base Silver Peak Range)	Evernden and James (1964), KA 1268, biotite	12.7	13.0
25. Esmeralda Fm., tuff (Fish Lake Valley)	Robinson and others (1968), no. 1, biotite	13.1	13.4
26. Andesite, hornblende (Cambridge Hills, North of Coal Valley)	Gilbert and Reynolds (1973), KA 2493, hornblende	14.88±0.47	15.3±0.5
27. Andesite, pyroxene (Mt. Ferguson)	Morton and others (1977), 2605-5	-------	15.4±0.5
28. Andesite, breccia (Stewart Valley)	Morton and others (1977), 11920-2, hornblende	-------	15.4±0.5
29. Andesite, biotite-pyroxene (Central Monte Cristo Range, south of Gilbert)	Silberman and others (1975), GL-2, biotite	15.1±0.5	15.5±0.5

Rock Unit (General Locality)	Reference, Sample No., and Material Dated	Age in M.Y. Old	Age in M.Y. New
30. Andesite, biotite	Albers and Stewart (1972), Gilbert Andesite, biotite	15.1±0.6	15.5±0.6
31. Andesite, or basalt (Candelaria Hills)	Marvin and others (1977), USGS-D2390R, whole rock	15.7±0.5	16.1±0.5
32. Andesite, hornblende (West of Candelaria Hills)	Marvin and others (1977), USGS-D24051Pl, plagioclase	17.4±0.6	17.9±0.6
33. Rhyolite, crystal tuff, Unit 7 of Speed and Cogbill (1979)= Belleville tuff (Candelaria Hills)	Marvin and others (1977), USGS-D2436Pl, plagioclase	21.4±0.9	22.0±0.9
34. Rhyolite, welded tuff, (Silver Peak Range, north of Emigrant Pk.)	Robinson and others (1968), no. 12, biotite	21.5±1.0	22.1±1.0
35. Rhyolite tuff (West of Miller Mtn.)	Gilbert and others (1968), KA 1979, sanidine	22.0±0.4	22.6±0.4
36. Rhyolite, vitrophyre (West of Miller Mtn.)	Gilbert and others (1968), KA 1970, sanidine	22.1±0.3	22.7±0.3
37. Rhyolite, crystal tuff Unit 9 of Speed and Cogbill (1979)= Candelaria Junction Tuff (Candelaria Hills)	Marvin and others (1977), USGS-D2381B, biotite; USGS-D2550S, sanidine	22.2±0.8 to 22.9±0.5	22.8±0.8 to 23.5±0.5

Rock Unit (General Locality)	Reference, Sample No., and Material Dated	Age in M.Y. Old	Age in M.Y. New
38. Rhyolite, welded tuff (Southeast flank of Miller Mtn.)	Robinson and others (1968), no. 14, biotite	22.8±1.0	23.4±1.0
39. "Upper Oligocene tuffs", complex of lithologically distinct units; includes Units 6, 5(Metallic City Tuff), 4, 3, and 2 of Speed and Cogbill (1979b) (Candelaria Hills)	Marvin and others (1977), USGS-D2380B, sanidine and biotite, respectively	22.1±0.4 to 24.2±0.9	22.7±0.4 to 24.8±0.9
40. Andesite, hornblende (East side of Pilot Mtns.)	Morton and others (1977), 16149-1, hornblende	--------	24.7±0.7
41. Rhyolite, crystal tuff, Unit 1 of Speed and Cogbill (1979b) (Candelaria Hills)	Marvin and others (1977), USGS-2379B, biotite	24.7±0.8	25.4±0.8
42. "Older tuff" of Speed and Cogbill (1979b) (North Pilot Mtns.)	Marvin and others (1977), USGS-D2464B, biotite	26.7±0.9	27.4±0.9
43. "Older tuff" of Speed and Cogbill (1979b) (Excelsior Mtns.)	Marvin and others (1977), B-3462, biotite	27.1±1.5	27.8±1.5

APPENDIX B: MEASURED STRATIGRAPHIC SECTIONS

Measured Section SS I

Stratigraphic section measured of Members 1 and 3 of the Blair Junction sequence of the Esmeralda Formation, in the Jackrabbit Draw area located in unsurveyed township T. 2 N., R. 38 E., M.D.M., approximately in sections 5 and 8 (SS I on fig. 14).

		Thickness (m)
Member 3 of Blair Junction sequence of the Esmeralda Formation (upper Miocene, middle to upper Clarendonian):		
Overlain by Quaternary older fan deposits:		
21.	Shale and tuff; shale white (N 9), tuffaceous and papery; interbedded with thin layers of grayish-yellow-green (5GY 7/2) vitric tuff, largely devitrified; thin interbeds of shale and tuff average 10 cm in thickness; minor sandstone lens near top composed largely of coarse and angular- to subangular grains of quartz and feldspar.....	15.0
20.	Tuff, white (N 9), fine-grained, composed of ash, and biotite and quartz phenocrysts....	1.5
19.	Shale and tuff; same as unit 21.....	7.0
18.	Siltstone, white (N 9) to light-greenish-gray (5GY 8/1), tuffaceous and platy	0.5
17.	Shale and tuff; same as unit 21, except with 0.5-m-thick, yellowish-gray (5Y 8/1), coarse- to very coarse-grained sandstone bed at base.....	5.6
16.	Shale and sandstone, white (N 9); shale breaks into small chunky, 0.5- to 3.0-cm, angular fragments; porcellaneous; coarse-grained white (N 9) to yellowish-gray (5Y 8/1), 0.4-m-thick sandstone lens at base	2.4
15.	Sandstone, moderate-brown (5YR 4/4), medium-grained; subangular grains; abundant feldspar and biotite.....	1.1

Measured Section SS I of Esmeralda Formation, Blair Junction sequence, member 3--Continued

		Thickness (m)
14.	Sandstone; same as unit 15, except contains lens of coarse-grained sandstone as described in unit 16.....	3.7
13.	Tuff, very light-gray (N 8); contains several coarse-grained sandstone lenses, each 0.1- to 0.3 cm thick; tuff composed mostly of vitric material with abundant biotite and quartz crystals.....	4.2
12.	Tuff; same as unit 20.....	12.5
11.	Pebbly sandstone, pale-brown (5YR 5/2); subrounded pebbles of weathered hornblende andesite averaging 1 cm in diameter, make up 3 to 5 percent of bed; poorly sorted, subangular, coarse- to medium-grained sandstone composes most of unit; minor crossbeds.....	10.5
10.	Granule conglomerate, grayish-yellow (5Y 8/4); small pebble- to granule-sized lithic material comprises about 10 percent of unit; poorly sorted sand to ash matrix; biotite-bearing quartz arenite; crossbedded.....	1.3
9.	Tuff, very light-gray (N 8), relatively homogeneous and structureless; composed mostly of ash with crystals of quartz and biotite; clasts of shale and sandstone incorporated at base of tuff.....	15.4
8.	Sandstone, yellowish-gray (5Y 7/2); subangular to subrounded grains; graded, fining upward, from very coarse grained to fine grained; tuffaceous; calcareous cement, local iron-oxide staining.....	1.9
7.	Shale, white (N 9) to very light-gray (N 8), tuffaceous, papery; some alteration of vitric material to clay.....	1.0
6.	Limestone, grayish-orange (10YR 7/4) to dark-yellowish-orange (10YR 6/6); flaggy, erosion-resistant beds; fossil-rich, mostly gastropods, some bivalves and ostracodes.....	0.8

Measured Section SS I of Esmeralda Formation, Blair Junction sequence, member 3--Continued

		Thickness (m)
5.	Claystone, grayish-orange (10YR 7/4), siliceous.....	0.9
4.	Limestone; same as unit 6, except less abundant fossil molluscs.....	0.2
3.	Siltstone, pale-yellowish-orange (10YR 8/6), soft, erodible, and tuffaceous.....	1.6
2.	Sandstone and shale, very light-gray (N 8), poorly exposed, alternating beds; tuffaceous; thinly bedded; sandstone beds grade upward into shale beds.....	13.0
1.	Siltstone and sandstone, very light-gray (N 8) to very pale-orange (10YR 8/2); alternating siliceous, chunky siltstone (breaking into 2- to 5-cm angular fragments) siltstone, with tuffaceous, graded, fining upward sandstone; thin beds 4 to 10 cm thick.....	3.5
	Total thickness of Member 3 measured.....	103.6

Member 1 of the Blair Junction sequence of the Esmeralda Formation. Fault contact with overlying member 3. Zone of intensely folded beds (not measured).

72.	Siltstone and claystone, very pale-orange (10YR 7/4) to pale-yellowish-orange (10YR 8/6); porcellaneous to siliceous siltstone breaks into roughly equant, angular chips; interbedded with friable, soft, tuffaceous very pale-orange (10YR 8/2) to dark-yellowish-orange (10YR 6/6) claystone that exhibits a "popcornlike" weathered surface (montmorillonite); very regular interbeds of alternating siltstone and claystone range from 0.05 to 0.45 m thick.....	3.5
71.	Shale, pale-yellowish-brown (10YR 6/2), carbonaceous; weathers into paper-thin, flexible chips 10 cm or less in width.....	0.5

Measured Section SS I of Esmeralda Formation, Blair Junction sequence, member 1--Continued

		Thickness (m)
70.	Shale, very pale-orange (10YR 8/2) to yellowish-gray (5YR 8/1); thin, 1- to 3-cm-thick interbeds of alternating porcellaneous and papery shale.....	2.5
69.	Shale, very light-gray (N 8), papery.....	1.5
68.	Silt shale, very pale-orange (10YR 8/2), porcellaneous.....	0.5
67.	Sandstone and shale; pale-yellowish-orange (10YR 8/6) sandstone, medium- to fine-grained, moderately well-sorted, sandstone; subangular grains; grades upward into yellowish-gray (5Y 8/1), papery shale; fibrous gypsum along fractures and partings in shale.....	0.24
66.	Shale, pale-yellowish-brown (10YR 6/2), carbonaceous, papery.....	0.06
65.	Silt shale; same as Unit 68.....	1.5
64.	Shale and sandstone, interbedded; shale, same as unit 66, occurring in 2- to 3-cm-thick beds; minor interbeds of dark-yellowish-orange (10YR 6/6) sandstone, medium-grained, moderately sorted.....	0.2
63.	Shale; same as unit 67.....	0.2
62.	Shale, yellowish-gray (5Y 8/1) to very pale-orange (10YR 8/2), papery, tuffaceous, and finely laminated.....	0.2
61.	Coal, dark-yellowish-brown (10YR 4/2), lignitic, ashy.....	0.05
60.	Shale; same as Unit 62.....	0.1
59.	Coal; same as Unit 61.....	0.15
58.	Shale; same as Unit 62.....	0.30

Measured Section SS I of Esmeralda Formation, Blair Junction sequence, member 1--Continued

		Thickness (m)
57.	Coal; same as Unit 61.....	0.2
56.	Shale; same as Unit 62.....	0.3
55.	Coal; pale-yellowish-brown (10YR 6/2), lignitic, bony coal with numerous thin (5- to 30-mm spaced shale partings).....	0.7
54.	Siltstone, very pale-orange (10YR 8/2), to pale-yellowish-orange (10YR 8/6) on weathered surface, hard, silicified to porcellaneous.....	5.0
53.	Shale, yellowish-gray (5Y 7/2), soft, erodible, tuffaceous; 2- to 4-cm-thick beds.....	7.5
52.	Shale; same as unit 53; locally intruded by weathered, greenish hornblende andesite dike up to 2 m thick.....	3.0
51.	Limestone, dark-yellowish-brown (10YR 4/2), unfossiliferous.....	0.5
50.	Shale; same as unit 53.....	0.75
49.	Limestone, dark-yellowish-brown (10YR 4/2); fossilferous, mostly gastropods.....	0.6
48.	Claystone and clay shale, dark-yellowish-brown (10YR 4/2), easily erodible, "popcorn-like" weathering surface (indicative of montmorillonite clay group).....	19.4
47.	Shale; same as unit 70, except color is pale-yellow-orange (10YR 8/6) to grayish-orange (10YR 7/4).....	2.0
46.	Limestone, pale-yellowish-orange (10YR 8/6) to grayish-orange (10YR 7/4); extremely fossiliferous, loaded with silicified gastropods and pelecypods 1 to 2.5 cm in diameter; abundant ostracodes.....	0.3

Measured Section SS I of Esmeralda Formation, Blair Junction sequence, member 1--Continued

		Thickness (m)
45.	Sandstone, grayish-orange (10YR 7/4); thinly-bedded; moderately sorted, fine- to medium-grained.....	7.7
44.	Silt shale, yellowish-gray (5YR 8/1), brittle, papery habit.....	2.5
43.	Siltstone, very pale-orange (10YR 8/2) to pale-yellowish-orange (10YR 8/6), hard, silicified.....	2.0
42.	Shale; same as unit 62.....	0.5
41.	Siltstone; same as unit 54.....	2.25
40.	Silty sandstone, grayish-orange (10YR 7/4), moderately-sorted.....	1.0
39.	Shale; same as unit 62.....	2.0
38.	Clay shale; same as unit 48.....	1.2
37.	Claystone, siltstone, and sandstone; grayish-orange (10YR 7/4) to dark-yellowish-orange (10YR 6/6) claystone and siltstone; interbedded with pale-yellowish-orange (10YR 8/6), fine- to medium-grained sandstone; repetitive sequence of alternating thin beds of sandstone, siltstone, and claystone; sandstones are notably graded, fining upward.....	19.8
36.	Claystone, siltstone, and sandstone; same as Unit 37, except contains a 1.5-m-thick lens of pebble conglomerate; most pebbles are subrounded, 3 cm or less in diameter, and mostly of andesitic composition.....	2.0
35.	Conglomerate, light-olive-gray (5Y 5/2), lensoidal; pebbles of andesitic composition average about 3 cm in diameter.....	0.5
34.	Sandstone, grayish-green (10GY 5/2), moderately sorted.....	2.0

Measured Section SS I of Esmeralda Formation, Blair Junction sequence, member 1--Continued

		Thickness (m)
33.	Conglomerate; same as unit 35.....	1.9
32.	Silty claystone, pale-yellowish-brown (10YR 6/2); laminated in 3-cm-wide bands; soft, erodible unit with "popcornlike" weathered surface.....	2.5
31.	Conglomerate; same as unit 35.....	1.8
30.	Tuff, light brown (5YR 6/4), about 2 percent biotite; friable.....	3.3
29.	Conglomerate; same as unit 35.....	2.75
28.	Tuff, grayish-orange (10YR 7/4); disseminated 1- to 4-mm fragments of lignite; vitric material largely altered to clay.....	1.9
27.	Conglomerate, grayish-olive (10YR 4/2); composed of subrounded, volcanic, mostly andesitic pebbles; largest clast to 25 cm in diameter; silty sand matrix composes about 40 percent of this unit.....	4.4
26.	Tuff and claystone, pale-yellowish-brown (10YR 6/2) to yellowish-gray (5YR 8/1); interbedded, thin, water-lain tuffs and tuffaceous claystone; vitric material is altered to montmorillonite clay.....	5.6
25.	Tuff, pale-yellowish-brown (10YR 6/2); vitric material partially altered to montmorillonite; thin interbeds of angular-grained siltstone and sandstone; friable and erodible; lower 3.5 m contains abundant silicified wood, very-pale-orange (10YR 8/2) to dark-yellowish-brown (10YR 4/2) with relict concentric growth rings, fragments up to 0.4 m across.....	12.2
24.	Siltstone and claystone, pale-yellowish-orange (10YR 6/2), tuffaceous, thin-bedded; common fragments of silicified wood.....	3.5

Measured Section SS I of Esmeralda Formation, Blair Junction sequence, member 1--Continued

		Thickness (m)
23.	Siltstone and claystone; same as unit 24, except without silicified wood.....	3.3
22.	Claystone, siltstone, and sandstone; same as unit 37; near top, intruded by a 2.8-m-wide, gray silicic dike that intrudes unit approximately along strike.....	5.5
21.	Sandstone, moderate-reddish-brown (10R 4/6), very fine- to fine-grained, moderately sorted, oxidized.....	5.5
20.	Tuff, yellowish-gray (5Y 7/2); common lignite fragments, some with woody texture.....	2.7
19.	Sandstone and shale; sandstone as in unit 21, interbedded with shale, pale-yellowish-brown (10YR 6/2).....	5.7
18.	Claystone; same as unit 48; carbonized wood fragments near base.....	14.2
17.	Tuff, white (N 9) to light-greenish-gray (5G 8/1), friable and erodible.....	1.6
16.	Tuff, pale-yellowish-brown (10YR 6/2), soft, friable, and easily eroded; partially altered to clay, probably montmorillonite; contains 1- to 5-cm, lath-like fragments of lignite, and scattered fragments of silicified wood.....	3.0
15.	Sandstone, moderate-reddish-brown (10YR 4/6), coarse-grained, moderately sorted, oxidized.....	5.1
14.	Conglomerate; composed mostly of light-olive-gray (5Y 5/2) to oxidized, moderate-reddish-brown (10YR 4/6), coarse- to very coarse-pebbles of andesitic composition, in a sandy matrix; maximum size of pebbles is 7 cm; subrounded clasts; moderately sorted.....	3.1

Measured Section SS I of Esmeralda Formation, Blair Junction sequence, member 1--Continued

		Thickness (m)
13.	Tuff, white (N 9) to very pale-orange (10YR 8/2); silicified wood fragments, several centimeters, long are concentrated in the upper 1.5 m; one minor 0.7-m-thick lens of andesite cobble and pebble conglomerate....	9.4
12.	Tuff; same as unit 16.....	0.8
11.	Tuff; same as unit 13, except without silicified wood.....	2.9
10.	Conglomerate; composed of cobble and pebbles of porphyritic andesite.....	0.7
9.	Claystone; same as unit 38.....	1.5
8.	Tuff, very light-gray (N 8); contains lapilli-size pumice.....	0.7
7.	Sandstone, moderate-brown (5YR 4/4), fine- to medium-grained, poorly sorted, tuffaceous; contains about 1 percent biotite..	1.6
6.	Conglomerate, composed of light-olive-gray (5Y 5/2), coarse pebbles and cobbles (2 to 18 cm in diameter); well-rounded clasts with high sphericity; about 60 percent poorly sorted sandy matrix.....	4.5
5.	Pebbly sandstone; sandstone is same as sandstone in unit 7; poorly exposed; has weathered clasts of andesite; locally intruded by a small, 1.5-m-wide hornblende andesite dike.....	13.0
4.	Cobbly sandstone, moderate-reddish-brown (10R 4/6); poorly sorted; subangular grains; a few cobbles of porphyritic andesite.....	9.3
3.	Conglomerate; same as unit 6.....	0.7
2.	Sandstone; same as unit 7, but contains common fragments of silicified wood.....	5.2

Measured Section SS I of Esmeralda Formation, Blair Junction sequence, member 1--Continued

	Thickness (m)
1. Pebbly sandstone, moderate-reddish-brown (10R 4/6), strongly oxidized, friable, poorly bedded, medium- to coarse-grained; several lenses of conglomerate with andesitic pebbles and rare cobbles.....	4.5
Total measured thickness of member 1.....	239.55

Castle Peak tuff, unwelded member (lower Miocene): not measured; unconformable contact with overlying member 1.

Measured Section SS II

Stratigraphic section measured of members 1, 2, and 3 of the Blair Junction sequence of the Esmeralda Formation, south of U.S. Highway 6/95 in the SE 1/4 sec. 22 and NW 1/4 sec. 23, T. 2 N., R. 37 E., M.D.M. (SS II on fig. 14).

Member 3 of the Blair Junction sequence of the Esmeralda Formation (middle Miocene, middle to upper Clarendonian): overlain by Quaternary alluvium.

		Thickness (m)
7.	Siltstone and sandstone, yellowish-gray (5Y 7/2) to moderate-yellowish-brown (10YR 5/4) siltstone, with lenses of very pale-orange (10YR 8/2), coarse-grained sandstone, cemented by calcite; sandstone lenses are composed primarily of angular grains of clear quartz and feldspar, lithic fragments, and biotite; extremely silicified, and breaks into angular, sharp-edged plates to small 2- to 4-cm fragments; major ridge former.....	5.0
6.	Siltstone, pale-yellowish-orange (10YR 8/6), silicified and platy, with impressions of reedy plant material.....	2.9
5.	Sandy limestone, moderate-yellowish-brown (10YR 5/4) to dark-yellowish-brown (10YR 4/2), platy, medium- to coarse-grained; angular sand grains are supported by dense calcite cement; very abundant fossils, mostly broken shells of gastropods.....	0.6
4.	Siltstone, white (N 9) to pale-yellowish-orange (10YR 8/6), tuffaceous, and thinly laminated.....	4.0
3.	Siltstone and sandstone, poorly exposed, pale-yellowish-orange (10YR 8/6), tuffaceous siltstone; interbedded, but less abundant, moderate-olive-brown (5Y 4/4), medium-grained sandstone.....	13.0

Measured Section SS II of Esmeralda Formation, Blair Junction sequence, member 3--Continued

		Thickness (m)
2.	Sandy limestone, light-gray (N 7) to dusky-yellowish-brown (10YR 2/2); sand grains within calcareous matrix are medium to coarse and subangular; unfossiliferous.....	1.0
1.	Covered by alluvium, and very poorly exposed, erodible; interbedded shale, tuff, minor siltstone.....	85.5
	Total thickness of Member 3.....	112.0

Member 2, conformable contact with overlying member 3.

21.	Conglomerate; composed of pale-brown (5YR 4/4), weathered andesite cobbles (to 15 cm in diameter) and pebbles; clasts are subrounded; poorly sorted, sandy matrix....	3.0
20.	Sandstone, moderate-olive-brown (5Y 4/4), moderately well-sorted, fine- to medium-grained; subangular grains; graded fining upward.....	3.0
19.	Sandstone, dark-yellowish-orange (10YR 6/6), platy and extremely siliceous, fine-grained; lath-shaped, wood-like impressions of plant material along partings in bed.....	0.9
18.	Sandstone and siltstone; sandstone same as unit 20, with siltstone, dark-yellowish-orange (10YR 6/6); beds range in thickness from about 0.5 to 1.0 m.....	5.0
17.	Sandstone, yellowish-gray (5Y 7/2), platy, siliceous, fine-grained.....	0.5
16.	Siltstone and sandstone; same as unit 18.....	12.0
15.	Sandstone; same as unit 19.....	0.5
14.	Sandstone; same as unit 20.....	1.0

Measured Section SS II of Esmeralda Formation, Blair Junction sequence, member 2--Continued

		Thickness (m)
13.	Limestone, dark-yellowish-brown (10YR 6/2) fissile and platy, with rare fossil gastropods.....	0.5
12.	Sandstone; same as unit 20, except contains common, broken fossil gastropods.....	1.0
11.	Limestone; same as unit 13, except rich in fossil gastropods.....	0.5
10.	Sandstone; same as unit 17.....	4.5
9.	Silt shale and sandstone, siliceous; containing a 1.0-m-thick interbed of sandstone, same as unit 20.....	3.0
8.	Sandstone, dusky-brown (5Y 6/4); subangular grains, quartz, feldspar and lithic fragments; laminated with several-cm-thick beds; graded, fining upwards, from coarse to fine grained.....	7.5
7.	Siltstone, dark-yellowish-orange (10YR 6/6) hard, erosion-resistant, tuffaceous and silicified.....	1.0
6.	Sandstone; same as unit 20.....	9.0
5.	Siltstone; same as unit 7.....	0.90
4.	Sandstone, dusky-yellow (5Y 6/4) to light-olive-brown (5Y 5/6), moderately well-sorted, fine- to medium-grained; graded, fining upwards; evenly thin bedded, 1- to 5-cm-thick beds.....	12.0
3.	Siltstone; same as unit 7.....	0.5
2.	Sandstone; same as unit 4.....	13.5

Measured Section SS II of Esmeralda Formation, Blair Junction sequence, member 2--Continued

	Thickness (m)
1. Sandstone, light-olive-brown (5Y 5/6) on fresh surfaces to moderate-olive-brown (5Y 4/4) on weathered surfaces; outcrop has massive appearance; 3- to 5-mm laminations; moderately sorted, subangular grains; graded, fining upward from fine- to very fine-grained, thin layers with impressions of woody material, size range of fragment impressions about 0.5 cm; minor crossbeds; sandstone composed mostly of comminuted lithic fragments (mostly andesite) with feldspar and quartz	9.0
Total thickness of Member 2.....	88.8

Member 1, partial thickness measured. Contact with overlying member 2 conformable.

1. Shale and sandstone, white (N 9) to very pale-orange (10YR 8/2), to dark-yellowish-orange (10YR 6/6) with more pronounced weathering; thin-bedded, generally 2- to 8-cm-thick shale beds, typically weathers into 1- to 10-mm, angular, flat chips; nature of shale varies from tuffaceous to porcellaneous, some beds breaking into papery layers; more minor tuffaceous sandstone interbeds, fine grained, with moderate sorting; generally forms poor outcrops.....	97.5
Total thickness of member 1 measured..... (Base of unit not exposed).	97.5

Measured Section SS III

Stratigraphic section measured of member 1 of the Blair Junction sequence of the Esmeralda Formation in NW 1/4 sec. 6, of unsurveyed township T. 2 N., R. 38 E., M.D.M. (SS III on fig. 14).

	Thickness (m)
Member 1 of the Blair Junction sequence of the Esmeralda Formation (middle Miocene, upper Barstovian-lower Clarendonian):	
Fault contact with younger intrusive hornblende andesite (Tai).	
12. Claystone and shale; interbedded tuffaceous claystone, and lignitic paper shales.....	17.8
11. Lignite, light-brown (5YR 6/4), papery, ashy low density; impressions of lath-like, woody plant material.....	0.3
10. Carbonaceous tuff and claystone, medium-light-gray (N 6); tuff is mostly altered to clay and locally contains abundant black (N 2) fragments of coaly or carbanaceous woody plant matter, or thin lignitic stringers; poorly exposed.....	13.8
9. Sandy tuff, grayish-orange (10YR 7/4); composed of fine-sand size, well-rounded quartz grains in ash matrix.....	1.8
8. Claystone, gray (N 7), tuffaceous.....	2.3
7. Lignitic claystone, yellowish-gray (5Y 8/1), tuffaceous; with fragments of black (N 2), woody lignitic material.....	0.20
6. Claystone and sandstone lenses, dominantly gray (N 7) to grayish-orange (10YR 7/4) tuffaceous claystone; with interbedded 0.2- to 0.8-m-thick, moderately sorted, fine- to medium-grained, tuffaceous sandstone lenses.....	9.2

Measured Section SS III of Esmeralda Formation, Blair Junction sequence, member 1--Continued

	Thickness (m)
5. Conglomerate, dark-yellowish-orange (10YR 6/2), granule- to pebble-, iron-oxide stained, moderately sorted; 3- to 8-mm diameter, rounded clasts of reworked rhyolitic tuff in a tuffaceous, matrix.....	0.8
4. Sandstone and shale, gray (N 7); sandstone with thin shale partings.....	1.1
3. Conglomerate, dark-yellowish-orange (10YR 6/2), with thorough iron-oxide staining; composed of fine- to coarse-pebbles 0.5 to 3.0 cm in diameter, with largest clasts about 7 to 8 cm; poorly sorted sand and silt matrix; friable; pebbles are rounded volcanic rocks, mostly porphyritic hornblende andesite with less abundant rhyolite; overall moderately sorted.....	3.5
2. Sandstone, shale, and conglomerate, very pale-orange (10YR 8/2) and conglomerate, poorly exposed; all contain a large component of reworked, tuffacaeous material; Sandstones are generally lensoidal and 0.3 to 0.7 m in maximum thickness; lensoidal granule- to pebble-conglomerate beds are graded, fining upward, and alternate with sandstone	15.7
1. Conglomerate, yellowish-orange (10YR 6/2), bouldery, poorly sorted; comprised mostly of weathered porphyritic, medium- to coarse-grained, biotite-hornblende-andesite clasts; andesite is probably derived from map unit Tca, (coarse-grained andesite); tuffaceous to clayey matrix; generally poorly exposed, but resistant subrounded boulders stand out in relative relief.....	1.7
Partial thickness of member 1 measured.....	68.2

Measured Section SS III of Castle Peak tuff, unwelded tuff member--Continued

	Thickness (m)
Castle Peak tuff, unwelded tuff member (upper Oligocene or lower Miocene): Fault contact with member 2 of the Blair Junction sequence of the Esmeralda Formation.	
1. Tuff, very light-gray (N 8) to light-greenish-gray (5G 8/1); 90 to 95 percent of rock is composed of fine rhyolitic ash and pumice fragments; common subrounded- to subangular-clasts of light-gray (N 7) to grayish-olive-green (5GY 5/2) andesite pebbles, pebbles averaging 1 to 5 cm in diameter, up to cobbles 15 cm in diameter; locally silicified tuff is partially compacted.....	9.9
Partial thickness measured of unwelded tuff member.....	9.9

Castle Peak tuff continues below, unmeasured.

Measured Section SS IV

Stratigraphic section measured of members 3 and 4, of the Blair Junction sequence of the Esmeralda Formation, in SE 1/4 sec. 15, and SW 1/4 sec. 14, T. 2 N., R. 37 E., M.D.M., (SS IV on fig. 14).

Member 4 of the Blair Junction sequence of the Esmeralda Formation (upper Miocene, Hemphillian):

		Thickness (m)
13.	Lahar, yellowish-gray (5Y 7/2) to pale-olive (10Y 6/2), overall color, multi-lithologic clasts of very light-gray (N 8), porphyritic rhyolite, and black and green chert and andesite; very poorly sorted, with clasts ranging from 1 to 2 cm as much as 1 m in diameter, averaging about 15 cm in diameter; most clasts are subangular to angular; pebble-to cobble-size clasts comprise about 40 percent of this unit; a tuffaceous, coarse- to very coarse-sandstone at base, reversely grades up into boulder-size clasts.....	4.5
12.	Siltstone, grayish-orange (10YR 7/4) to dark-yellowish-orange (10YR 6/6), thin-bedded, siliceous to tuffaceous.....	7.0
11.	Limestone, dark-yellowish-brown (10YR 5/4), very thin-bedded; unfossiliferous.....	0.7
10.	Siltstone; same as unit 12.....	1.3
9.	Conglomerate and sandstone, pale-olive (10Y 6/2), conglomerate is composed mostly of small pebbles; with lenses of coarse-grained sandstone.....	7.2
8.	Lahar, pale-olive (10Y 6/2); contains clasts of rhyolite up to 1.5 m; very poorly sorted; coarse, tuffaceous sandstone matrix.....	1.8
7.	Conglomerate and sandstone; same as unit 9...	1.5

Measured Section SS IV of Esmeralda Formation, Blair Junction sequence, member 4--Continued

	Thickness (m)
6. Pebbly sandstone, light-olive-gray (5Y 5/2), graded (fining upward), coarse- to fine-grained; with scattered subrounded pebbles averaging about 1 cm in diameter.....	1.9
5. Lahar, light-olive-brown (5Y 5/6), very poorly sorted; up to about 1-m-diameter boulders of rhyolite in a tuffaceous to sandy matrix; poorly developed reverse grading of volcanic clasts.....	1.6
4. Sandstone, yellowish-gray (5Y 7/2), massively bedded, medium-grained sandstone, moderately sorted.....	3.0
3. Conglomerate, pale-olive (10Y 6/2) to light-olive gray (5Y 6/2), lensoidal; mostly cobble-sized volcanic (mostly andesitic) clasts, in moderately-sorted sandy matrix..	1.0
2. Sandstone; same as unit 4.....	3.0
1. Lahar, moderate-olive-brown (5Y 4/4) tuffaceous silty to sandy matrix, with 3 to 15 cm diameter angular clasts of mostly rhyolite, with lesser andesite and Paleozoic chert clasts; overall unit is very poorly sorted.....	4.5
Partial thickness measured of Member 4.....	39.0

Member 3 of the Blair Junction sequence of the Esmeralda Formation (upper Miocene, Clarendonian):

Disconformable contact with overlying member 4.

22. Sandstone, light-olive-brown (5Y 5/6), small-scale trough crossbeds; moderately sorted, graded, fining upward; several thick beds.....	6.5

Measured Section SS IV of the Esmeralda Formation, Blair Junction sequence, member 3--Continued

		Thickness (m)
21.	Siltstone, dusky-yellow (5Y 6/4), platy, and tuffaceous.....	1.0
	---------Fault-----(Undetermined thickness missing)----------	
20.	Limestone, dark-yellowish-brown (10YR 5/4), platy, resistant bed locally contains common fossil bivalves.....	1.0
19.	Sandstone, grayish-yellow (5Y 8/4), coarse-grained; graded, fining upwards; contains thin, papery silt shale parting.....	2.4
18.	Tuff, grayish-orange (10YR 7/4) fine-ash; very well lithified and siliceous; breaks into small angular, brittle chips; common angular quartz phenocrysts, and biotite....	2.8
17.	Sandstone, very-pale-orange (10YR 8/2), coarse- to very coarse-grained; moderately sorted; subangular grains; lenses of conglomerate, with angular, medium-size pebbles; calcareous, finer sand to silt matrix and cement, contains quartz, feldspar, and biotite.....	4.8
16.	Sandstone and siltstone, grayish-yellow (5Y 8/4); medium-grained, poorly sorted sandstone; crossbedded; interbedded with dark-yellowish-orange (10YR 6/6), platy siltstone.....	8.2
15.	Sandstone, grayish-orange (10YR 7/4), moderate- to well-sorted impure sandstone; grains are mostly subangular, quartz and feldspar, with lesser dark grains of hornblende; locally crossbedded; calcite cement.....	1.1
14.	Limestone, dark-yellowish-brown (10YR 5/4); several thin (average 5 cm thick) beds, with siltstone partings.....	0.7
13.	Shale, very pale-orange (10YR 8/2), papery, slightly calcareous to carbonaceous.....	1.5

Measured section SS IV of Esmeralda Formation, Blair Junction sequence, member 3--Continued

		Thickness (m)
12.	Limestone, pale-yellowish-orange (10YR 8/6) to grayish-orange (10YR 7/4), fine-grained, thin-bedded, very platy to flaggy; abundantly fossiliferous, with fragmented fish bones, vertebrae, and teeth; gastropods and ostracods; bivalves (probably Sphaerium or Pisidium sp.).....	0.5
11.	Shale; same as unit 13.....	0.8
10.	Limestone; same as unit 12, but less fossiliferous.....	0.5
9.	Shale; same as unit 13.....	0.5
8.	Limestone; same as unit 12.....	0.2
7.	Shale; same as unit 13.....	0.5
6.	Tuff, very light-gray (N 8) to more weathered grayish-orange (10YR 7/4); fine-grained matrix of vitric material with visible quartz and feldspar phenocrysts.....	0.5
5.	Shale; same as unit 13.....	6.2
4.	Tuff, pale-yellowish-brown (10YR 6/2), fine-grained, well-lithified.....	0.8
3.	Silty sandstone, light-olive-gray (5Y 6/1), friable, poorly exposed.....	10.0
2.	Siltstone, dark-yellowish-orange (10YR 6/6), sandy, well-sorted, siliceous; splits into 1- to 5-cm, erosion-resistant, flaggy, layers; with small lenses of coarse sandstone and small pebble conglomerate.....	1.7
1.	Shale, white (N 9), tuffaceous and friable.....	13.3
	Partial thickness of member 3..... (Base of unit not exposed).	65.5